

WHY WALK AND RUN: ENERGETIC COSTS AND
ENERGETIC OPTIMALITY IN SIMPLE
MECHANICS-BASED MODELS OF A BIPEDAL
ANIMAL

A Dissertation

Presented to the Faculty of the Graduate School

of Cornell University

in Partial Fulfillment of the Requirements for the Degree of

Doctor of Philosophy

by

Manoj Srinivasan

May 2006

© 2006 Manoj Srinivasan

ALL RIGHTS RESERVED

WHY WALK AND RUN: ENERGETIC COSTS AND ENERGETIC
OPTIMALITY IN SIMPLE MECHANICS-BASED MODELS OF A BIPEDAL
ANIMAL

Manoj Srinivasan, Ph.D.

Cornell University 2006

This thesis is a model-based exploration of the classic hypothesis that animals locomote in a manner that minimizes the metabolic cost of the task.

First, we formulate perhaps the simplest mathematical model of a bipedal animal that is capable of an infinite variety of gaits — including many types of walking, running, and skipping. The model, first described by Alexander (1980), consists of a point-mass upper body and massless legs which are capable of performing work on the upper body when in contact with the ground. We determine the positive and negative work required by the model to perform idealized versions of various familiar gaits. Approximating the total metabolic cost as being only due to positive and negative work, we find that inverted pendulum walking is preferable to, specifically, impulsive running at low speeds and impulsive running is preferable to inverted pendulum walking at higher speeds. Further, we find that skipping is always a little more energetically expensive than impulsive running.

We then ask a larger question: why do people choose to walk and run when their legs are, in theory, capable of an infinite variety of gaits? Using numerical optimization on the minimal model, we show that from among an infinite variety of gaits that the minimal model is capable of, inverted pendulum walking requires

the least energy at low speeds. Impulsive running requires the least energy at high speeds. At a small range of intermediate speeds and large step lengths, a new gait we have dubbed “pendular run” is found to be optimal.

Next, we provide an analytical proof of the energetic optimality for walking at low speeds and running at high speeds in an informal simplification of the minimal biped model.

Finally, we present simple models for the energetics of swinging the leg. Combining this simple leg-swing model with the previously derived model of the work done by the leg during stance, we find that as an animal moves faster, the ratio of the cost for swinging the leg to the cost of the work done during stance is approximately a constant, as has been shown in some experiments.

BIOGRAPHICAL SKETCH

Manoj was born in 1979 in Mannargudi, South India. Most of his childhood and schooling was spent shuttling between various cities in the state of Tamil Nadu. Manoj studied engineering at the Indian Institute of Technology, Madras, majoring in Naval Architecture. Manoj came to Cornell University for graduate studies in 2000. At Cornell, Manoj worked with Andy Ruina on the mechanics of bouncing disks and rolling eggs, mechanics of throwing, and various other related topics including the eventual subject of his Ph.D. thesis, the mechanics of legged locomotion.

To my parents

Indira Srinivasan and K. R. Srinivasan

ACKNOWLEDGEMENTS

Most of the ideas in this thesis have been inspired by being around Andy Ruina and/or developed by discussions with him. I thank Andy for his encouragement, his advice and most of all, a perhaps-misplaced generosity with his time.

Thanks to John Bertram (University of Calgary, Canada) for access to his extensive data on human walking energetics, although not used in this thesis. Much of the work in this thesis was indirectly motivated by earlier collaborative work with John.

I'm indebted to Professors John Guckenheimer and Hod Lipson for serving on my special committee and for the many comments that have helped improve this thesis various ways. They were part of an informal group of faculty and students that met every week for a seminar on various biomechanics and motor control issues. This seminar series, created due to the initial efforts of Andy Ruina and Francisco Valero Cuevas, has been an important source of topical intellectual stimulation for the last four years.

This thesis has also benefited from informal discussions with David Cabrera, Mario Gomes, Madhusudhan Venkadesan, Sam Walcott, and others. Finally, I must thank all the graduate students, professors, and staff at the friendly department of Theoretical and Applied Mechanics, and especially all of my sometime roommates for making my stay in Ithaca quite pleasant.

The author was supported, in part, by a McMullen fellowship, various assistantships at Cornell teaching math and mechanics courses, and a National Science Foundation grant in Robotics.

TABLE OF CONTENTS

1	Introduction	1
1.1	Theories of locomotion and motor coordination.	1
1.2	Optimality as a predictive theory in biology.	1
1.3	The best way to move: energetic optimality in animal movement.	4
1.4	Muscle modeling	7
1.5	Brief overview of locomotion research	10
1.6	Optimal control in locomotion biomechanics	11
1.7	Outline of this thesis	13
2	Simple models of walking, running, skipping, and level walking.	15
2.1	Minimal model of a bipedal animal	15
2.1.1	Relation to “external work” calculations	19
2.2	An additive cost for swinging the legs	20
2.3	Walking	21
2.3.1	Inverted pendulum walking	22
2.3.2	The limits of inverted pendulum walking.	26
2.3.3	Comparison of model prediction with human data	29
2.3.4	The smoothest gait: Constant speed level walking	31
2.3.5	Another smooth gait: Level walking with no double support	33
2.4	Running	34
2.4.1	Impulsive running	34
2.4.2	Compliant running: the spring-mass model of running	37
2.4.3	Pseudo-elastic spring-mass running	39
2.5	Skipping	40
2.6	Comparing the cost of various gaits	45
2.7	Conclusions	46
3	Computer optimization of a minimal biped model discovers walking and running	49
3.1	Methods	57
3.1.1	Formulation	57
3.1.2	Numerical solution of the optimal control problem	58
3.2	Further comments about Srinivasan and Ruina (2006)	59
3.2.1	A consequence of periodicity on the objective function	59
3.2.2	Description of the optimal control problem	60
3.2.3	Trick-1: Smoothing the non-smooth integrand	61
3.2.4	Trick-2: Assume the non-smoothness away	63
3.2.5	Convergence of the numerical optima	64
3.2.6	Non-smoothness of the objective function	65
3.2.7	Discovering level walking in the optimizations	69
3.2.8	Cost of pendular running	69

3.2.9	Optimal duty factor for pendular running at small step-lengths	70
3.2.10	Generating the phase boundaries	71
3.2.11	Possible discontinuity at the boundary between pendular running and impulsive running	71
4	Minimal biped model at small step lengths: a heuristic proof of optimality of walking and running	75
4.1	Introduction	75
4.2	Problem A: Symmetry assumptions.	76
4.3	Problem B: Riding a circular arc with vertical telescoping legs . . .	78
4.4	Small step lengths: Problem B is “similar” to Problem A	80
4.5	The “elevator problem”: Riding a constant acceleration vertical el- evator.	83
4.6	Optimal “gaits” in the elevator problem.	85
4.7	Discussion	90
5	Cost of swinging the leg.	94
5.1	Introduction	94
5.2	Model of leg-swinging: No tendons	94
5.2.1	Strategies for the total positive work	96
5.3	Analytical expressions for the cost of impulsive work.	97
5.4	Effect of tendons	99
5.5	Discussion	101
6	Power laws: why cost of swinging is approximately a constant proportion of the total cost of locomotion.	103
6.1	Introduction	103
6.2	Optimal trade-off between two power laws	103
6.3	Metabolic cost components can be approximated by power laws . .	104
6.4	Optimal trade-offs between the stance and leg-swing cost	105
6.5	Discussion	106
6.6	Conclusions	107
7	Conclusions	108
8	Future work	110
8.1	Less restrictive calculations with the minimal model	110
8.2	More calculations with the minimal model	110
8.2.1	Optimal state-based feedback control	111
8.2.2	Adding force and power constraints	111
8.2.3	Adding a cost for force	111
8.2.4	Tendons in series with muscles	112
8.3	A kinematically accurate minimal model of a bipedal animal	112

LIST OF TABLES

3.1	<p>Symmetric smooth problem. Optimal value for various N for $V = 0.5, D = 0.5$ is shown in terms of its difference from the accurate cost obtained for inverted pendulum walking (0.019913159). Optimal value for $N \rightarrow \infty$ is obtained by extrapolation using a linear and quadratic curve-fits. The mean square errors for the two curve-fits are respectively about 5×10^{-5} and 1×10^{-5} (a cubic fit does not do any better). The accuracy of the extrapolations seem to be consistent with these mean square errors.</p>	66
3.2	<p>Convergence of the smoothed optimal control problem in N. Optimal values for a sequence of N for $V = 0.5, D = 0.5$ are plotted in terms of their differences from the accurate collisional walking cost. Each of these numbers were obtained by solving a sequence of ϵ-smoothed optimal control problems (with the smoothing function f_1) and extrapolating to $\epsilon = 0$ as in Figure 3.6. We note that the extrapolation to $h = 0$ and $\epsilon = 0$ is different from the result of the collisional value by about 10^{-5} — somewhat higher than would be expected superficially from the mean-square errors of the linear (error: 5×10^{-6}) and quadratic (error: 5×10^{-7}) curve-fits. The source of this inconsistency is not clear.</p>	67
3.3	<p>Co-vary ϵ and N in smoothed optimal control problem. ϵ and N were varied according to the relation $\epsilon = \frac{1}{5N}$. The optimal values are then extrapolated to $\epsilon = 1/N = 0$ by fitting a cubic polynomial to the data. Mean-square error of the cubic fit was about 10^{-7} — the agreement of the extrapolation with the accurate collisional value of the walking cost is only about 10^{-4}.</p>	67

LIST OF FIGURES

2.1	Point-mass biped model. The biped has a point-mass body and massless legs. (a) Single stance: the configuration shown is partway through the stance phase. (b) Double stance: both legs are in contact with the ground. (c) Free body diagrams of the leg and the point-mass body during flight, single stance and double stance.	17
2.2	Inverted pendulum walking. (a) The body travels in a sequence of circular arcs. (b) The transition from one circular arc to the next is accomplished by two impulses: a push-off impulse and a heel-strike impulse. (c) Push-off zoomed in. The leg and hence the impulse is perpendicular to the incoming velocity \mathbf{v}_i , performs some positive work to redirect the velocity to \mathbf{v}_m	23
2.3	Feasibility of inverted pendulum walking. Shaded region represents the region in which inverted pendulum walking is possible without tensional leg-forces. For a bipedal animal with a point-mass body and mass-less legs. Dashed line represents the boundary of feasibility. The oval represents roughly where humans on a treadmill cease to walk. $P(2\sqrt{5}/3 \approx 1.4905, 0)$ is where the dashed line intersects the $V = 0$ axis.	28
2.4	Comparison of the inverted pendulum walking model with human data Bobbert (1960) gives metabolic data for human walking. Kuo et al. (2005) gives estimates of the work done by the legs from the ground reaction forces – the plotted points correspond to metabolic cost estimates arising from these external work estimates, assuming $b_1 = 4$ and $b_2 = 1$. That the external work estimate of metabolic cost overestimates the actual metabolic cost suggests the possibility that some of the leg-work in walking is performed, not by muscles, but by tendons.	30
2.5	Two types of level walking. (a) is a level walk without constant speed and with no double support. b is level walking with constant speed and with double support at all times. Also shown are the forces on the point-mass body at a typical point in each of the two gaits (free-body diagrams).	32
2.6	Impulsive run. The flight phase is a symmetric parabola. During the short stance phase, the leg is vertical and applies a vertical impulse.	35

2.7	Metabolic cost of running The metabolic cost of real runners is plotted as a function of speed. Also plotted for comparison are the metabolic costs estimated by an impulsive running gait, and a pseudo-elastic running gait. These estimates assume that muscles do all the work. Both impulsive running and compliant pseudo-elastic running seem to overestimate the real running cost because apparently, in real running much of the work is done by springy tendons costing little metabolic cost.	36
2.8	Effective leg stiffness Nondimensional spring constant obtained by fitting a spring mass model to speed, step length and duty factor data for real human running from Wright and Weyand (2001). . . .	41
2.9	Compliant run. The minimal model can simulate the compliant running motions of a spring-mass model of running.	41
2.10	Simple skipping gaits. The body flies through the air in a parabolic free-flight at the end of which the legs land in sequence – the trailing leg first provides an impulse, then the leading leg provides an impulse. (a) In bilateral skipping, the legs interchange their roles every stride. (b) In unilateral skipping, the legs have asymmetric roles; one leg is always in front of the other. If the legs are identical and massless, the difference between unilateral and bilateral skipping vanishes. (c) and (d) show the effect of an impulse by leg-1, the trailing leg on the velocity of the center of mass. Case 1: (c), when $\alpha < \theta$, a mixture of positive and negative work is done by leg-1. Case 2: (d) when $\alpha \geq \theta$ only positive work is done by leg-1.	42
2.11	Comparing costs. The regions where each of the 3 gaits (inverted pendulum walking, impulsive running and level walking with no double support) have the lower cost in a three-way comparison are shown. Interestingly, the boundary that separates level walking and inverted pendulum walking here is identical to the boundary of infeasibility of inverted pendulum walking in Figure 2.3	47
3.1	Body motion in human gaits. (a) Trajectories of the center of mass for a few possible gaits. Solid lines, stance; dotted lines, flight. (b), Trajectory for inverted-pendulum walking. (c) Trajectory for impulsive running. (d) Trajectory for a new gait: pendular running. At least one of the gaits (b), (c) and (d) turns out to use less work than any other candidates (for example, from (a) according to the calculations here.	50

3.2	<p>Point-mass biped model and its optimal solutions. (a) The configuration shown is part way through the stance phase. The next stance leg is oriented to prepare for a new contact at a distance d from the last. (b-d) Dimensionless force and length shown as functions of dimensionless time, for the three optimal gaits, (b) pendular walk; (c) impulsive run; (d) pendular run), before full convergence of the numerical optimization. The finite forces in the figures are approximations to the converged impulsive (collisional) forces. In the extrapolated optimum, as the grid size $h \rightarrow 0$ and the allowed force upper bound F_{max}, the optimizations find that $e_1, e_2 \rightarrow 0$ and that the maximum forces used go to infinity (Methods). In these limits the walking gait (b) is an inverted pendulum with heel-strike and push-off impulses, the running gait (c) is an impulsive bounce between free flights, and the pendular run (d) has constant-length pendulum phases and flight phases separated by impulses.</p>	53
3.3	<p>The regions in which each of the three collisional gaits are optimal. Inverted-pendulum walking ceases to be locally optimal at the pendular-run interface. The oval indicates the approximate speed and step length range at which humans switch from walking to running (Thorstensson and Robertson., 1987; Minetti et al., 1994). The dashed line indicates where compression-only inverted-pendulum walking becomes mechanically infeasible ((typically approximated Alexander, 1976, as $V = 1$, which is correct for small D). At the right part of the intermediate region, the pendular run is almost impulsive running; at the left edge, it is almost inverted-pendulum walking.</p>	54
3.4	<p>Cost of transport versus speed. (a) For small D ($= 0.50$), all periodic gaits (that do not involve leg tension) have nearly equal costs near $V = 1$. Inverted-pendulum walking is optimal at low speeds, pendular running at a narrow range of intermediate speeds, impulsive running at high speeds, and flat walking is never optimal. b, However, for large D ($= 1.00$) and for $V \approx 0.8-0.9$, flat walking, perhaps like a ‘Groucho walk’ (Bertram et al., 2002), although not optimal, has lower cost than both inverted-pendulum walking and impulsive running. The colors used in (a) and (b) indicate the following gaits: red, impulsive running; blue, pendular walking, green, level walking; purple, optimal gait. (c) Body trajectories for a pendular walking gait (blue; kink angle is independent of speed), a low-speed impulsive running gait (red; kink angle is large), a high-speed impulsive running gait (orange; kink angle is small) and level walking (green; no kinks, but generally more costly), all with the same step length.</p>	56

3.5	Three smoothings of x. (a) $f_1(x, \epsilon) = \frac{2}{\pi}x \tan^{-1}(x/\epsilon)$ approaches $ x $ from below as ϵ goes to zero. (b) $f_2(x, \epsilon) = \sqrt{x^2 + \epsilon^2}$ and (c) $f_3(x, \epsilon) = x + \epsilon \log(1 + e^{-x/ \epsilon })$ approach $ x $ from above as ϵ goes to zero. In these figures, the smoothed versions are visually indistinguishable from $ x $ for $\epsilon = 0.01$. (d) The smoothed and unsmoothed versions of a hypothetical $ P(t) $ are shown. $\epsilon = 0.1$ was used for the smoothing.	62
3.6	Convergence of the smoothed optimal control problem in ϵ. Optimal value for a sequence of ϵ -smoothed optimal control problems for fixed $N = 17$. As before, $V = 0.5$, $D = 0.5$. Two types of smoothing were used to obtain, respectively, a sequence of overestimates of the optimal value for $N = 17$ and a sequence of underestimates. Such sequences are extrapolated to $\epsilon = 0$ for a range on N for use in Table 3.2.	66
3.7	Non-smoothness of the objective function. Shown is the variation of the objective function when (a) one or (b) two control parameters are varied with all other parameters are kept fixed at their optimal values. The objective function does not seem continuously differentiable at the optimum – in both (a) and (b), the optimum lies at the kink. We solved the symmetric smooth problem ($N = 12$, $V = 0.5$, $D = 0.5$), found the optimum, then changed the objective function to include an absolute value sign, and obtained this plot as the force values at the first and second grid points were changed. The function looks non-smooth at finer scales as well.	68
3.8	Pendular run. The impulsive change in velocity due to push-off at the end of a pendular stance phase is shown.	72
3.9	Classified optimal gaits We solved the symmetric optimal control problem with $N = 11$ for a number of different (V, D) combinations and classified the resulting optimal solution as inverted pendulum walking, impulsive running or pendular running. Because of the low grid-size, the regions over which a given gait is optimal is slightly different from that obtained by solving the more-restricted optimization problem of Section 3.2.10.	72
3.10	Optimal pendular running The optimal duty factor given that the gait is a pendular run is plotted as a function of V at a constant $D = 1.0$	74

3.11	Unique optimal duty factor?	Or are there multiple local minima? (a) shows only one minimum. (b) shows two minima, while (c) again shows one minimum. Thus there seems to be a very small window of non-uniqueness. (d) shows the contour plot of the cost with respect to V and the duty factor at a constant D . (e) zooms in on the region shaded yellow in (d). Vertical sections through this region are depicted in (a), (b), and (c). The contours in (e) were created using MATLAB's contour, with 30 grid points on each axis.	74
4.1	Problem A	(a) One step of a gait that is symmetric about the mid-step. (b) Assumptions that all steps are identical and that each step is symmetric about mid-step imply that the vertical component of the velocity is zero at mid-step and the end of the step.	79
4.2	Problem B: riding a circular track	(a) The radial telescoping leg of Problem A has been replaced by a vertical telescoping leg in Problem B. The foot of the vertical telescoping leg moves on a circular track. (b) The action of the vertical telescoping leg riding on a circular track is shown in detail. Note that the vertical velocity components vanish at mid-step and end of step.	79
4.3	Problem C: Riding an accelerating elevator.	Both the point-mass and the elevator start at the same position (START) with zero vertical speeds. The elevator maintains a constant downward acceleration e . The point-mass can react push or pull against the elevator using arbitrarily strong vertical telescoping legs. When the elevator reaches END, the vertical speed of the point-mass should again be zero. The objective is to ensure this by doing the least amount of work with the vertical telescoping legs.	92
4.4	Solution to the elevator problem.	(a), Case 1: $g > e$. The thin parabolic contours are constant energy lines. The goal is to go from the origin O to the dotted line AB with the least positive work. Optimal strategy is the vertical line OM . Two alternate suboptimal strategies ON and OPQ are shown as thin dashed lines. (b) Case 2: $g < e$. Optimal strategy is the path ORS . An alternate path OT is shown as a thin dotted line. (c), Case 3, $g = e$. All trajectories (e.g., OF , OG , OH) that do not backtrack have the same cost and hence are optimal. (d) shows the set of accessible velocity directions – directions in which the trajectory can proceed. In the upper half-plane, the trajectories can never move left. In the lower half plane, the trajectories can never move to the right. No magnitude information is intended by the equal length of the arrows.	93

5.1	Mechanics of leg-swinging. (a) The leg is modeled as a compound pendulum attached to a rigid support. (b) Phase portrait θ vs. $\dot{\theta}$ for the pendulum. The concentric ellipses are denote constant energy contours for the mechanical system; the ellipses coincide with the trajectories of unforced oscillations of the pendulum. Thick solid line is the optimal motion for amplitude θ_{max} when the required swing frequency is less than or equal to the natural frequency at this amplitude. (c) Thick solid line is the optimal motion for a swing frequency greater than the natural frequency at the given θ_{max}	95
5.2	Nondimensional positive work $W_{p/oscillation}/mgr\theta_{max}^2$ as a function of the ratio of swing frequency and natural frequency $\frac{\omega_s}{\omega_n}$. Three cases are shown. Solid curve is the cost of work-minimizing strategy in the presence of gravity. Thick long-dashed curve is work-minimizing in the absence of gravity. Thin short-dashed curve is the cost of a sinusoidal oscillation at the required frequency.	99
5.3	Leg-swinging with tendon springs (a) shows a model for the leg in the absence of gravity. (b) gravity in a simple pendulum model is equivalent to a sping in parallel to the muscles.	102
6.1	Minimum of the sum of two power law functions.	103

Chapter 1

Introduction

1.1 Theories of locomotion and motor coordination.

Voluntary motion in most animals consists of a complex of interactions between the mechanical structure of the body, the muscles, the nervous system, the circulatory system, and to perhaps lesser extents, other physiological systems. Researchers hope to untangle this complex of interactions into dynamical equations. These equations will predict the physiological consequences (including movement of limbs) of a high-level volitional decision by the brain or predict the responses to an external stimulus. These attempts at “dynamical theories” of motor coordination could be reductionist in the extreme, building up from the level of individual neurons and muscle fibers. Such reductionist syntheses are likely to be more fruitful for simple rhythmic movements (e.g., Marder and Bucher, 2001) in simple lower animals (e.g., Grillner et al., 1991, 1995; Grillner, 1996) and/or simple reflex behavior (e.g., Kandel et al., 2000). For humans exhibiting more elaborate behavior, a more realistic near-term goal would be to understand the dynamical coupling between systems-level behaviors of the relevant physiological components: writing equations that describe, at a blurred-out level, the interactions between human free will, whole muscles, some gross efferent motor signals, gross afferent sensory signals, and the relevant physiological systems. We do not have such detailed dynamical descriptions of the human motor system (or of any animal for that matter).

Eventually we might have enough data to put the pieces together, to create more and more complete, behaving animals in the computer. Complementary to such attempts at dynamical theories are theories that assume optimality or some variation thereof in animal behavior. The neo-Darwinian argument goes like this: Much of animal movement has a purpose. Animals move to forage, predate, evade, reproduce, migrate, etc. These activities are critical to the eventual reproductive success of the animal. There is, therefore, a strong evolutionary pressure on animals to move “well”. The hope, then, is that optimization of behavior in mathematical models of animals will predict, at least approximately, what they are likely to do to achieve a specific goal, say locomotion. This thesis is almost entirely concerned with this second kind of theory.

1.2 Optimality as a predictive theory in biology.

Optimality in biological systems is an ancient hypothesis:

“If one way be better than another, that — you may be sure — is nature’s way.”

– Aristotle, 384 BCE-322 BCE, quoted in Sutherland (2005).

“A perpetual law of nature consists of acting with the smallest work.”
 – Borelli, 1608–1679 (Borelli, 1680).

However there is some skepticism whenever optimization is touted as a predictive theory in biology (Gould and Lewontin, 1979). A thorough discussion of the utility and rationale for optimization in biology is provided in Smith (1978). Other good references are Smith (1982), Alexander (2001) and Sutherland (2005). For completeness, we briefly discuss the main issues here.

An optimization study requires a definition of what “good” means. For biological systems shaped by natural selection, a “good” trait is often defined roughly as that which survives better, say, over a time-scale much longer than the life-time of a single organism. This rough notion of “fitness” can be variously formalized in simple mathematical models of animal competition and evolution (Smith, 1982). We can then seek the evolutionarily stable strategies (if such exist) within the simple models of animal evolution. However, in many situations (including animal locomotion, we shall argue), the effectiveness of a behavior of a particular animal can be well-characterized by a single scalar quantity, that depends only on the behavior of the particular animal, but not on the behavior of the other animals in the population. In such situations, it is appropriate to replace the problem of finding the evolutionarily stable strategy (Smith, 1982) in some model of evolution by a more tractable proxy problem – that of finding that adaptation that maximizes or minimizes the scalar “objective function”. We can then see how well optimization of this objective function can explain particular adaptive behavior or structure. A reasonable objective function that characterizes the effectiveness of locomotion is the metabolic cost (e.g., Margaria, 1976; Alexander, 1989) for traveling unit distance. As will be discussed in the next section, there is some experimental evidence for energetic optimality in animal locomotion.

Optimization studies are often criticized as being circular, tautological and irrefutable. For example, some of these optimization studies posit an optimization principle, determine the theoretical optimum and if it does not agree with experiment, change the objective function and constraints appropriately to make better predictions. Sutherland (2005) deflects this criticism by pointing out that this circularity is a common feature of most scientific enterprise. On the other hand, the new refined theory should (as should all new theories) not be judged by the data that motivated it, but be judged by the accuracy of its novel predictions (e.g., Smith, 1978).

Nevertheless, the hypothesis of optimality with respect to *some*, possibly unknown, objective function is irrefutable (Smith, 1978). It might be possible to explain a lot of an animal’s behavior by attributing it to the optimization of a rather complicated objective function. For some problems, we might be able to derive, by repeated human guesswork, the objective function that is (perhaps) being optimized. Such guesswork can sometimes be automated into a procedure called inverse optimization (e.g., Ahuja and Orlin, 2001), in which a computer algorithm searches for the objective function (typically from a finitely-parameterized family

of objective functions) that when optimized with appropriate constraints predicts the observed behavior. Especially when the structure of the resulting objective function is complicated, such optimization is unlikely to offer simple understanding, but might well be a reasonable way to codify a wide range of animal behavior. Inverse optimization in combination with (forward) optimization has been used successfully to derive ingenious rules for animation of human motion (Liu et al., 2005).

Sometimes no single objective function seems likely to predict observed behavior and the adaptive behavior might be a compromise for multiple functional consequences. In such cases, we might still get good predictions from composite objective functions or multi-objective formulations¹ of the optimization problem (for e.g., Ringuest, 1992). More generally, evolution by natural selection is never strictly an optimizing process. Given that animals compete, the fitness of a particular animal is determined not only by its own actions and adaptations but also those of other animals and plants in a dynamic ecosystem. Co-evolution of species takes them away from any given objective ideal of optimality. In many of these cases, non-cooperative evolutionary game theory might be the more appropriate approach (Smith, 1982).

Another common criticism of optimization studies is their apparent inability to account for evolutionary or developmental constraints. The usual response to this criticism is that all optimization studies require a description of the “the feasible region”, the set of possible solutions from which the best is sought. The feasible region is specified either explicitly as constraints on the optimization or implicitly via modeling assumptions. The feasible region, therefore, implicitly defines the space of possible phenotypes – implicitly modeling the evolutionary and developmental constraints. However, the phenotypic variation thus assumed in optimization studies are based more on convenience, rather than our current knowledge about developmental constraints and trade-offs. Detailed data on the possible phenotypic variation is virtually non-existent for most situations (Nijhout and Emlen, 1998). More generally, the underlying assumption in optimization studies is that most such constraints can always be violated on a longer time-scale.

Theories based on optimality can be complementary to more dynamical or mechanistic descriptions of say, how a particular efficient locomotor behavior is implemented in an animal with muscles and neurons or how a particularly effective structure is developed as a consequence of developmental trade-offs. Of course, it is neither fruitful nor reasonable to expect to understand every little feature in an organism by optimization. Nevertheless, functional adaptation (optimization is a special case) of structure and behavior remains one of the few unifying themes in biology.

¹in which the set of non-dominated Pareto-optimal solutions are sought

1.3 The best way to move: energetic optimality in animal movement.

The best way to locomote depends on the situation. High accelerations and maneuverability may be required to successfully catch an evading prey or to successfully evade a pursuing predator (e.g., Alexander, 2003). At other times, ability to maintain a slow but sufficient speed for long periods of time (endurance) might be important (e.g., Alexander, 2003). Energetic economy, only subtly different from endurance, is useful in most situations. And not losing stability — not falling down — is a hard constraint in all these situations (e.g., Kubow and Full, 1999). These are not necessarily mutually exclusive goals. For example, an animal can accelerate quickly when it wants to, but be energetically economical when it has reached the intended steady speed. Energetic optimality could be pursued, for example, with stability as a constraint.

More generally, minimization of an energy-like quantity might not be appropriate for discovering optimal strategies for maximum performance tasks such as maximum-velocity throwing or maximum speed running. However, many adaptations for maximum speed running, for example, would help energy efficiency and vice versa (e.g., low friction joints, long light legs). Further, the relationship between energy efficiency and some other performance measure can be understood by the study of appropriate dual problems. Given, say a throwing velocity, maximal or otherwise, one can ask how one should attain this throwing velocity with minimum energetic cost. An animal might usefully seek to minimize its metabolic energy expenditure subject to the constraint that it escape a pursuing predator with probability one.

This thesis is mostly concerned with energetic optimality of steady legged locomotion. In particular, we will consider only the energetic optimality of the locomotor *behavior*, as opposed to the optimality of the locomotor *structure*. However there is some evidence of structural adaptations that help locomotor energy economy. For example, the long tendons in animals store and return energy during running, and arguably, walking as well — thus minimizing the work requirements of these gaits (e.g., Alexander, 1988).

Unlike optimality with respect to some as-yet-undetermined criterion, energetic optimality is an experimentally refutable hypothesis. And as noted earlier, studies have found some evidence for energetic optimality in animal movement. This evidence is of two types:

1. **Direct experimental evidence.** The metabolic energy expenditure during a preferred locomotion pattern is compared with those of nearby not-preferred locomotion patterns. The preferred locomotion pattern tends to have the least metabolic cost. The metabolic cost here is typically estimated by monitoring the oxygen (“VO₂”) and carbon dioxide (“VCO₂”) exchange through the lungs (e.g., Brooks et al., 2000).

2. **Consequences of Optimality.** This kind of evidence is less direct. A researcher uses a model of the animal to determine the consequences of optimality for the model and compares that to observed behavior (e.g., Alexander, 1980, 1992, 1997; Kuo, 2001; Srinivasan and Ruina, 2006).

Before discussing the experimental evidence of the first type, we need to more clearly define what we mean by “animals pursue energetic optimality”. When an animal is resting – that is, not moving – it expends metabolic energy to support the various physiological processes that keep it alive. But “not moving” is not a single state, and depending on what processes are going on in the body, the resting metabolic rate will vary (e.g., Alexander, 1999). For simplicity in specific applications, this rate R_{rest} is often assumed to be a constant. When the animal starts moving, voluntary muscles are employed to perform work on the body and exert forces as appropriate. Voluntary muscle contraction requires energy. Further, sustained voluntary muscle use requires increased blood flow to the corresponding muscles, increased breathing rates to keep up the oxygen required for aerobic glycolysis and increased motor neuronal firing; all these increases entail energetic costs. The increase in metabolic rate due to use of voluntary muscles for movement is the sum total of all such changes in the energy requirements.

What should an animal minimize? It is easiest to discuss this question in the context of steady horizontal locomotion. Let the total metabolic rate (energy per unit time) while moving steadily at speed v be $R_{mov}(v)$. Then the total metabolic cost per unit distance would be R_{mov}/v . If the animal needs to travel a given distance, perhaps it should travel in a manner that minimizes the total metabolic cost required to travel this distance – hence minimizing R_{mov}/v . Note that R_{mov} includes the resting cost R_{rest} . This minimization problem results in an optimal speed of travel v_{opt} . v_{opt} is greater than zero because the cost per unit distance at zero speed is infinity, given that $R_{mov}(v = 0) > R_{rest} > 0$ (Tucker, 1975; Radhakrishnan, 1998).

Minimization of the total cost per unit distance is equivalent to selecting the speed that maximizes the distance traveled on a given energy budget, say without eating. So v_{opt} is also called the maximum-range speed (Alexander, 1999). This speed might be the appropriate evolutionary adaptation during periods of spatial scarcity of food.

In humans, minimizing the total cost per unit distance R_{mov}/v for walking gives an energy-optimal speed of about 1.30 ms^{-1} . And people’s self-selected walking speeds tend to be close to 1.30 ms^{-1} (Ralston, 1976; Bastien et al., 2005). Hoyt and Taylor (1981) showed a similar result in horses. They first trained horses to walk, trot and gallop at a wide range of speeds on a treadmill. The energetic costs of these gaits were then measured at these speeds. They then calculated the energetic cost per unit distance as a function of speed for each of these three gaits – without subtracting the resting metabolic cost. They also determined the speeds at which the horses tended to employ each of these gaits most often, when not on a treadmill. They found that these self-selected speeds for each of the three

gaits line up with the minima of the respective gait's total metabolic cost per unit distance.

Self-selected speeds of animals moving on slopes are different from self-selected speeds on level ground. At a range of slopes, the changes in self-selected speeds are well-predicted by the changes in the energetically optimal speed in horses (Wickler et al., 2000) and in humans (Ralston, 1976; Minetti et al., 1994). Self-selected speeds in walking while carrying loads of up to 75% body weight matched the energetically optimal speed (Bastien et al., 2005). Also, physically challenged subjects, using crutches or prosthesis seem to have self-selected speeds that minimize their (much higher) metabolic cost per distance (Ralston, 1958).

Curiously, there seems to be some evidence that unencumbered walking speeds on streets differ from country to country (e.g., Bornstein and Bornstein, 1976; Levine and Norenzayan, 1999). And this variation has been correlated to some measure of “the pace of life”, wealth and affluence of the various countries. Some of this variation in walking speeds is probably a result of the differences in the non-trivial cost for time in various countries, as the authors conjecture. However, it would be interesting to determine the metabolic cost per distance as a function of speed for individuals drawn from the various countries to see how much of the variation in walking speeds can be explained by minimization of the metabolic cost (people from different countries might have different mean values of height, weight, and other physiological parameters that determine the metabolic cost of walking).

The speed of progression is just one variable among the infinitely many that is required to completely characterize how an animal moves. There is evidence that animals (humans) choose these other variables in an energetically optimal manner as well. In the above discussion of the optimal speed of travel, we implicitly assumed that at any particular speed the animals move in a way that minimizes energy per unit distance at that speed. For any given speed, humans select the stride-length (Högberg, 1952; Cavanagh and Williams, 1982; Kuo, 2001; Bertram and Ruina, 2001) that seems to minimize the metabolic cost. They also seem to choose their step-width based on energetic considerations (Donelan et al., 2001).

In humans, gait transition from walking to running or running to walking happens close to where energetic cost of walking and running are approximately equal (Margaria, 1976; Thorstensson and Robertson., 1987; Minetti and Alexander, 1997; Hreljac, 1993). Some of these studies show that there is a small but significant difference between the speed at which humans prefer to change gait and the speed at which the walking and running cost curves cross. Similarly, there is some conflicting evidence regarding the trot-to-gallop transition in horses. While one study (Farley and Taylor, 1991) found a statistically significant difference between the minimum sustained galloping speed and the energetically optimal transition speed, another study (Wickler et al., 2003) found no significant difference.

Humans seem to be able to do constrained energy-optimization dynamically, as the situation demands it. For instance, the relationship between speed and step length is different for different constraints and the particular relationship seems to be consistent on average with the optimization of metabolic cost subject to

the specific constraints (Bertram and Ruina, 2001). This suggests that humans (and animals) have evolved an ability to quickly find the energy optimum even in unfamiliar and novel situations, rather than be energy efficient in only the more often used tasks such as steady unconstrained locomotion. However, more experiments are needed to more thoroughly demonstrate the natural constrained optimization capabilities of humans in strange and unfamiliar situations.

The experiments described above provide evidence that some aspects of animal behavior might be a consequence of, or at least correlated with, energetic optimality. However, the experiments described above were narrow in scope. They do not say that among all the possible gaits that our legs are capable of, we choose the best possible. To show this, we have to compare the energetic cost of the preferred gait with every other possible gait. This takes far too many experiments. Moreover even if we did perform a large number of experiments and found that the self-selected gait has the lowest metabolic cost, the result would be subject to the criticism that strange and unpracticed gaits are energetically expensive exactly because they are unfamiliar. Thus the more elaborate tests of energetic optimality might best be carried out with mathematical models. Such mathematical models, having assumed energetic optimality, should be able to make a variety of testable predictions about the locomotor behavior of animals.

Energetic optimality is not yet a well-tested theory. Optimization, especially of a single scalar objective, can probably be never a very accurate theory for complex animal behavior. Nevertheless, in many cases, even if animals are not exactly optimal by any particular measure, optimality might provide useful approximations of its behavior. The extent to which optimality predicts motor coordination and locomotion cannot be discerned without detailed models predicting the consequences of optimality.

We do not know what the limits of the hypothesis of energetic optimality are for the particular case of steady legged locomotion. We do know, through experiments described in the previous section, that animals tend to behave in a manner that is more or less energetically optimal in some specific situations. While there have been many optimization studies whose predictions have been compared with some experimental measurements (e.g., Alexander, 1980, 1992, 1997; Yamaguchi and Zajac, 1990; Anderson and Pandy, 2001a), we do not know if the theory is likely to apply quantitatively in a wider class of situations.

1.4 Muscle modeling

A key component of a model of the energetics of a locomoting animal is a model of its muscles.

Energy for muscle activity Muscle activity of some kind is required for an animal to interact mechanically with its environment. The energy for muscle con-

traction comes most immediately from the hydrolysis of ATP stores in the muscle. On a longer time-scale, ATP is synthesized by metabolizing glycogen and fatty acid, which in turn are obtained from more complex food molecules (e.g., Brooks et al., 2000; Alexander, 1999). As pointed out in a previous section, if we really wanted an accurate estimate of the energetic cost of a particular motor activity, we would have to include the energetic cost of pumping the blood at an increased rate, the energetic cost of faster breathing, and a host of other things that accompany the motor activity. Using the amount of oxygen consumed (“VO2”) as a measure of metabolic cost naturally accounts for all these extra “systemic” energy costs. And when constructing a mathematical model of the energetics of voluntary muscle activity, it is usually implicitly assumed that these extra systemic energy costs scale in proportion to the energy directly consumed by the voluntary muscles themselves (“direct” energy costs).

Muscle activity has a direct cost whether the muscle is performing external mechanical work or not. Isometric (constant muscle length) force generation has, for instance, a non-trivial energetic demand. However, the simple model that we will use in this thesis assumes that the metabolic cost of muscle use solely depends on the positive and negative work performed by it. In this model, if a muscle is exerting force but performing no work, it does not require energy i.e., there is no energetic cost for isometric force. This approximation is based on experiments (Margaria, 1976) that showed that the metabolic rate of walking and running up or down large-enough slopes at a given speed scales in proportion the rate of change of potential energy of the person. Assuming that when a person is climbing up a steep-enough slope his leg muscles mostly do positive work, and when going down a steep-enough slope, the leg muscles mostly do only negative work, we can estimate the respective efficiencies of positive work and negative work (Alexander, 1976). The metabolic cost for each muscle for a task lasting a time duration T can then be approximated by a linear combination of the total positive and negative work.

$$E_m = \int_0^T (b_1[P]^+ + b_2[P]^-)dt \quad (1.1)$$

Here the mechanical power of the muscle $P = F \times v$ where F is the muscle force and v is the muscle contraction speed. $[P]^+$ is the positive part of the power: $[P]^+ = P$ if $P \geq 0$ and $[P]^+ = 0$ if $P < 0$. $[P]^-$ is the negative part of the power, defined by $[P]^- = [-P]^+$. For a task that requires activity of more than one muscle, the total metabolic cost could be obtained by summing the metabolic cost over individual muscles. Typically, $b_1 \approx 4$ and $b_2 \approx 0.8$ (Margaria, 1976). In this thesis, we will make the approximation that $b_1 + b_2 = 5$.

Is a purely work-based energetic cost any good? The mechanics of many tasks are dominated by a need to perform a certain amount of mechanical work. For these tasks, work is often a good first approximation of metabolic cost. Even in legged locomotion, where the net work done is zero, work seems to account for a

substantial fraction of the total metabolic cost (Ruina et al., 2005; Donelan et al., 2001). But we want to use work as an objective function in an optimization study to see how well it can predict the locomotor behavior of animals. Is this likely to give reasonable results? Naive optimization has a curious way of exposing the inadequacies in the objective function or the inadequacies in the formulation of the constraints, by often discovering physically unrealistic minima. An animal, for instance, could drive the muscle work done during locomotion to zero (in the absence of frictional and viscous dissipation) by evolving springy tendons in series with the muscles. A purely work-based metabolic cost model would suggest that the energy cost of locomotion would be close to zero. This conclusion would be incorrect as the muscles in series with the tendons will need to match the tension in the spring and this will cost some energy even if the muscles do no work. Nevertheless, it is useful to understand in detail the predictions of work optimization in locomotion, if only as a starting point for more elaborate analysis.

Muscle model with a cost for isometric force. A second model for the cost of muscle use might have an additional term for force, isometric or otherwise, like $\int_0^T |F| dt$.

$$E_m = \int_0^T (b_1[P]^+ + b_2[P]^- + b_3|F|) dt \quad (1.2)$$

Why $|F|$ and not, say a higher power of F like F^2 ? The linear scaling of the cost of force with the force is consistent with a simple model of muscle-force production. This model assumes that the rate of energy consumption is proportional to the number of active sarcomeres and that muscles produce higher forces by activation of more sarcomeres in parallel. By a similar argument, b_3 has a natural scaling. Longer muscles producing the same force will have more cross-bridges in series, implying that b_3 scales in proportion to muscle length, for a given muscle cross-sectional area. In general, it is likely that different muscles are best described by different values for these constants b_1 , b_2 and especially b_3 .

Minetti and Alexander (1997) used a more elaborate model that captures the velocity dependence of force and energy efficiency. Their equations were numerical fits to the experimental data in Ma and Zahalak (1991).

Other researchers have used models for energetic costs such as the integral of muscle tension raised to some power (e.g., $\int c|F|^\alpha dt$ in Crowninshield and Brand, 1981; Anderson and Pandy, 2001b) or variations thereof. Studies of voluntary goal-directed hand-movements have used other objective functions not directly related to muscle energetic costs: Flash and Hogan (1985) suggest a measure of “jerk” $\int \left(\frac{d^3x}{dt^3} \right)^2 + \left(\frac{d^3y}{dt^3} \right)^2 dt$ where (x, y) was the position of the hand.

Doke et al. (2005) suggest that the cost of muscle use, especially for high-frequency motions, can have terms that penalize the rapidity of force production (cost proportional to high derivatives of force). We will discuss their experiments in greater detail in chapter 5.

Finally, we must note that the decomposition of the total muscle cost into a weighted sum of individual terms is only a convenient first guess.

Limits on muscle performance. Muscles can only produce a finite amount of force (maximum muscle stress is, very roughly, 0.33 MPa). The force exerted by a muscle depends (Zajac, 1989) on its current length, its current shortening velocity, some measure of neuronal activation, its recent history of its use, as in stretch-induced force enhancement (Lee and Herzog, 2002), or more long-term history, as in injury or training. One can imagine a sequence of muscle models, varying in complexity, that incorporate one or more of these features. In this thesis we use the simplest, where the forces a muscle can exert are conceptually unbounded, not constrained by the values of any other variables.

Muscle kinematics. Finally, one requires a model of how a muscle is connected to the body, and how its contraction affects motion. Again, there are various degrees of realism possible. At one extreme, lie the remarkably detailed modeling of muscle kinematics, including the wrapping of the muscles around realistically shaped bones in detailed models of the animal body (Delp and Loan, 2000). In this thesis, we choose the other extreme of model simplicity. For instance, we model each leg with all of its muscles as a single telescoping actuator that can change length, exert force, and perform mechanical work on the upper body (Chapters 2–4). Somewhere in between these two extremes is the approximation of muscles as simple torque actuators, uni-articular or multi-articular.

1.5 Brief overview of locomotion research

Researchers from a wide variety of fields have studied and continue to study the various aspects of walking and running. Researchers at various gait analysis laboratories have studied walking (not so much running) in normal and pathological subjects, to diagnose and correct specific locomotor deficiencies in patients (e.g., Perry, 1992). Physical anthropologists interested in the evolution of the human bipedality have studied locomotion to understand the role it played in shaping our functional morphology (e.g., Bramble and Lieberman, 2004; Wang et al., 2004; Nagano et al., 2005; Sellers et al., 2004). Roboticians who wish to build legged robots that approach human or animal nimbleness of feet at similar energetic costs have contributed much to our understanding of legged locomotion (e.g., Raibert, 1986; McGeer, 1990b,c; Pratt, 2000; Collins et al., 2005). Computer scientists who wish to produce natural-looking graphic animations of humans and animals (e.g., Brotman and Netravali, 1988; Liu et al., 2005) have developed tools that might be of use in studying locomotion.

Then there is a large mainstream biomechanics literature on walking and running. A complete discussion of this literature is beyond the scope of this thesis. A part of this literature attempts to model humans, or parts of humans, in great

detail. These models tend to have a large number of degrees of freedom. Body segments are approximated as being rigid. Muscles might have realistic origins and insertions (Zajac, 1993), but have simplified Hill-type transient properties (Zajac, 1989). Contact is typically modeled with stiff springs and dashpots. Impressive whole body models have been assembled and various analyses performed. The building of such complex models have been made easier by the development of various software, for example, SIMM (Delp and Loan, 2000), that combine musculo-skeletal modeling capability with a dynamics package. These models have been made to track human motion capture data (Neptune et al., 2004, 2001) using inverse dynamics calculations. Detailed models have also been used in large-scale optimization calculations to predict the details of human motion from first principles (see Sec. 1.6).

Mathematical models of sufficient realism will be required for specific medical interventions: for example, rehabilitation of muscle function through electrical stimulation (Yamaguchi and Zajac, 1990). Unfortunately, there exists insufficient understanding of the many components that such complex models require — for instance, *in vivo* muscle behavior is not understood well enough (Alexander, 2002a). Further, complex models typically imply high computational cost (Anderson and Pandy, 2001a).

The mathematical models in this thesis are much simpler and might be viewed as being complementary to the models that incorporate more of the complexities of an animal body. The hope here is to understand, in detail, the consequences of energetic considerations in the context of these simple models. There is a great tradition of simple models in biomechanics of legged locomotion, exemplified by the tens of papers and books on similar topics by R. McNeill Alexander. This thesis draws much from this literature.

1.6 Optimal control in locomotion biomechanics

The core of this thesis is the numerical solution of an optimal control problem in Chapter 3. In a typical optimal control problem, one seeks to minimize a scalar quantity J by choosing appropriate shapes for a finite number of functions $f_i(t)$ and appropriate values for a finite number of parameters c_i . The scalar quantity J is often related to $f_i(t)$ and c_i via the dynamics of some differential equations: $\dot{x}(t) = g(t, x(t), f_i(t), c_i)$. The minimization problem might be subject to various constraints on the state variables $x(t)$, the control functions $f_i(t)$, and the parameters c_i .

The hypothesis that animals move in a manner that minimizes the metabolic cost of locomotion can be translated into an optimal control problem. The functions f_i in such an optimal control problem in the context of legged locomotion often correspond to muscle forces or muscle activations or joint angles as functions of time. And the differential equations are simply the Newtonian equations of motion that relate forces to the accelerations.

A (biomechanics) optimal control problem is often called a “dynamic optimization problem” (Davy and Audu, 1987) to differentiate it from a “static optimization problem” (Hardt, 1978), which does not involve the solution of an optimal control problem. A number of authors have discussed the so-called dynamic optimization problem in the context of the biomechanics of legged locomotion.

Chow and Jacobson (1971) seem to have been the first to formulate an optimal control problem as a means to predicting the motion of a human from first principles. For computational expedience, the authors make a number of simplifications that make extensive use data of humans walking data. In particular, they completely specify the motion of the hip (to decouple the dynamics of the two legs) and also make use of ground reaction forces (to obtain estimates of ankle forces and torques). As the authors themselves point out, these assumptions constrain the model in a manner that only the swinging of the non-stance leg can be optimized.

Since this paper, the most common use of dynamic optimization in biomechanics has been to determine those sets of muscle activation or muscle force histories that make a particular mathematical model of a human body closely track various aspects of human walking data (Davy and Audu, 1987; Yamaguchi and Zajac, 1990; Tashman et al., 1995). In these studies, the objective function was a linear combination of some model of metabolic cost and the squared deviation of the model’s motion from the human data. The solution of such “tracking problems” can be valuable as they provide information about hard-to-measure *in vivo* muscle forces.

In order to be able to generate meaningful predictions about how a person will move (walk) in a novel situation, it is important that the formulation of the basic metabolic cost optimization problem does not contain references to kinematic data from human-subject walking trials. Anderson and Pandy (2001a) come closest to this ideal. They use a mechanical model of a human consisting of 23 degrees of freedom, actuated by 54 muscles. Briefly, they seek a periodic walking motion that “starts” from a given posture (obtained from human data) and minimizes the metabolic cost per unit distance. Specifying the initial posture seems somewhat unsatisfactory. However the overall effect of such a specification may be evaluated by detailed sensitivity analysis. Anderson and Pandy (2001a) point out that their optimization problem was so computationally expensive that the only attempted numerical solution² exhibited clear signs of non-convergence – for example, the periodicity constraints were not met after 10,000 hours of CPU time (assume CPU speeds circa 1999-2000).

The mechanical model of a biped employed in this thesis is much simpler (and somewhat less realistic) than those used in the above studies. Because of the simplicity of the model, we will see that it is possible to obtain reasonable convergence to (what we believe to be) the solution of the corresponding optimal control problem without specification of initial posture.

²using a gradient-based parameter optimization method similar to the one used in this thesis

Finding minimal energy bipedal gaits is obviously of interest to roboticists who wish to design and build efficient walking robots. Consequently, many roboticists have attempted the solution of the optimal control problem for finding the minimum-energy bipedal gaits. Here, “energy” almost always refers the integral of the sum over all the joints of squared joint-torque, and typically does not involve work-like terms. Interestingly, most of these robotics papers (e.g., P H Channon, 1990; Roussel et al., 1998; Chevallereau et al., 1999; Hardt et al., 1999) use the same 4-DOF bipedal robot model with torque-motors at all joints. Many of these papers do assume the initial posture as given *a priori*. The paper by Hardt et al. (1999) probably contains the most elaborate solution of the optimal control problem among these robotics papers. Hardt et al. (1999) used DIRCOL — a software for numerical solution of optimal control problems by direct collocation techniques, developed by von Stryk and coworkers (von Stryk, 1999).

Liu et al. (2005) solve locomotion-related optimal control problems in the context of computer animation. As described earlier, this paper is quite novel in its use of inverse optimization to obtain the objective function, which when minimized predicts a pre-specified locomotion pattern. The mechanical model used in this work has passive springs in parallel with muscles. Although biomechanically somewhat unrealistic, these parallel springs presumably mitigate some of the instabilities inherent in a multi-body system — possibly promoting robust convergence to solutions that “look” reasonable (the primary objective in computer animation).

We have so far discussed some studies that formulate optimal control problems in the context of legged locomotion. There exist a few other papers that solve other biomechanics-related optimal control problems: examples include rising up from a chair (Pandy et al., 1995; Menegaldo et al., 2003), maximum-speed pedaling (Raasch et al., 1997), maximum-height jumping (Pandy et al., 1990; Anderson and Pandy, 1999), and kicking (Hatze, 1976). We shall not review these papers here. Gomes and Ruina (2003, 2005a,b) implicitly solve optimal control problems by finding zero-work dissipation-free periodic solutions in simple models of ape brachiation and in a biped model with springs.

Finally, it seems appropriate to mention a sequence of classic papers by Alexander (1980, 1992) and Minetti (1997) even though they did not contain explicit optimal control formulations. Instead, the optimizations were over a two-parameter family of gaits for every speed and step length.

1.7 Outline of this thesis

In Chapter 2 of this thesis, we describe a minimal model of a bipedal animal that is capable of a range of gaits. This minimal model has a point-mass upper body and massless telescoping legs. We discuss the mechanics of some familiar gaits such as walking, running and skipping as well as some not-so-familiar gaits such as level walking in the context of this minimal bipedal model. We estimate the metabolic costs of these various gaits and determine which of these particular gaits have the

lowest energetic cost at a given forward speed and step-length. In Chapter 3, we ask a more general question. We determine which gait, from an infinite variety of gait possibilities (subject to some restrictions), minimizes the energetic cost of moving unit distance for the minimal biped model. Numerical optimization shows that a classic simple description of walking is optimal at low speeds and a classic simple description of running is optimal at high speeds. In Chapter 4, we present an approximate simplified version of the optimization problem in Chapter 3 and provide an informal proof of the global optimality of the analogs of walking and running at low and high speeds respectively in the simplified optimization problem. In Chapter 5, we describe simple models of the cost of swinging the leg. In Chapter 6, we present a simple theory of why the cost of leg-swinging as a fraction of the total metabolic cost changes little with change in speed. We conclude the thesis with a list of short-term goals of the line of research begun in this thesis.

Chapter 2

Simple models of walking, running, skipping, and level walking.

Human legs are capable of much more than just walking, running and skipping. With appropriate, but perhaps unusual muscle activations, human legs can be made to simulate a variety of unusual locomotor patterns. We would like a simple general model of a bipedal animal that is capable of describing a similar large variety of locomotor possibilities.

In this chapter, we describe a minimal mechanics-based model of a bipedal animal as relevant to legged locomotion. This model was first described by Alexander as a special case of a quadruped model (Alexander, 1980). This minimal model can be made to track the center of mass motion for a number of characteristic patterns of locomotion (“gaits”). In particular, various classical descriptions of walking and running such as inverted pendulum walking (Alexander, 1976, 1989; Kuo, 2002; Kuo et al., 2005; Ruina et al., 2005), level walking (Alexander, 1976, 1991), impulsive running (Rashevsky, 1944, 1948), a more compliant spring-mass running gait (Blikhan, 1989; Blickhan and Full, 1993) can be treated as special cases of this minimal model. We will discuss the energetics of these and other idealized gaits in the context of the simple model. This chapter is, in part, a review of these classic idealizations of bipedal locomotion, but contains a number of new results as well.

2.1 Minimal model of a bipedal animal

The model here is based on the basic assumption that humans have compact bodies and light legs. For humans, the upper body is about 70% of the total body mass and each leg is about 15% of the total mass. During walking and running, the upper body has little or no rotational dynamics. This is presumably due to some stabilizing muscular control preventing rotation of the upper body during stance. But the lack of body rotation is mostly because the forces the legs exert on the upper body act more or less through the center of mass, and therefore, applying very little rotational moment on the upper body. So it is convenient to entirely neglect any rotational motion and idealize the upper body as a point-mass (Alexander, 1976, 1980) at position (x, y) , as shown in Fig. 2.1.

The two legs are identical and indistinguishable. But where their functional roles are distinct, it is convenient to label them leg-1 and leg-2. One or both or neither of the two legs might be in contact with the ground at any point in time. The two legs are modeled as having zero mass. A leg therefore can have no meaningful dynamics of its own when it is not in contact with the ground. Instead, when not in contact with the ground, we assume that a leg can be swung around arbitrarily quickly, if so required. We will discuss the rationale and the consequences of this modeling assumption in greater detail in Section 2.2.

We assume here that the leg does not have an extended foot, and has only a point-foot. Since we have assumed that the leg is massless and that the body is a point-mass, the leg can only transmit an axial force. That is, the force is always in the direction of the line joining the point-foot and the point-mass upper body. A massless leg, even if its length fluctuations are mediated by hip and knee flexion, acts mechanically like a telescoping actuator (Fig. 2.1). The respective lengths of leg-1 and leg-2 as functions of time are $l_1(t)$ and $l_2(t)$. These lengths must always be less than or equal to l_{max} , the maximum length of the legs. When they are on the ground the legs support compressive time-varying forces – respectively $F_1(t)$ and $F_2(t)$. We assume that the legs are arbitrarily strong, both structurally and in the active force-producing sense, so that there is no upper bound on the magnitude of these forces. This means that the leg can instantaneously change the velocity of the upper body by applying suitable impulses — infinite forces over infinitesimal durations.

When not in contact with the ground, the forces through the legs are identically zero. Also, when not in contact with the ground, the legs can be lengthened or shortened arbitrarily quickly, without any cost. Finally, real muscles are connected to the body via tendons. The tendons are elastic and act as springs in series with the muscles. In the simple model here, we have assumed that there are no springs in series with the telescoping actuator. We shall explore some of the consequences of this assumption in Section 2.4.

Equations of motion. When neither leg is on the ground (**flight phase**), the governing equations for the upper body are:

$$\ddot{x} = 0 \tag{2.1a}$$

$$\ddot{y} = -g \tag{2.1b}$$

where g is the acceleration due to gravity.

When a foot is in contact with the ground, it does not slip. Note that we do not simply assume frictional contact. Rather we impose zero foot-slip as being inviolable during stance. When only leg-1 is on the ground (**single stance phase**), the governing equations are:

$$m\ddot{x} = \frac{F_1(x - x_{c1})}{l_1} \tag{2.2a}$$

$$m\ddot{y} = -mg + \frac{F_1(y - y_{c1})}{l_1} \tag{2.2b}$$

where (x_{c1}, y_{c1}) is the point of contact of the foot of leg-1 with the ground. For locomotion on a flat horizontal plane, $y_{c1} = 0$.

And when both the legs are on the ground exerting a force on the upper body

Model

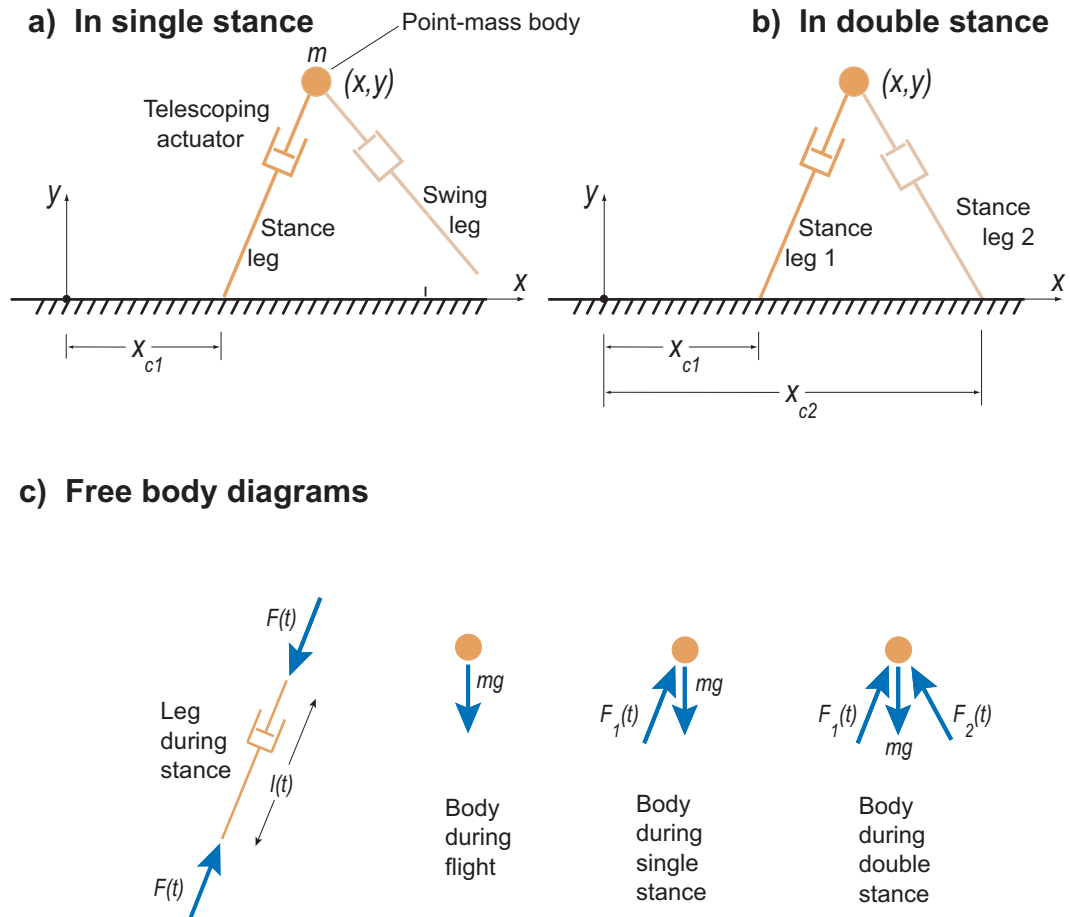


Figure 2.1: **Point-mass biped model.** The biped has a point-mass body and massless legs. (a) Single stance: the configuration shown is partway through the stance phase. (b) Double stance: both legs are in contact with the ground. (c) Free body diagrams of the leg and the point-mass body during flight, single stance and double stance.

(**double stance phase**), the equations are:

$$m\ddot{x} = \frac{F_1(x - x_{c1})}{l_1} + \frac{F_2(x - x_{c2})}{l_2} \quad (2.3a)$$

$$m\ddot{y} = -mg + \frac{F_1(y - y_{c1})}{l_1} + \frac{F_2(y - y_{c2})}{l_2} \quad (2.3b)$$

where (x_{c2}, y_{c2}) is the point of contact of the foot of leg-2 with the ground. As before $y_{c2} = 0$ if the ground is horizontal.

Gait, step, stride, periodicity. A particular gait can have flight, single stance and double stance phases in any permutation. The model here can quantitatively track the center of mass motion of *any* conceivable bipedal gait by appropriate actuation of the telescoping legs. And it can be made to qualitatively match the footfall pattern of any conceivable bipedal gait.

For unknown reasons (perhaps energetic economy), gaits observed in nature are periodic to a fair degree¹. Therefore we consider only periodic gaits here. In a periodic gait on level ground, all relevant state variables except the horizontal position of the center of mass repeat themselves after a duration t_{period} .

For simple periodic gaits, terms such as “step” and “stride” are closely related to the periodicity of the gait. In symmetric walking and running, two steps make a stride. And one stride is equal to one period of the motion (when the two legs are considered as being distinguishable). Such terms are less well-defined when considering asymmetric gaits or gaits with higher periodicity (as in some skipping gaits). For clarity, we shall define these terms again in the respective section on skipping (Sec. 2.5).

Metabolic cost of locomotion. Given the leg forces $F_{1,2}(t)$ and the leg lengths $l_{1,2}(t)$ over one period of a periodic gait, the total positive and negative work done by each leg can be evaluated by integrating, respectively, the positive and negative part of the leg-powers P_1 and P_2 . These quantities can then be used to obtain a work-based estimate of the metabolic cost as described in Sec. 1.4:

$$P_1 = F_1\dot{l}_1, \quad P_2 = F_2\dot{l}_2 \quad (2.4)$$

$$E_{\text{m/period}} = b_1 \int_0^{t_{\text{period}}} ([P_1]^+ + [P_2]^+) dt + b_2 \int_0^{t_{\text{period}}} ([P_1]^- + [P_2]^-) dt \quad (2.5)$$

¹But some evidence of deterministic non-periodic behavior, chaos, has been reported in the so-called passive dynamic walking models (e.g., Garcia et al., 2000). Various studies have looked at the statistics of step-to-step variability in walking (e.g., Hausdorff et al., 1995). Some studies wonder if this variability is random noise or due to some deterministic process (e.g., Dingwell and Cusumano, 2000). We note that the assumption of periodicity of gaits simplifies the definition and analysis of the stability of gaits via poincare maps (e.g., Hurmuzlu and Moskowitz, 1987a,b)

Recall that $[P]^+ = P$ if $P \geq 0$ and $[P]^+ = 0$ if $P < 0$ is the positive part (or the “rectification”) of P . Also, $[P]^- = [-P]^+$ is the absolute value of the negative part of P . If the horizontal distance travelled over a single period is d_{period} , the nondimensional cost of transport is given by:

$$c_t = \frac{E_{\text{m/period}}}{mgd_{\text{period}}} \quad (2.6)$$

Dynamic similarity and nondimensionalization. For a given gait to be completely described, many parameters need to be specified: for instance, the average speed v , the step-length d , the leg-forces as a function of time, the trajectory of the center of mass (not all independent). All these relevant variables can be nondimensionalized by expressing them in terms of m, l_{max} and g . The forces are nondimensionalized by dividing by mg , the lengths by l_{max} , the velocities by $\sqrt{gl_{\text{max}}}$, time by $\sqrt{l_{\text{max}}/g}$ and so on. A gait of one (model) animal can be said to be “dynamically similar” to the gait of another animal if the nondimensionalized set of all parameters describing the two gaits are identical. Since the cost of transport is a nondimensional quantity, it will be equal for dynamically similar gaits.

Two nondimensional parameters that are especially useful are the nondimensionalized speed: $V = v/\sqrt{gl_{\text{max}}}$ and the nondimensionalized step-length: $D = d/l_{\text{max}}$. Note that V^2 is the so-called Froude number (Alexander, 1976). For the idealized gaits we discuss in this chapter (for instance, inverted pendulum walking with push-off before heel-strike, and impulsive running), the two parameters V and D suffice to specify a family of dynamically similar gaits².

2.1.1 Relation to “external work” calculations

Analogous to the calculation of positive and negative work in the model above, it is similarly possible to estimate the work done by each leg when a real person walks or runs. This is achieved by measuring the ground reaction forces for each leg $\mathbf{F}_{g1}(t)$ and $\mathbf{F}_{g2}(t)$, say, by using force plates (Cavagna, 1975) on the ground or a force treadmill (Kram et al., 1998). Given the initial velocity of the center of mass \mathbf{v}_0 , and knowing the external forces, namely, the ground reaction forces and gravity as functions of time, we can compute the center of mass velocity as a function of time: $m\mathbf{v}(t) = m\mathbf{v}_0 + \int_0^t (-mg\mathbf{j} + \mathbf{F}_{g1} + \mathbf{F}_{g2})dt'$. Having determined the velocity of the center of mass, the work done by each of the legs can be approximated as the work done by the two ground reaction forces *as if they were acting on a point-mass upper body*: the respective leg powers are thus approximated by $P_1 = \mathbf{F}_{g1} \cdot \mathbf{v}$ and $P_2 = \mathbf{F}_{g2} \cdot \mathbf{v}$ respectively. Exactly as in Eq. 2.5, we can then estimate the metabolic cost from the positive and negative work done by each leg separately.

²because in these special gaits, the nondimensional leg-forces and leg-impulses are only dependent on V and D and no other parameters

This procedure was proposed by Donelan et al. (2002b) and they called it the “individual limbs method” for estimating the so-called “external work”. They suggested this as an alternative to the more older notion of “external work” in legged locomotion, first described in Fenn (1930a,b) for running and which has since been used for walking and other gaits in various studies (Cavagna et al., 1963, 1964; Cavagna, 1975). This older “external work”, dubbed “the *combined* limbs method” by Donelan et al. (2002b), did not consider the two legs as separate actuators. Instead of using the integral of $[P_1]^+ + [P_2]^+$ for the total positive work as in the *individual* limbs method, the combined limbs method uses the integral of $[P_1 + P_2]^+$. The two methods give the same answer for running, as in this gait not more than one leg is on the ground at any time. However the two-limbs method is sometimes liable to underestimate the quantity of interest, as it cannot account for one leg doing positive work, while the other leg simultaneously doing negative work (Donelan et al., 2002b). In other words, $[P_1 + P_2]^+ < [P_1]^+ + [P_2]^+$, when P_1 and P_2 are of opposite signs. This situation can and does arise in walking, for example.

We remark that the term “external work” as used in the biomechanics of legged locomotion is misleading in a thermodynamic sense as it is not the work done by the environment on the body (A. Ruina, unpublished note). After all, the point on the body in contact with the ground slips very little during stance phase (and not at all in most idealized models). So the forces on the body exerted by the ground typically do essentially zero mechanical work (Ralston, 1976). However the prefix “external” comes presumably from how the quantity is most often calculated — by using the external forces on the body. Perhaps a change in terminology is in order: a more descriptive and less misleading, but somewhat long term could be **point-mass stance-leg work estimate**. This estimate is identical to the positive-work-based mechanical cost estimate that we use for our minimal model.

2.2 An additive cost for swinging the legs

The simple model here has the property that the metabolic cost per unit distance can be reduced to zero by taking the limit of zero step-lengths ($d \rightarrow 0$). In particular, all the idealized gaits to be discussed in this chapter have the property that their metabolic costs per distance approach to zero as the step length d approaches to zero. This is analogous to the rolling of a rimless wheel becoming more like that of a circular wheel as the number of spokes increase (resulting in small step-lengths).

For a given speed, a small step length implies a large step frequency and a large step frequency requires moving the legs at correspondingly large frequencies. Swinging a leg with non-zero mass entails a metabolic rate that increases rapidly with the leg-swing frequency. Therefore, the unrealistic prediction of the small costs at small step-lengths can be avoided if the simple model was endowed with legs having non-zero masses (Kuo, 2001).

As an alternative to replacing the massless legs of the simple model with legs with masses, one can augment the simple model with massless legs with an *additive cost* for swinging the legs (Alexander, 1976; Kuo, 2001). Such an additive cost for swinging a leg in a model with massless legs is only a convenient simplification. But it lets us ignore the dynamics of swinging legs, and restrict our attention to only the motion of the center of mass due to lengthening and shortening of the stance leg.

Simple expressions for this leg-swing cost can be derived in terms of the amplitude and the time duration of the leg-swing (see Doke et al., 2005, and chapter 5 of this thesis). We will not use any such specific additive cost for leg-swing in Chapters 2-4. Instead, we will simply refrain from calculations that are meaningless without including a leg-swing cost (for example, take the limit of small step-length locomotion). We will compare the energetic costs of two gaits (without adding the leg-swing costs) only when they have the same speed and stride-length. The implicit assumption here is that the additive leg-swing cost is simply a function of the speed and step-length³.

Finally, we remark that the energetic costs derived in this chapter might be considered as underestimating the true metabolic cost because we do not explicitly include the leg-swing costs. Of course, these model-based energetic costs will not be strict underestimates because of all the other simplifications here.

2.3 Walking

When humans wish to go slowly from point A to B, they choose to walk. All gaits that have no flight phase – no period of time when neither leg touches the ground – are often classified as walking. Clearly, by this definition, there are infinitely many such walking gaits. But the term “walking” in this thesis will usually mean some idealization of normal walking as practiced by healthy individuals.

In normal walking at not-too-high speeds, body pivots over relatively straight legs during single stance. This motion is often compared to that of an inverted pendulum. Close to the end of one such single stance phase, the leg in contact with the ground, say leg-1, starts to push-off with the foot, just as the heel of the contralateral leg, leg-2, strikes the ground. There is a small period of double stance phase in which leg-1 finishes pushing-off and loses contact with the ground. The double stance is followed by another single stance phase, now with leg-2 on the ground. During the single stance of one of the legs, the other leg swings forward, partly bending at the knee to avoid scuffing the ground, orienting itself for the next heel-strike and the subsequent single stance phase. This swinging of the leg is not all passive pendular motion due to gravity but involves some muscular effort (Braune and Fischer, 1895-1904).

³While this assumption is especially inaccurate for gaits dominated by double support phase, all gaits discussed in this chapter, except one, have no double support phase.

2.3.1 Inverted pendulum walking

We can make the minimal model describe the actual center of mass trajectory during normal walking. But it is easier to understand a limiting case of the above picture of normal walking. We shall call this idealized walking gait, “inverted pendulum walking” in this thesis. The specific idealizations seem to have been first described in detail by Ruina (unpublished) and Kuo (2002), while models with minor variations have been described previously, especially by Alexander (1976, 1991). Later in this section, we discuss the history of inverted pendulum walking model in somewhat greater detail. Kuo et al. (2005) present a review of various aspects of inverted pendulum walking. For completeness here, we will derive expressions for the energetic cost for inverted pendulum walking. The key simplifications are:

- There is no extended double stance phase.
- Assume that the stance leg is always at its maximum length. The single stance phase is, therefore, exactly circular.
- At the end of a single stance phase, the leg on the ground pushes off impulsively. There is an instantaneous change in the velocity, but no change in position. The other leg then strikes the ground, again impulsively, changing the velocity of the upper body. The push-off and the heel-strike together change the downward-pointing velocity at the end of one circular arc to the upward-pointing velocity at the beginning of the next circular arc.

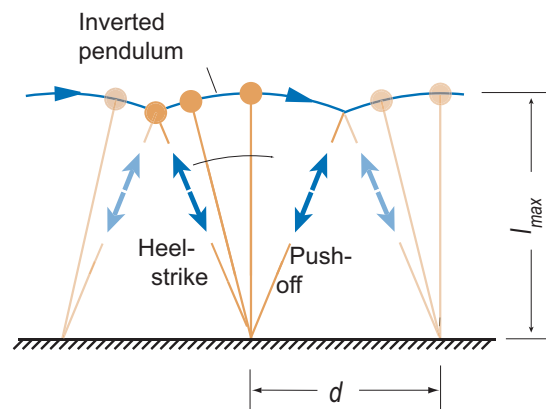
This abstraction of walking has a sequence of exactly circular single stance phases, stitched together by push-off/heel-strike impulse-pairs.

The inverted-pendulum phase requires no work, and hence entails no energetic cost in our cost-accounting. All the work in a period is done at the transition from one pendular arc to the next – “the step-to-step transition” (Donelan et al., 2002a). During the push-off, the leg performs only positive work and during heel-strike, it performs an equal amount of negative work.

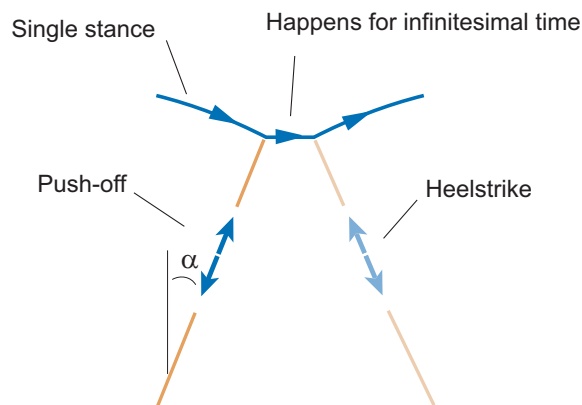
Fig. 2.2b shows, in detail, the changes in velocity direction during the impulsive push-off and the impulsive heel-strike. Fig. 2.2c focuses on just the push-off. α is the angle made by the leg with the vertical at the end of the stance phase. v_i is the magnitude of the velocity at the end of the stance phase — that is, just before the push-off impulse. And v_m is the magnitude of velocity just after push-off but just before heel-strike.

From conservation of linear momentum perpendicular to the push-off impulse, we find that $v_i = v_m \cos \alpha$ (see Fig. 2.2c). Because the push-off impulse does no negative work, the positive work performed during push-off can be obtained as the change in the kinetic energy of the body due to the push-off. This is given by (Kuo, 2001; Ruina et al., 2005):

a) Inverted pendulum walking



b) Transition from one step to the next



c) Push-off

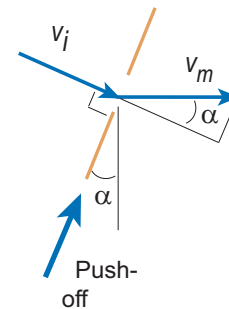


Figure 2.2: **Inverted pendulum walking.** (a) The body travels in a sequence of circular arcs. (b) The transition from one circular arc to the next is accomplished by two impulses: a push-off impulse and a heel-strike impulse. (c) Push-off zoomed in. The leg and hence the impulse is perpendicular to the incoming velocity \mathbf{v}_i , performs some positive work to redirect the velocity to \mathbf{v}_m .

$$W_{p/\text{step}} = \frac{m(v_m^2 - v_i^2)}{2} = m \frac{v_i^2 / \cos^2 \alpha - v_i^2}{2} \quad (2.7)$$

$$= \frac{mv_i^2 \tan^2 \alpha}{2} \quad (2.8)$$

Ruina et al. (2005) used a small-angle approximation of the above expression. Because the gait is steady and periodic, the positive work W_p during the push-off is equal to the negative work W_n done during heel-strike.

Small angle approximation. When α is small, $\tan \alpha \approx \alpha \approx d_{\text{step}}/2l$ and $v_i \approx v$. Using these in Eq. 2.8 gives:

$$W_{p/\text{step}} \approx \frac{mv^2 d_{\text{step}}^2}{8l^2} \quad (2.9)$$

The cost of transport is therefore (Ruina et al., 2005),

$$c_t = \frac{(b_1 + b_2)W_{p/\text{step}}}{mgd_{\text{step}}} \quad (2.10)$$

$$\approx \frac{b_1 + b_2}{8} \cdot \frac{v^2}{gl} \cdot \frac{d_{\text{step}}}{l} \quad (2.11)$$

$$= \frac{b_1 + b_2}{8} \cdot V^2 D_{\text{step}} \quad (2.12)$$

where $D_{\text{step}} = d_{\text{step}}/l_{\text{max}}$.

Relationship between v and v_i . While the magnitude v_i of the velocity just before push-off is approximately equal to the average horizontal speed v for small angles α , v_i is not exactly equal to v . More exactly, the relationship between v_i and v is obtained by taking the dynamics of the inverted pendulum into account. If $\theta(t)$ is the angle that the leg makes with the vertical at time t and $t = 0$ corresponds to mid-stance, conservation of energy gives:

$$\frac{m\dot{\theta}(t)^2 l_{\text{max}}^2}{2} + mgl_{\text{max}} \cos \theta = \frac{mv_i^2}{2} + mgl_{\text{max}} \cos \alpha. \quad (2.13)$$

Therefore,

$$\dot{\theta}(t) = \sqrt{\left(\frac{v_i}{l_{\text{max}}}\right)^2 + \left(\frac{g}{l_{\text{max}}}\right) (\cos \alpha - \cos \theta)} \quad (2.14)$$

Now we can calculate the time t_{step} spent by the inverted pendulum leg in one circular arc (one step), in terms of v_i , g , l_{max} and α .

$$t_{\text{step}} = 2 \int_0^\alpha \frac{dt}{d\theta} d\theta = 2 \int_0^\alpha \frac{d\theta}{\dot{\theta}(t)}. \quad (2.15)$$

This integral can be evaluated in terms of elliptic functions, or evaluated by numerical quadrature (Bertram et al., 1999; Usherwood, 2005). v can then be obtained as a function of v_i , g , d and l_{max} by noting that $v = d_{step}/t_{step}$, where $d_{step} = 2l \cos \alpha$ and t_{step} is given by Eq. 2.15.

Other variants of inverted pendulum walking. So far, we have assumed that the push-off happens entirely before heel-strike in inverted pendulum walking. Another extreme possibility is that of heel-strike happening entirely before push-off (but this requires tensional leg forces: Ruina et al., 2005). Ruina et al. (2005) point out that infinitely many possible variants of inverted-pendulum walking gaits exist between these two extremes – each distinguished by a different amount of overlap between the impulsive push-off and the impulsive heel-strike. It turns out that the energetic costs of these variants of inverted pendulum walking depend on the details of this short impulsive contact period. Ruina et al. (2005) show that the extreme of pushing-off entirely before heel-strike has the least cost among these variants (assuming among other things, that the animal has a point-foot).

In the light of these considerations, when we compare the energetic costs of inverted pendulum walking with other gaits, we shall use the variant of inverted pendulum walking with the least energetic cost — in which push-off occurs entirely before heel-strike.

A brief history of inverted pendulum walking. The key modeling assumption in inverted pendulum walking is that the center of mass describes an arc of a perfect circle during each single stance phase and that the leg is more or less straight during this stance phase. We could not find this approximation in the two great nineteenth century treatises on locomotion (Marey, 1874; Braune and Fischer, 1895-1904), even though the latter obtained detailed trajectories of the center of mass of a walking person. Saunders et al. (1953)⁴ introduced the idea of a compass gait – a walking gait in which the leg is relatively straight during stance, reminiscent of a compass. Following this, idealizations of walking with a constant leg-length stance phase are often called compass gaits. Bekker (1956) seems to have been one of the first to idealize the stance phase as being exactly circular in a mathematical model. However, he does not seem to have treated the inverted pendulum phase as being work-free — he ascribed a work-based energetic cost to the up and down motion of the body during the inverted pendulum phase. Bekker seems to have also been the first to draw an analogy between bipedal walking and the motion of a rimless wheel, later mentioned again by Margaria (1976). Alexander (1976) described an inverted pendulum walking gait, and derived an energetic cost that is identical to that described here. This energetic cost was derived without specification of how exactly the transition between the circular arcs is effected. McGeer (1990a) presented an analysis of the collisional energy losses in a rimless wheel rolling down a slope. Alexander (1991) modified this analysis to make it

⁴as described in McMahon (1984)

apply for a point-mass human walking on a level surface. He assumed that the heel-strike came before the push-off. This seems to have been the first complete description of the energetics of (any variant of) inverted pendulum walking. Inverted pendulum walking, with push-off before heel-strike, alluded to by Tucker (1975) and McGeer, seems to have been first described in detail by Ruina and Kuo (Kuo, 2002; Kuo et al., 2005; Ruina et al., 2005).

2.3.2 The limits of inverted pendulum walking.

Alexander (1976), among other things, derives a simple upper limit on the speed of progression for inverted-pendulum walking gaits. Imagine a point-mass animal vaulting over a straight mass-less leg. If the speed of the upper body is too high, a purely compressive leg-force cannot keep the foot on the ground, the legs will need to *pull* on the body to keep the foot in contact with the ground — the centripetal acceleration required would have exceeded the acceleration due to gravity. If the horizontal speed at midstance was v_{mid} , then the (compressive-is-positive) leg-force at mid-stance is $F = mg - mv_{mid}^2/l_{max}$. For a non-tensional leg-force at midstance, we require that $F > 0$. Consequently a necessary condition for pendular walking is $v_{mid}^2/(l_{max}g) \leq 1$. Since for small step lengths, the average horizontal speed v is approximately equal to v_{mid} , the above necessary condition was approximated by Alexander (1976) as $v^2/(gl_{max}) \leq 1$.

This elegant reasoning requires slight modification for two reasons: 1) In inverted pendulum walking, the compressive leg-force in the legs is minimum, not at midstance, but at the end of stance. In fact, the leg-force is maximum at mid-stance. So as the speed is increased, the leg will lose contact with the ground first, not at midstance but close to the end of stance. This means that a necessary condition based on the midstance velocity (as derived above) will not be a “strict” necessary condition. 2) The formula needs to be accurate for large step lengths. Further, in some biomechanics circles, the infeasibility of inverted pendulum walking is treated as a theory for gait transitions — this is a questionable premise as will be discussed later in this section.

Here we derive expressions for the boundary of infeasibility that is applicable for large-step-length inverted pendulum walking. Consider a gait with step-length d_{step} and average horizontal speed v . The linear momentum balance along the leg at the maximum leg angle $\alpha = \sin^{-1}(d_{step}/2l_{max})$ gives:

$$mv_i^2/l_{max} = mg \cos \alpha - F \quad (2.16)$$

where F is the force on the leg and v_i is the velocity magnitude at the end of a stance phase, but just before the impulsive push-off. If F is to be greater than zero, we need:

$$v_i^2/(gl_{max} \cos \alpha) \leq 1 \quad (2.17)$$

As derived earlier in this section, v_i and α are related to v , d , g and l_{max} , so this inequality can be translated into a feasible region in the v - d plane, or more usefully,

the non-dimensional V - D plane. The shaded region in Fig. 2.3 shows where the above condition is satisfied. The dotted line is the boundary of this region. This figure indicates that at larger step-lengths inverted pendulum walking with only compressive leg-forces becomes infeasible at a lower speed. These observations were first made by Usherwood (2005), and independantly rediscovered here.

The point P in Fig. 2.3 is where the boundary of infeasibility intersects the $V = 0$ axis. The coordinates of this point can be determined analytically as follows: Imagine the point-mass attached to the mass-less leg is initially vertical. This is an unstable equilibrium. And the leg-force is compressive in this configuration. Now let the mass topple over from this position due to an arbitrarily small perturbation. The inverted pendulum will gain angular speed as it topples (taking an arbitrarily long amount of time) and the leg-force will eventually go to zero at some angle α_{max} to the vertical. This leg-angle specifies a corresponding step-length $d_{max} = 2l_{max} \sin \alpha_{max}$. Note that this motion of the inverted pendulum corresponds to zero horizontal speed (because it takes infinitely long to topple from a perfectly vertical position).

By conservation of energy, when started from $v_{mid} = 0$, the speed magnitude v_{max} of the mass at leg-angle α_{max} is given by

$$0 = v_{mid}^2 = v_{max}^2 - 2gl_{max}(1 - \cos \alpha_{max}) \quad (2.18)$$

Further, speed v_{max} is such that the leg-force is exactly zero at $\alpha = \alpha_{max}$. So $v_{max}^2 - gl_{max} \cos \alpha_{max} = 0$ from Eq. 2.17. Using this in Eq. 2.18, we get $gl_{max} \cos \alpha_{max} = v_{max}^2 = 2gl_{max}(1 - \cos(\alpha_{max}))$. Which means that $\cos \alpha_{max} = 2/3$. The corresponding step length is $d_{max}/l_{max} = 2 \sin \alpha_{max} = 2\sqrt{1 - (2/3)^2} = 2\sqrt{5}/3$. As seen in Fig. 2.3, d_{max} is an upper bound on the feasible step-lengths for any forward speed. This upper bound, however, is not independent of the boundary of infeasibility (dashed line) in Fig. 2.3 as noted by Usherwood (2005); rather, it is one special point on this boundary, corresponding to the limit of zero-speed inverted pendulum walking.

The above considerations were based on the idealized model of exact inverted-pendulum walking of an animal with point-mass body, massless legs and impulsive step-to-step transitions. Obviously the predictions of the model will change as these assumptions are revised. In particular, if the push-off is not impulsive but spread out over a finite amount of time, the parameter regime over which the nominally inverted-pendulum walking is possible will be extended. Because the push-off and the heel-strike are compressive impulses, smearing them out over an extended period of time will increase the compressive forces on the legs close to the step-to-step transition, so there would be less danger of the compressive leg-force going to zero. Such a gait, however, would not quite be exactly inverted-pendulum walking. Because when there is an extended (as opposed to impulsive) step-to-step transition, the gait does not resemble the motion of an inverted pendulum throughout the stance phase. Further, the relationship between v_i and v will be different when the massless leg is replaced with a leg that has, say, 15% of the

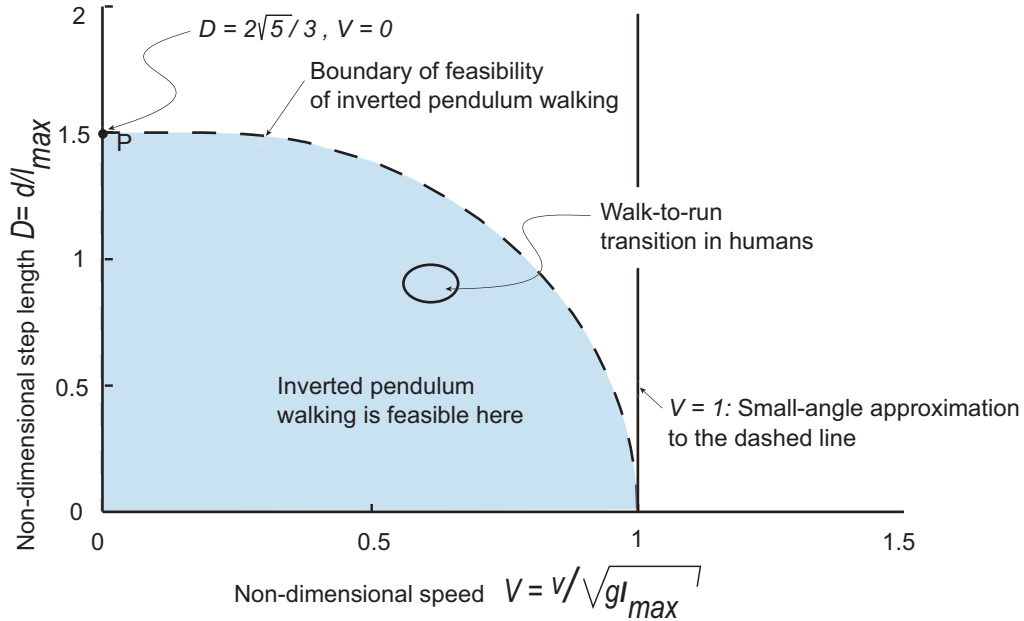


Figure 2.3: **Feasibility of inverted pendulum walking.** Shaded region represents the region in which inverted pendulum walking is possible without tensional leg-forces. For a bipedal animal with a point-mass body and mass-less legs. Dashed line represents the boundary of feasibility. The oval represents roughly where humans on a treadmill cease to walk. $P(2\sqrt{5}/3 \approx 1.4905, 0)$ is where the dashed line intersects the $V = 0$ axis.

total mass. This means that the limit of inverted pendulum walking with legs with masses would be slightly different. The swinging of the other (contralateral) leg will further modify the dynamics of the “inverted pendulum”.

As noted briefly above, the infeasibility of inverted pendulum walking is sometimes considered a theory, if only an approximate theory, of why people switch gait to running. We believe, however, that it cannot be a reasonable theory of gait transition. Inverted pendulum walking is only one of an infinite variety of possible walking gaits. Many of these other walking gaits (like the level walking gaits of the next section) are not subject to a similar upper bound on the speed. So the reason that inverted pendulum walking is infeasible above a certain speed is not good enough to change from a gait without flight phase (that is, a walking gait) to one that has a flight phase (that is, running gait). The above calculation, therefore, is only a curiosity, relevant only in the presence of artificial constraints such as in race-walking (in which sport, the walker is not supposed to bend his legs at the knees for the first half of a stance phase).

2.3.3 Comparison of model prediction with human data

Bobbert (1960) provides simple regression formulas for the metabolic rate of walking as a function of walking speed. Converting these formulas to SI units, we have:

$$\text{Metabolic rate per unit mass} = \left(2.2 + 1.155 \left(\frac{v}{1 \text{ ms}^{-1}} \right)^2 \right) \text{ Watts/kg} \quad (2.19)$$

Subtracting a resting metabolic rate of about 1.4 Watts/kg, and dividing by v and g we get the cost of transport (over and above the resting cost) to be:

$$c_t = \frac{0.8 \text{ Watts/kg}}{vg} + \frac{1.155 \text{ Watts/kg}}{vg} \left(\frac{v}{1 \text{ ms}^{-1}} \right)^2 \quad (2.20)$$

We plot this regression equation in Figure 2.4 along with the estimate of the cost of transport from the inverted pendulum walking model (Equation 2.10). For the calculation of the cost of inverted pendulum walking, we used the following regression formula of Alexander and Maloij (1984) relating nondimensional step length and speed in walking humans, accurate over the speeds considered.

$$D = 1.25V^{0.6}. \quad (2.21)$$

We find that the inverted pendulum walking model overestimates the cost for higher speeds. This overestimation could be due to any of the many simplifications in the inverted pendulum walking model. Addition of a leg-swing cost to the energetic cost obtained here, will further exaggerate the overestimation.

Inverted pendulum walking is simply an idealization of the walking kinematics. Better estimates of the positive and negative work performed by the legs while walking can be obtained by using the actual center of mass motion during human walking. We present such work-estimates obtained in Kuo et al. (2005) (based on Donelan et al., 2002b). See Section 2.1.1 for a brief description of how these estimates were obtained. The corresponding metabolic cost estimate is also shown in Figure 2.4⁵.

We find that these estimates of the metabolic cost based on the actual kinematics of human walking also *exceed* the actual metabolic cost (in spite of not including the leg-swing cost). This overestimation is instructive. In real animals, muscles are in series with elastic tendons. So what is observed as work done by the “legs” is likely to be a combination of muscle work and passive tendon work. But we have assumed that none of the leg-work was due to tendons. Perhaps the overestimation of the metabolic cost by these “leg-work” estimates is due to a non-negligible fraction of the leg-work being performed passively by tendons without incurring any energetic cost. As we will discuss in Section 2.4.3, such “elastic recovery” plays a more prominent role in the energetics of human running — where the aforesaid overestimation of the metabolic cost is much more dramatic (Cavagna et al., 1964).

⁵We note that the subjects in the two studies were of similar stature and weight, and therefore presumably have similar energetics and walking characteristics.

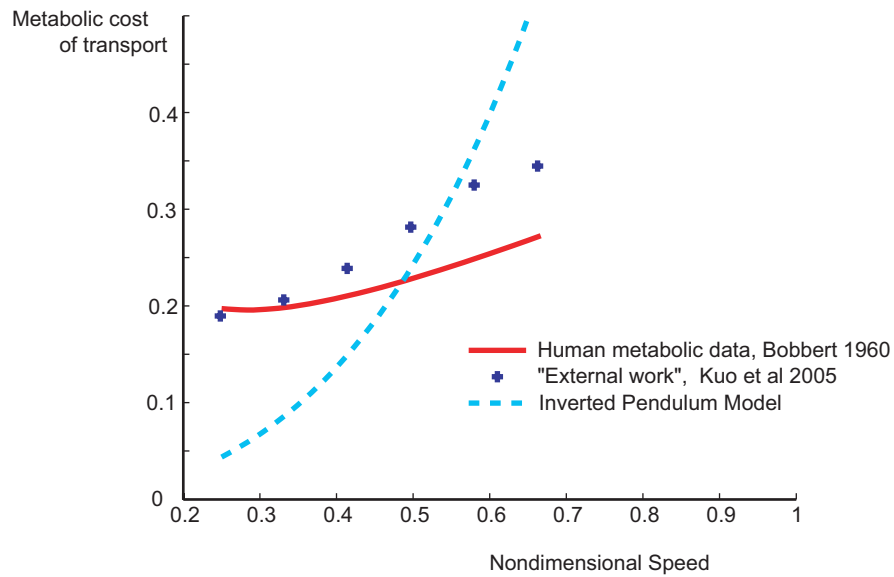


Figure 2.4: **Comparison of the inverted pendulum walking model with human data** Bobbert (1960) gives metabolic data for human walking. Kuo et al. (2005) gives estimates of the work done by the legs from the ground reaction forces – the plotted points correspond to metabolic cost estimates arising from these external work estimates, assuming $b_1 = 4$ and $b_2 = 1$. That the external work estimate of metabolic cost overestimates the actual metabolic cost suggests the possibility that some of the leg-work in walking is performed, not by muscles, but by tendons.

2.3.4 The smoothest gait: Constant speed level walking

Ortega and Farley (2005) showed that a person expends more energy while walking with a constant-height center of mass trajectory than while walking naturally at the same speed. These experiments were in response to the hypothesis (Saunders et al., 1953) that walking smoothly, perhaps with no vertical motion of the center of mass and little change in horizontal speed, will improve energy efficiency. This hypothesis was based on the reasoning that only changes in kinetic and potential energies required work. So, the reasoning went, if there were no changes in kinetic and potential energy, there would be no requirement for work. As alluded to in Alexander (1980), this reasoning is faulty – because even when there is no net work, each leg might be doing positive and negative work that might cancel out. Such positive and negative work will have an attendant metabolic cost. It is thought that many contemporary robots waste energy in a similar manner by simultaneously performing positive and negative work (Chris Atkinson, personal communication and Collins et al., 2005).

For the minimal model here, there are many ways to walk with a perfectly horizontal center of mass trajectory. Here we discuss only two types of level walking. We will first consider the smoother of these two gaits. This gait, not only has no vertical excursion of the center of mass, but also has no fluctuations in the horizontal speed. Fig. 2.5a shows the progression of the upper body and the leg-postures in this gait. Since there is no acceleration, there is no net force on the body. This gait requires double support to balance gravity at all times.

Also, it is clear from Fig. 2.5a that this gait requires infinitely quick leg-swings between two consecutive steps. However, the point we wish to make here is that even without consideration of the (possibly large) leg-swing cost, the work required for this smooth gait is greater than the other gaits discussed in this chapter.

We measure the horizontal position x from the mid-stance of leg-1. The trailing leg (leg-1) supports a compressive force of magnitude F_1 and the leading leg (leg-2) supports F_2 . As the body moves forward, the trailing leg does positive work and the leading leg does negative work. If l_1 is the length of the trailing leg and l_2 that of the leading leg, then force balance gives:

$$\frac{F_1 x}{l_1} - \frac{F_2 (d_{\text{step}} - x)}{l_2} = 0 \quad (2.22)$$

$$\frac{F_1 h}{l_1} + \frac{F_2 h}{l_2} - mg = 0 \quad (2.23)$$

Eq. 2.23 gives $F_2 = mgl_2 x / (hd_{\text{step}})$. If the (vector) force due to leg-2 is $\mathbf{F}_2 = F_{2x}\mathbf{i} + F_{2y}\mathbf{j}$ and the velocity of the body is $\mathbf{v} = (dx/dt)\mathbf{i}$, the negative work done

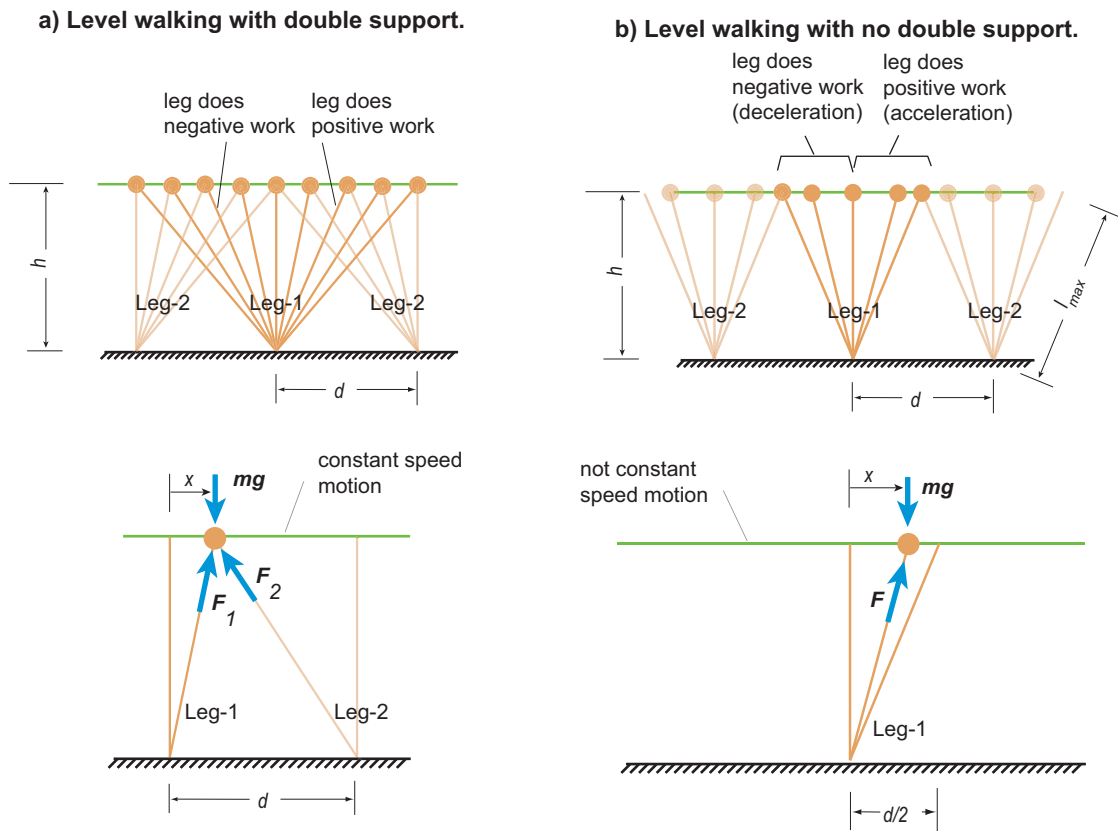


Figure 2.5: **Two types of level walking.** (a) is a level walk without constant speed and with no double support. b is level walking with constant speed and with double support at all times. Also shown are the forces on the point-mass body at a typical point in each of the two gaits (free-body diagrams).

by the trailing leg over a distance d_{step} is:

$$W_{n/\text{step}} = \int_0^{t_{\text{step}}} (\mathbf{F}_2 \cdot \mathbf{v}) dt \quad (2.24)$$

$$= \int_0^{d_{\text{step}}} F_{2x} dx \quad (2.25)$$

$$= \int_0^{d_{\text{step}}} \frac{F_2(d_{\text{step}} - x)}{l_2} dx \quad (2.26)$$

$$= \int_0^{d_{\text{step}}} \frac{mgl_2 x}{hd_{\text{step}}} \cdot \frac{d_{\text{step}} - x}{l_2} dx \quad (2.27)$$

$$= \frac{mgd_{\text{step}}^2}{6h} \quad (2.28)$$

Noting that the positive work is equal to the negative work, we find the cost of transport is given by

$$c_t = (b_1 + b_2) \frac{mgd_{\text{step}}^2}{6h} \cdot \frac{1}{mgd_{\text{step}}} = (b_1 + b_2) \frac{d_{\text{step}}}{6h} \quad (2.29)$$

The cost per unit distance is independent of velocity.

We will find that the energetic cost of this smooth variant of level walking is higher than the not-so-smooth version of level walking to be discussed below. Because the smoother version of level walking requires infinitely quick leg-swings, this observation is quite robust to adding a metabolic cost for leg-swing.

With double support, we have a whole function space of possible level walks, parameterized by the horizontal acceleration as a function of x during the double support. However exactly one of these gaits (described above) has a constant horizontal speed and requires only non-tensional (non-negative) leg-forces.

2.3.5 Another smooth gait: Level walking with no double support

Level walking is possible even in the limit of no double support. Fig. 2.5b shows such a level walking gait — one that is symmetric about each mid-stance. There is a one parameter family of such level walking gaits with no double support, parameterized by the degree of asymmetry about mid-stance (for example, the distance from the center of the switch from leg-1 to leg-2). We will only consider the symmetric case here, discussed first by Alexander (1976, 1991). The following discussion is similar to Alexander (1991).

In this level walking gait with no double support, each leg performs negative work until mid-stance and performs positive work from mid-stance until the step-to-step transition. Let the compressive force supported by leg-1 be $\mathbf{F}_1 = F_{x1}\mathbf{i} + F_{y1}\mathbf{j}$ of magnitude F_1 . Since the acceleration in the vertical direction is zero, force balance gives $mg = F_{y1} = F_1 h/l_1$, where h is the height of the center of mass, and

l_1 is the length of the leg. This gives $F_{x1} = mgx/h$. The positive work performed by the legs is:

$$W_{p/step} = \int_0^{d_{step}/2} \frac{mgx}{h} dx = \frac{mgd_{step}^2}{8h} \quad (2.30)$$

The corresponding cost of transport is $c_t = (b_1 + b_2)d_{step}/8h$. This cost has the same functional form as the level walking with constant speed, except for the smaller leading constant, $\frac{1}{8}$ instead of $\frac{1}{6}$. The cost is similarly independent of speed.

For the simple model here, numerical calculations similar to those in Chapter 3 show that symmetric non-constant-speed level walking gait with no double stance described in this section has the least metabolic cost (without considering leg-swing costs) among all level walking gaits, for given speed and step length.

2.4 Running

Broadly, running is defined as any gait in which all the legs are off the ground at some point during a gait cycle i.e., any gait that has a flight phase. This definition is mildly confusing because humans have many gaits that involve a flight phase: normal running, unilateral skipping (often called galloping) and bilateral skipping (typically just called skipping), hopping on one or two legs, etc, but only one of these gaits (normal running) is called running in the popular parlance. In this section, we will restrict our discussion to normal bipedal running. However, note that for the minimal model, hopping with one or two legs will be energetically indistinguishable from running.

2.4.1 Impulsive running

Impulsive running is conceptually the simplest running gait that our minimal model can perform. The motion of the center of mass during impulsive running is shown in Fig. 2.6. The stance phase is reduced to a vertical impulse of infinitesimal duration. Between two such impulsive stance phases, the body flies through the air in a parabolic trajectory. This idealization of running seems to have been first discussed in Rashevsky's papers (Rashevsky, 1944, 1948).

During the short stance phase, the vertical impulse first performs negative work reducing the vertical component of the body velocity to zero and then performs positive work to restore the vertical velocity to its pre-impulse magnitude, but now in opposite direction. The positive work is, therefore, equal to $W_{p/step} = mv_y^2/2$, where v_y is the magnitude of the vertical component of the velocity just before and just after the stance phase. Noting that the flight phase is parabolic, we have $v_y = gT_{step}/2 = gd_{step}/(2v)$. So $W_{p/step} = mg^2d_{step}^2/(8v^2)$. The cost of transport is then:

$$c_t = (b_1 + b_2) \frac{mg^2 d_{\text{step}}^2}{8v^2} \cdot \frac{1}{mgd_{\text{step}}} \quad (2.31)$$

$$= (b_1 + b_2) \frac{gd_{\text{step}}}{8v^2} \quad (2.32)$$

$$= (b_1 + b_2) \frac{1}{8} \cdot \frac{d_{\text{step}}}{l_{\text{max}}} \cdot \frac{gl_{\text{max}}}{v^2} \quad (2.33)$$

$$= (b_1 + b_2) \frac{D}{8V^2} \quad (2.34)$$

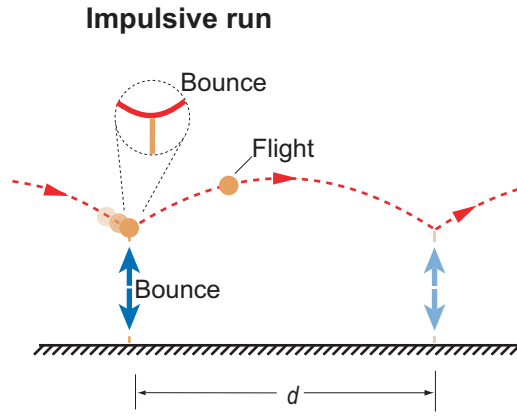


Figure 2.6: **Impulsive run.** The flight phase is a symmetric parabola. During the short stance phase, the leg is vertical and applies a vertical impulse.

Given the speed vs step-length data (here we use data from Wright and Weyand, 2001) for real human running, the above expression can be evaluated for the cost of transport and compared with the actual metabolic cost of transport in human running (Wright and Weyand, 2001). This comparison is shown in Fig. 2.7. We use $b_1 = 4$ and $b_2 = 0.8$. We see that the metabolic cost estimates of the impulsive run far exceed the actual metabolic cost of running. This could mean many things. That impulsive running is an inefficient way to run and a more compliant gait, where the leg forces change more gradually, could cost less energy (and agree better with human metabolic data). Or it could just mean that impulsive running is a bad model of human running. The primary deficiency in this model is that all the work is attributed to the telescoping actuator (muscles) and hence entails metabolic cost. Whereas when there are tendons in series with the muscles – springs in series with the telescoping actuator – some or all of the negative and positive work during the stance phase could be performed by passive springs. We explore these issues in the next two sections.

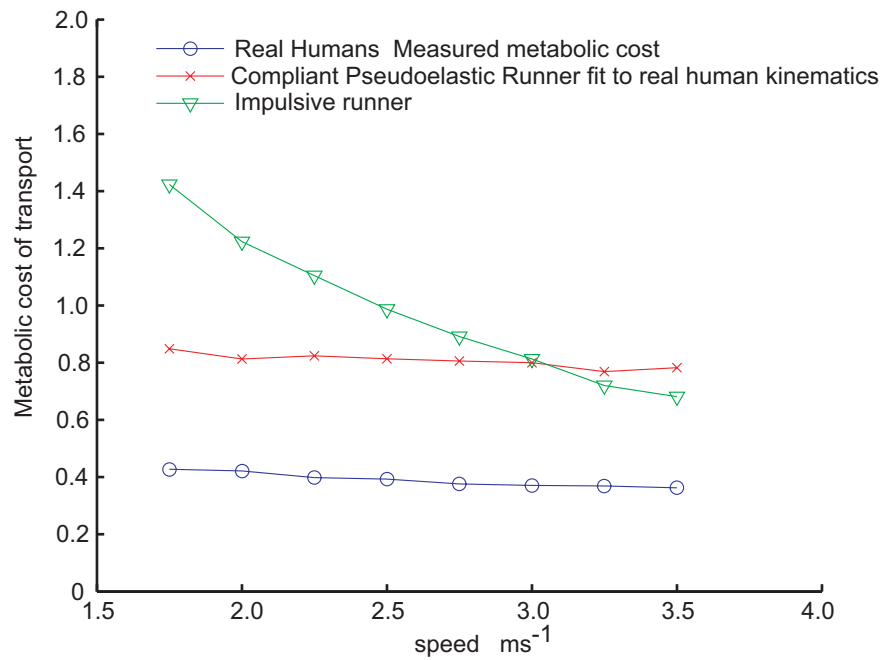


Figure 2.7: **Metabolic cost of running** The metabolic cost of real runners is plotted as a function of speed. Also plotted for comparison are the metabolic costs estimated by an impulsive running gait, and a pseudo-elastic running gait. These estimates assume that muscles do all the work. Both impulsive running and compliant pseudo-elastic running seem to overestimate the real running cost because apparently, in real running much of the work is done by springy tendons costing little metabolic cost.

2.4.2 Compliant running: the spring-mass model of running

Human running gaits are not impulsive. The duty factor for any gait is defined as the time-fraction of a stride (one stride = one period = two steps of running) over which a given leg is in contact with the ground. Running has a maximum duty factor of 0.5, each leg touching the ground for less than half a stride. Slow running typically has high duty factors, over 0.4 at speeds lower than 1.75 ms^{-1} in humans. While running at higher speeds has lower duty factors (e.g., 0.31 at 3.5 ms^{-1} ; see Wright and Weyand, 2001), the duty factor never goes below 0.1 for humans in steady running (as can be verified by observing a sprinter at top speed).

Normal human running has flight phases interspersed with the extended stance phases of alternating legs. This gait has often been compared to a perfectly elastic ball bouncing along a flat surface for two reasons (Margaria, 1976). Firstly, the changes Δl in the length of the leg during a stance phase seem to approximately obey the law of a Hookean spring: $F_{\text{leg}} = k\Delta l$, where k is some effective spring constant (Blikhan, 1989; Farley and Gonzalez, 1996). Secondly, human legs have large tendons in series with the major muscles (although these tendons are not as prominent as in many other animals). These tendons serve as elastic storage mechanisms. If human legs did not have these springs, the compression and extension of the leg would be entirely powered by active muscle contraction. However, the tendons seem to store some of the energy during the compression phase, and this stored energy seems to be used to partly power the leg extension (Cavagna et al., 1964; Alexander, 1997). Direct evidence for this elastic storage has been obtained in running turkeys (Roberts et al., 1997), horses (Biewener, 1998), and guinea fowls (Marsh et al., 2004) by various experimental means (Alexander, 2002b). These studies show, for instance, that the length changes in the muscles are much smaller than the length changes in the tendons. In particular, many of the muscles do little work, but only provide isometric forces that brace the stretching tendon in series.

These experimental observations have led to extensive research about spring-mass running (e.g., Blikhan, 1989; McMahon and Cheng, 1990; Farley et al., 1991; Carver, 2003; Ghigliazza et al., 2005; Seipel and Holmes, 2005; Seyfarth et al., 2002; Geyer et al., 2005). The central mechanical model in such research is the “spring-mass model of running”, sometimes called the Spring-Loaded Inverted Pendulum (SLIP) model of running. This model consists of a point-mass upper body and a massless leg. This leg, however, is a simple linear spring with a given spring constant k , rather like a person riding on a pogo stick. The spring-mass model can be obtained by replacing telescoping actuator in the minimal model here by a linear spring. The spring force is zero during a flight phase and non-negative during a stance phase. The end of a stance phase is determined by the spring force going to zero.

Fitting the spring-mass model to human running data. Briefly, the parameters that define the spring-mass model are m , g , l_{max} and k . These can be combined into one nondimensional parameter: a non-dimensional stiffness $k_{\text{eff}} = kl_{max}/mg$. For simplicity, we consider only in running-like motions of the spring-mass model that are symmetric about mid-stance. This symmetry requires that the velocity at mid-stance has to be horizontal (zero vertical component). For given spring-mass model parameters, there is a two parameter family of such symmetric running motions⁶ – the leg length l_{mid} at mid-stance and the horizontal speed at mid-stance v_{x-mid} . We can nondimensionalize these two parameters by respectively dividing by l_{max} and $\sqrt{gl_{max}}$.

A real human running gait can be simply characterized by the average horizontal speed v , step-length d_{step} and the duty factor μ_d . Toward this end of fitting the spring-mass model to human running data, for every specification of $(v, d_{\text{step}}, \mu_d)$ of human running, we wish to find a motion of the pogo-stick model that has the same $(v, d_{\text{step}}, \mu_d)$. We noted in the previous paragraph that the set of spring-mass motions is characterized by two parameters, for a specified value of non-dimensional stiffness. If we choose to vary the stiffness as well, we have access to three parameters $(l_{mid}, v_{x-mid}, k_{\text{eff}})$ which we can vary to obtain a motion of the pogo-stick model that have the specified values three parameters $(v, d_{\text{step}}, \mu_d)$. The appropriate $(l_{mid}, v_{x-mid}, k_{\text{eff}})$ for a specified $(v, d_{\text{step}}, \mu_d)$ can be (and is here) obtained by a numerical root-find.

When asked to run at a particular speed on a treadmill, people automatically select their preferred step-length and duty factor. That is, the preferred step-length and the preferred duty factor can be represented as functions of the forward speed. Wright and Weyand (2001) present such data: $(v, d_{\text{step}}(v), \mu(v))$ combinations that humans use as they naturally run at a variety of speeds. Such human running data can be fit by the pogo-stick model as described in the previous paragraph. Among other things, this model-fit indicates how the effective stiffness k_{eff} changes with speed (Fig. 2.8). Somewhat remarkably, it is found that the effective non-dimensional stiffness that best fits the human data for a range of speeds is approximately a constant ($k_{\text{eff}} \approx 15$). It does act as if the human leg is a linear spring whose stiffness does not change with speed. This intriguing result was first obtained by somewhat different arguments by McMahon and Cheng (1990).

The pogo-stick model with a *constant* leg-stiffness is perfectly capable of going at a given forward speed at a variety of step-frequencies. But when humans are forced to choose a non-preferred step-frequency at a given speed, the effective spring constant of 15 is no longer a good description of leg-behavior, but rather, the leg seems to behave like a spring with lesser or greater apparent stiffness (Farley et al., 1991; Farley and Gonzalez, 1996). This suggests that perhaps the constancy

⁶Not all values of these parameters lead to symmetric running-like solutions but every symmetric running-like solution is characterized by these two parameters. For instance, some values of the parameters, the spring force would never go to zero, and the leg would never leave the ground.

of leg-stiffness during natural running may not be a simple mechanical consequence of passive elastic elements in the leg. As a consequence, it is not clear why the stiffness is approximately a constant for natural running (with self-selected step frequencies and duty factors) in the first place.

Why does the leg behave like a spring at all? Calculations in Chapter 3 show that energetic optimality for the minimal model imply that running should “look” perfectly elastic even when the legs do not have no springs in them. These calculations predict elastic-looking *impulsive* running as opposed to a more realistic compliant running gait. We conjecture (Chapter 8) that the details of the spring-like behavior can be still be explained as a consequence of energetic optimality but in a more realistic mechanical model of the running animal, perhaps including springs in series with muscles and incorporating a metabolic cost for isometric force.

2.4.3 Pseudo-elastic spring-mass running

The minimal biped model of Section 2.1 has no springs. Nevertheless the minimal model can *simulate* the running motion of a spring-mass model by appropriately changing the length of the telescoping actuator — the telescoping actuator of the minimal model could be made to actively duplicate the behavior of a linear spring of a specified spring constant. We shall call this *pseudo-elastic* spring-mass running because the compliance is simply simulated.

Simulating spring-mass running using the telescoping actuators requires energy. For any particular pseudo-elastic running gait, the energy required can be easily calculated by noting that because the forces and length changes are identical to that of an actual spring-mass model, the positive and negative work done by the telescoping actuator is identical to the positive and negative work performed by the linear spring of the spring-mass model that is being simulated. And these quantities are both equal to the energy stored in the spring when it is maximally compressed. That is, $W_{p/step} = W_{n/step} = 0.5k(l_{max} - l_{mid})^2$. Thus given a running-like motion of the spring-mass model, we can estimate a metabolic cost for the motion *as if* it were performed in the absence of springs. Fig. 2.7 shows the metabolic cost estimates thus obtained by fitting a spring-mass model to real human running as described in the previous section and attributing metabolic cost to the spring work.

Fig. 2.7 shows that the metabolic cost estimate from the pseudo-elastic runner is almost twice as much as the actual metabolic cost for running. Cavagna et al. (1964) did a similar calculation, and obtained essentially the same result. They did not of course fit a pseudo-elastic running model to real human running. Instead, they estimated the work of the legs during stance by measuring the ground reaction forces and calculating the “external work” as described in Sec. 2.1.1. The “external work” was found to be only about 50% of the total metabolic cost, which means a muscle efficiency of about 50% if all the leg-work is due to muscles. Since other experiments have established that muscles are not more than 25% efficient, the inference was that some of the leg-work must have been done for free by real

springs in the leg.

Note that it is not surprising that the estimate of the leg work from fitting the pseudo-elastic runner (as in this section) is essentially the same as the external work estimate of the leg work (not shown: Cavagna et al., 1964). This agreement is because the spring-mass model was originally intended as an approximation of actual human running ground reaction forces and hence also center of mass kinematics (these are the only determinants of the “external work” estimate).

What fraction of the leg work is performed by the springs and what fraction by active muscle contraction? Recall that the above numbers indicate that the leg work (which is a sum of tendon work and muscle work) is about 50% of the metabolic cost. For clarity, consider the following two extreme cases:

- All the leg-work is due the springy tendons and all the metabolic cost is due to isometric contraction of muscles to stretch the spring. Then the so-called elastic recovery, the fraction of the total positive leg-work that is performed by stored elastic energy, would be 100%.
- On the other hand, if we assume that no metabolic cost is consumed for isometric contraction, and assume that all the metabolic cost is due to muscle work at 25% efficiency, then the fraction of the total leg-work due to the elastic elements would be about 50%.

Reality is somewhere between these two extremes — the elastic work probably accounts for more than 50% of the total leg work, and the total metabolic cost is probably, in part, due to force.

2.5 Skipping

Children skip more often than adults do. And it seems like children can skip much more easily than adults can. Skipping also seems to be a preferred form of locomotion for astronauts on the moon and some birds when not flying (Minetti, 1998). While there is a long history of modeling the metabolic cost for walking and running, there seems to be no such for skipping.

There are two types of skipping gaits. The first type, **unilateral skipping**, is sometimes called galloping. It is an asymmetric gait in which one leg is always in front of the other (Fig. 2.10b). **Bilateral skipping**, on the other hand, is a symmetric gait in which each leg takes turns leading the skip. An idealization of a bilateral skipping gait is shown in Fig. 2.10a. Bilateral skipping is obtained when we replace the single stance phase of inverted pendulum walking with a flight phase. In the model here, half a period of bilateral skipping (assuming that the legs are distinguishable) is equal to one period of unilateral skipping. Otherwise the two idealizations are identical.

In Fig. 2.10, the distance covered over one period of unilateral skipping or half a period of bilateral skipping is denoted d_2 . The subscript “2” is to indicate that the event of leg contacting the ground happens twice during this distance. For

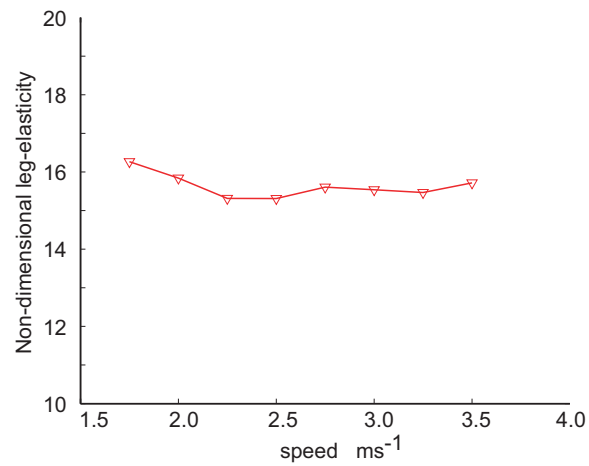


Figure 2.8: **Effective leg stiffness** Nondimensional spring constant obtained by fitting a spring mass model to speed, step length and duty factor data for real human running from Wright and Weyand (2001).

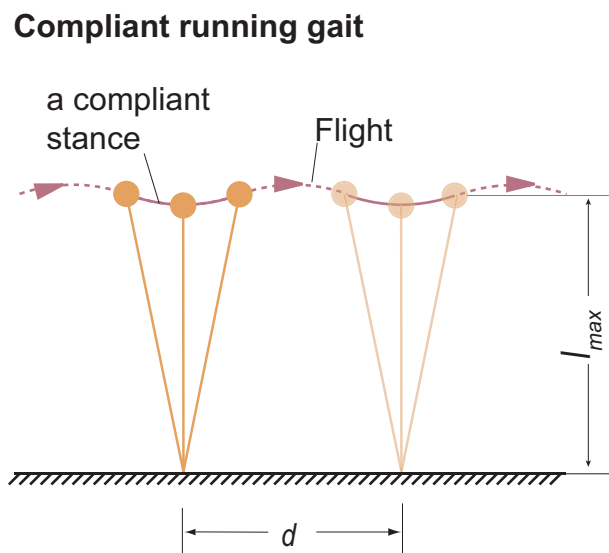


Figure 2.9: **Compliant run.** The minimal model can simulate the compliant running motions of a spring-mass model of running.

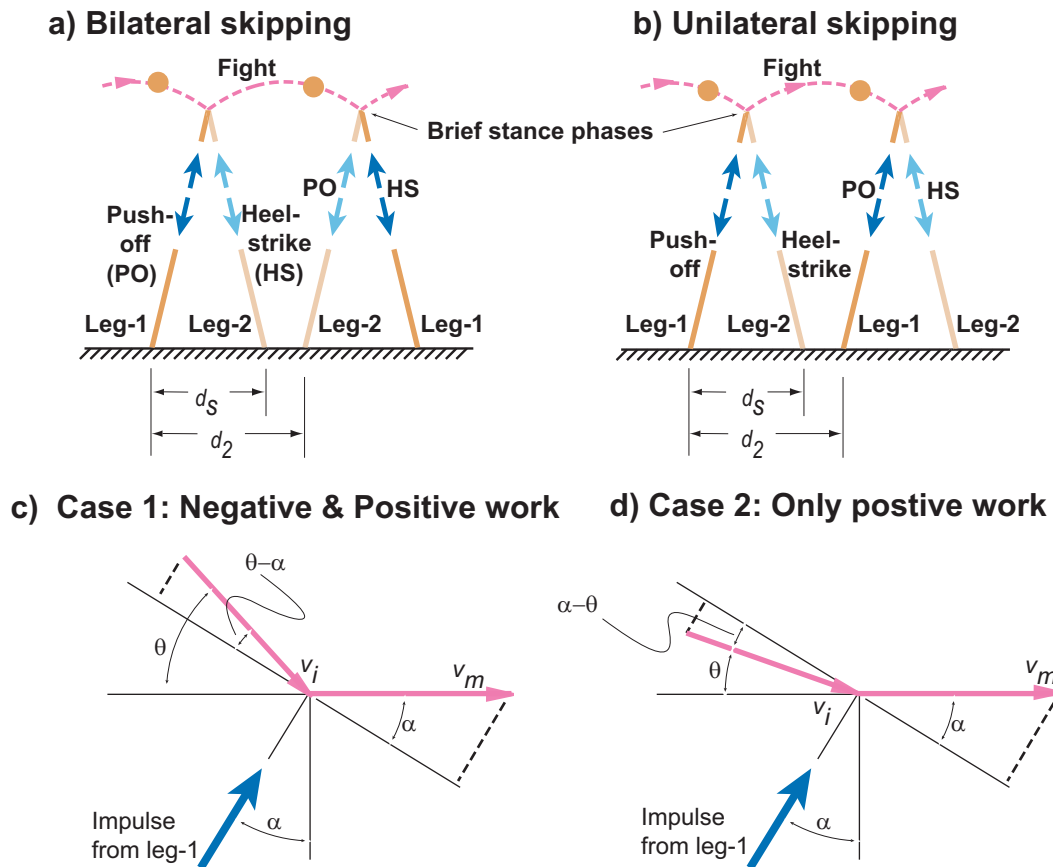


Figure 2.10: **Simple skipping gaits.** The body flies through the air in a parabolic free-flight at the end of which the legs land in sequence – the trailing leg first provides an impulse, then the leading leg provides an impulse. (a) In bilateral skipping, the legs interchange their roles every stride. (b) In unilateral skipping, the legs have asymmetric roles; one leg is always in front of the other. If the legs are identical and massless, the difference between unilateral and bilateral skipping vanishes. (c) and (d) show the effect of an impulse by leg-1, the trailing leg on the velocity of the center of mass. Case 1: (c), when $\alpha < \theta$, a mixture of positive and negative work is done by leg-1. Case 2: (d) when $\alpha \geq \theta$ only positive work is done by leg-1.

convenience, we shall call one period of unilateral skipping, a stride. The angle between the legs when they impact the ground in sequence is 2α . As in walking, the push-off is assumed to be complete before the heel of the other leg strikes the ground. The magnitude of the velocity just before the stance phase is v_I as in walking, and the angle the velocity vector makes with the x-axis is θ . Since the average horizontal speed is v , and in the idealization here, almost all the time is spent in flight, we have $v = v_I \cos \theta$ or $v_I = v / \cos \theta$.

The action of leg-1 and leg-2 are assumed anti-symmetric. That is, the amount of negative work performed by leg-1 is equal to the amount of positive work performed by leg-2 and vice versa. Just like in inverted pendulum walking. So it suffices to look at the energetics of leg-1 in detail. This is shown in Figs. 2.10c,d. Also, again by symmetry, the velocity is horizontal just after the impulse due to leg-1 and just before the impulse due to leg-2.

Ruina et al. (2005) briefly discuss the energetics of skipping in the limit of small step lengths (and therefore small angles θ and α). Here we generalize the small angle analysis to large angles.

Whether leg-1 performs both negative work and positive work, or performs only positive work, depends on the relation between the leg-angle α and the angle θ of incoming velocity at the end flight phase. We consider two cases.

Case 1. Steep incoming angle $\theta \geq \alpha$ Here, leg-1 first does negative work, and then does positive work (Figs. 2.10c). The component of the incoming velocity in the direction opposite to that of the leg is lost to negative work in this case:

$$W_{n/\text{leg}1} = \frac{m}{2} v_I^2 \sin^2 (\theta - \alpha) \quad (2.35)$$

We see that the velocity after the leg impulse has a positive component in the direction of the leg. This is due to the positive work performed by leg-1.

$$W_{p/\text{leg}1} = \frac{m v_m^2 \sin^2 \alpha}{2} \quad (2.36)$$

Since leg-2 does exactly the same as leg-1 but only in reverse, positive work done by leg-2 is equal to the negative work done by leg-1. This means that the total positive work over the stride is simply $W_{p/\text{stride}} = W_{n/\text{leg}-1} + W_{p/\text{leg}-1}$, which is also equal to the total negative work $W_{n/\text{stride}}$. This gives us the following expression for the metabolic cost:

$$E_{m/\text{stride:case1}} = \frac{1}{2} \cdot m(b_1 + b_2)(v_I^2 \sin^2 (\theta - \alpha) + v_m^2 \sin^2 \alpha) \quad (2.37)$$

Linear momentum balance in the direction perpendicular to the leg gives

$$v_m \cos \alpha = v_I \cos \theta - \alpha. \quad (2.38)$$

Using this relation and $v_I = v / \cos \theta$, we have:

$$E_{m/\text{stride:case1}} = \frac{(b_1 + b_2) m v^2}{2 \cos^2 \theta} (\sin^2 (\theta - \alpha) + \tan^2 \alpha \cos^2 (\theta - \alpha)) \quad (2.39)$$

Case 2: Shallow incoming angle $\theta \leq \alpha$ In this case, the incoming velocity has a non-negative component in the direction of leg-1 (Fig. 2.10d). This means that no negative work can be done. All work by leg-1 is positive and this is given by the change in the kinetic energy across the impulse by leg-1.

$$W_{p/\text{stride}} = \frac{m}{2}(v_m^2 \sin^2 \alpha - v_I^2 \sin^2 (\alpha - \theta)) \quad (2.40)$$

$$= \frac{mv^2}{2 \cos^2 \theta} (\tan^2 \alpha \cos^2 (\theta - \alpha) - \sin^2 (\theta - \alpha)) \quad (2.41)$$

This gives,

$$E_{m/\text{stride:case2}} = \frac{(b_1 + b_2)mv^2}{2 \cos^2 \theta} [\tan^2 \alpha \cos^2 (\theta - \alpha) - \sin^2 (\theta - \alpha)] \quad (2.42)$$

$$= \frac{(b_1 + b_2)mv^2}{2 \cos^2 \theta} R \quad (2.43)$$

$$\text{where, } R = \tan^2 \alpha \cos^2 (\theta - \alpha) - \sin^2 (\theta - \alpha) \quad (2.44)$$

Cost of transport for skipping. Consider Eq. 2.39. Making the small angle approximation that $\theta \ll 1$ and $\alpha \ll 1$,

$$E_{m/\text{stride:case1}} \approx \frac{(b_1 + b_2)mv^2}{2} \cdot ((\theta - \alpha)^2 + \alpha^2) \quad (2.45)$$

$$E_{m/\text{stride:case2}} \approx \frac{(b_1 + b_2)mv^2}{2} \cdot (\alpha^2 - (\theta - \alpha)^2) \quad (2.46)$$

For fixed values of v , θ , m , etc., the small-angle expression for $E_{m/\text{stride:case1}}$ above is minimized with $\alpha = \theta/2$. The minimum value is $(b_1 + b_2)mv^2\theta^2/4$. On the other hand, the small angle expression for $E_{m/\text{stride:case2}}$ increases with α and is minimized at $\alpha = \theta$ with value of $(b_1 + b_2)mv^2\theta^2/2$. The minimum value for case 1 ($\alpha \leq \theta$) is smaller than the minimum value over case 2 ($\alpha \geq \theta$) for small angles.

From Eqs. 2.35 and 2.36, we see that when $\alpha = \theta/2$ each leg performs an equal amounts of negative work and positive work. That is, each leg acts in a ‘‘pseudo-elastic’’ manner. Note that $\tan \theta = d_2 g / (2v^2)$, which for small angles reduces to $\theta \approx g d_2 / (2v^2)$. Substituting this expression for θ and $\alpha = \theta/2$ in Eq. 2.45, we get a simpler expression for the cost applicable to locomotion restricted to shallow angles.

$$E_{m/\text{period}} = (b_1 + b_2)mv^2 \left(\frac{\theta}{2}\right)^2 \quad (2.47)$$

$$= \frac{(b_1 + b_2)mv^2}{4} \left(\frac{g d_2}{2v^2}\right)^2 \quad (2.48)$$

$$= \frac{(b_1 + b_2)mv^2 g^2 d_2^2}{16} \quad (2.49)$$

The corresponding cost of transport is given by:

$$c_t = \frac{(b_1 + b_2)D_2}{16V^2} \quad (2.50)$$

where $D_2 = d_2/l_{max}$ and $V = v/\sqrt{gl_{max}}$ are the nondimensional versions of d_2 and v . This small angle approximation is also obtained in Ruina et al. (2005).

Comparing skipping with impulsive running. We now compare the cost of idealized skipping, derived above, with the cost of impulsive running. One stride of unilateral skipping has two footfalls. We can roughly match the leg-swing costs of the compared gaits by ensuring that the number of footfalls per unit time is the same for both gaits. Therefore, we compare one stride of unilateral skipping with two steps (therefore two footfalls) of impulsive running — that is, the step-length d for the compared running gait is chosen to be $d_2/2$.

We find that the small angle expression for the energetic cost of skipping (Eq. 2.50) is exactly the same as the cost of covering the distance D_2 by impulsive running (Eq. 2.34) with two equally spaced vertical impulses.

More detailed calculations show that for large angles, the costs of impulsive running with two impulses and skipping are not identical. Is skipping better or worse than impulsive running? To make this comparison for a given v and d_2 , we use numerical optimization on the large angle expressions for the skipping cost (Eqs. 2.39, 2.42) to determine the α that gives the least skipping cost. For the small angle approximation above, the optimal α was equal to $\theta/2$. More generally, for large angles, we find that the optimal α is not equal to $\theta/2$ but less than $\theta/2$, approaching $\theta/2$ asymptotically with small θ . Using this optimal skipping cost, we find that impulsive running with two equally spaced impulses is always slightly better than skipping. Thus it seems like, while the cost of skipping asymptotically approaches that of running for small step-lengths and high velocities, impulsive running is still cheaper than skipping in general in this model.

2.6 Comparing the cost of various gaits

Now that we have estimates of the metabolic costs of a few salient gaits, we can compare these to determine which gait the animal should choose at a given speed and step-length. We have already noted above that skipping is always more expensive than impulsive running, for given speed and given distance over which two footfalls are allowed. So skipping need not be included in the comparison. Among the two level walking gaits, the one with constant horizontal speed is always more expensive than the one with non-constant horizontal speed and no double stance. So only the latter level-walking gait needs to be considered for gait choice.

For simplicity, we ignore compliant spring-mass running and compare the costs of inverted pendulum walking, level walking with no double stance, and impulsive running for a range of speeds and step-lengths. The results of the comparison are

shown in Fig. 2.11. We find that inverted pendulum walking is best at low speeds, impulsive running is better at high speeds. Level walking (with no double support) is better than inverted pendulum walking and impulsive running in a region that starts out as a small sliver at $V = 1$ and grows at larger step-lengths. Alexander (1976) presents similar results.

Fig. 3.4a shows the cost of the three gaits for two step-lengths $D = 0.5$ and $D = 1.00$. We see that for low V , inverted pendulum walking is least expensive. At high V , impulsive running seems least expensive. Level walking with no double support seems least expensive for a small range of speeds – near $V = 1$ for $D = 0.5$ and between $V = 0.8$ and $V = 0.9$ for $D = 1.00$.

The energetic trade-offs between inverted pendulum walking and impulsive running is easily understood for small step lengths. At small step-lengths, the cost of transport for walking is $c_{walking} = DV^2/8$ and the cost of transport for running is $c_{running} = D/(8V^2)$. This implies that at $V = 1$ and small D , $c_{walking} = c_{running}$.

This energetic trade-off between inverted pendulum walking and impulsive running can be understood with following geometric argument. Both walking and running have essentially work-free motions interrupted collisional work. The work-cost of these gaits at a given speed are determined by the collision angle (Ruina et al., 2005). The energetic trade-off between inverted-pendulum walking and impulsive running can be understood as a minimization of collision angles for a specific step length D . At low speeds, the circular arc of walking has shallower collisions than the parabolic free-flight of running and at high speeds, the situation is reversed (Fig. 3.4).

We omitted pseudo-elastic running from the above comparison. When we compared the costs of inverted pendulum walking, impulsive running and pseudo-elastic running (but omitted level walking), we obtained a picture quite similar to Fig. 2.11 with level walking more-or-less replaced by pseudo-elastic running. That is compliant pseudo-elastic running is better than impulsive running for some values of V and D . For instance, we see in Fig. 2.7 that for the particular speeds and step-lengths used by humans, an impulsive run requires more work than the pseudo-elastic spring-mass running. In brief, the next chapter shows that impulsive running requires the least work for some range of speeds and step-lengths. But the human running data used here (Wright and Weyand, 2001) does not fall in the speed-step length region where impulsive running is optimal for this model.

2.7 Conclusions

In this chapter, we presented a simple model of a general bipedal animal that is capable of a wide variety of gaits. We found that particular abstractions of various bipedal gaits discussed in the literature are special cases of this simple model. We used the simple model to estimate the energetic costs of a few idealized gaits, compared these costs, and found that among these few gaits considered walking seems best at low speeds, and impulsive running at high speeds and level walking at

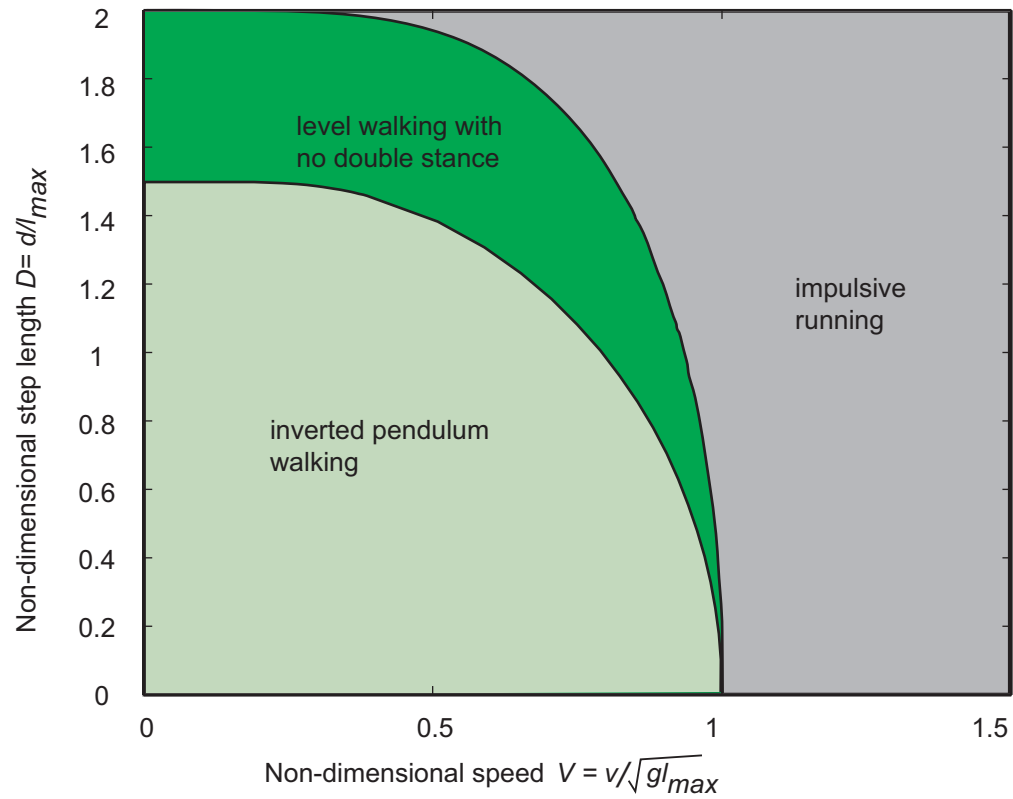


Figure 2.11: **Comparing costs.** The regions where each of the 3 gaits (inverted pendulum walking, impulsive running and level walking with no double support) have the lower cost in a three-way comparison are shown. Interestingly, the boundary that separates level walking and inverted pendulum walking here is identical to the boundary of infeasibility of inverted pendulum walking in Figure 2.3

a narrow range of intermediate speeds and step-lengths. This result is generalized in the next two chapters, where we show that inverted pendulum walking and impulsive running are optimal (in terms of the work-based metabolic cost model here) respectively at low and high speeds, even when compared against many other strange gaits of the simple biped model.

Chapter 3

Computer optimization of a minimal biped model discovers walking and running

The first part of this chapter is word-for-word the text of Srinivasan and Ruina (2006), except where noted as footnotes. Five minor typographical errors in the published version have been corrected in this version, as also a small error in Figure 3.3. Also, since Srinivasan and Ruina (2006) was a short paper, it could give only a cursory treatment of some of the more technical details. These details are provided in the second half of this chapter, starting from Sec. 3.2 titled “Further comments”.

Although people’s legs are capable of a broad range of muscle-use and gait patterns, they generally prefer just two. They walk, swinging their body over a relatively straight leg with each step, or run, bouncing up off a bent leg between aerial phases. Walking feels easiest when going slowly, and running feels easiest when going faster. More unusual gaits seem more tiring. Perhaps this is because walking and running use the least energy (Borelli, 1680; Margaria, 1976; Hoyt and Taylor, 1981; Alexander, 1980, 1989, 1992; Minetti and Alexander, 1997). Addressing this classic (Borelli, 1680) conjecture with experiments (Margaria, 1976; Hoyt and Taylor, 1981) requires comparing walking and running with many other strange and unpracticed gaits. As an alternative, a basic understanding of gait choice might be obtained by calculating energy cost by using mechanics-based models. Here we use a minimal model that can describe walking and running as well as an infinite variety of other gaits. We use computer optimization to find which gaits are indeed energetically optimal for this model. At low speeds the optimization discovers the classic inverted-pendulum walk (Alexander, 1976; Cavagna et al., 1977; Alexander, 2003; Kuo, 2002; Ruina et al., 2005; Kuo et al., 2005), at high speeds it discovers a bouncing run (Ruina et al., 2005; Rashevsky, 1944)¹, even without springs, and at intermediate speeds it finds a new pendular-running gait that includes walking and running as extreme cases.

One way of characterizing gaits is by the motions of the body (Fig. 3.1a). In these terms, walking seems well caricatured (Kuo et al., 2005) (Fig. 3.1b) by the hip joint going from one circular arc to the next with push-off and heel-strike impulses in between. Similarly, running could be caricatured by a sequence of parabolic free-flight arcs (Fig. 3.1c), with impulses from the ground at each bounce (Rashevsky, 1944; Alexander, 1988; McMahon and Cheng, 1990).

Why do people not walk or even run with a smooth level gait (Alexander, 1976), like a waiter holding two cups brim-full of boiling coffee? Why do people select walking and running from the other possibilities? We address such questions

¹The published version incorrectly referred to Ruina et al. (2005); Kuo et al. (2005)

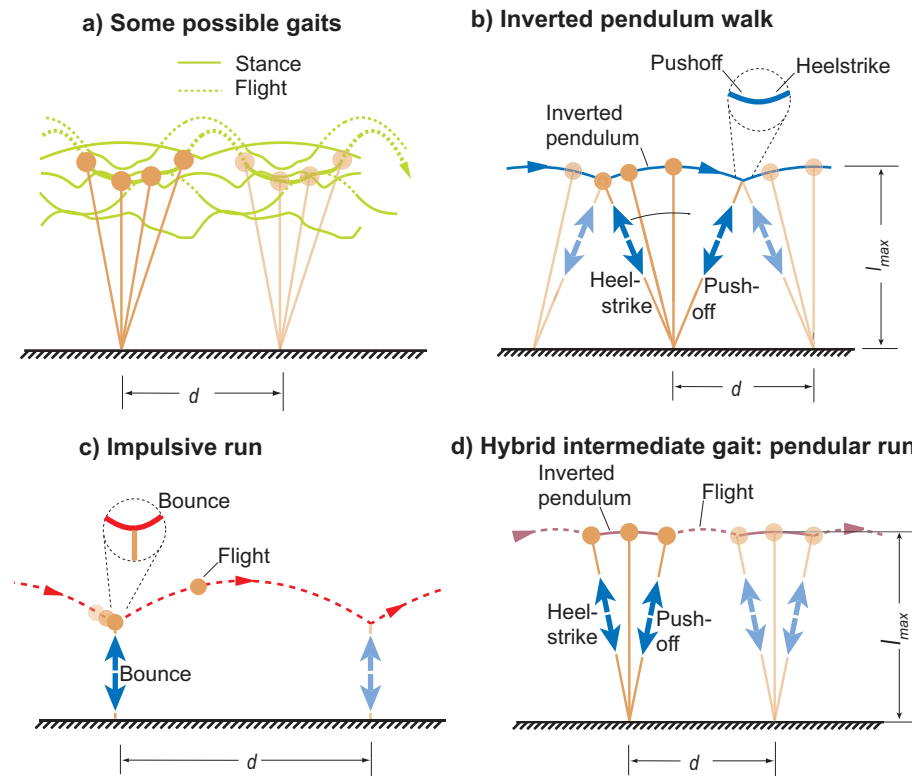


Figure 3.1: **Body motion in human gaits.** (a) Trajectories of the center of mass for a few possible gaits. Solid lines, stance; dotted lines, flight. (b), Trajectory for inverted-pendulum walking. (c) Trajectory for impulsive running. (d) Trajectory for a new gait: pendular running. At least one of the gaits (b), (c) and (d) turns out to use less work than any other candidates (for example, from (a) according to the calculations here).

by modelling a person as a machine describable with the equations of newtonian mechanics. The basic approximations are: first, that humans have compact bodies and light legs; second, that gait choice is based on energy optimization (Borelli, 1680; Alexander, 1980); and third, that energy cost is proportional to muscle work (Margaria, 1976; Alexander, 1980, 1976). We use a simplification of previous models (Alexander, 1980, 1992; Minetti and Alexander, 1997), perhaps the simplest mechanical model that is capable of exhibiting a broad range of gaits that includes walking and running. Although the model is a mechanical abstraction that is not physically realizable, it is subject to the laws of physics. Because of its simplicity, the model is amenable to interpretation. It can also be studied with exhaustive and accurate simulation experiments, far beyond what is possible with human subjects.

We wish to find how a person can get from one place to another with the least muscle work W (Methods). We treat the body as a point mass m at position (x, y) at time t (Fig. 3.2a). The legs are massless and therefore, when not in ground contact, they can be oriented, lengthened and shortened with no energy cost. The fluctuations of the leg length $l(t)$ due to flexion of the hip, knee and ankle are incorporated in a single telescoping axial actuator (Alexander, 1980) that carries a compressive time-varying force $F = F(t)$. For simplicity, we seek an explanation of gait choice with no essential dependence on elastic energy storage; we assume no springs (tendons) in series or parallel with the actuators.

We assume that during the stance phase, when a foot is in contact with the rigid level ground, that it does not slip. At most one foot can be in contact with the ground at a time. During stance, both gravity mg and F act on the body (Fig. 3.2a). During the flight phase, when neither leg touches the ground, gravity is the only force. We seek periodic motions, in which each step is like the previous step. The left and right legs have identical force and length profiles. A single step consists of one stance phase (possibly short, as in high-speed running) and one flight phase (possibly of zero duration, as in walking).

A gait is characterized by the position and velocity of the body at the start of a stance phase relative to the stance foot, by the step period, and by $F(t)$. Given these, we can integrate the newtonian equations of motion forwards in time to find the body trajectory and leg length as functions of time (including the maximum leg length l_{max}). At the end of the step, we assume that the next foot is placed on the ground at the same position relative to the body as at the start. We can thus calculate the step length d , the average forward speed v , and the work done by the leg per unit weight and distance $C = W/(mgd)$. For random $F(t)$, the final body height and velocity generally do not match the starting conditions and therefore do not generate a periodic gait. Nonetheless, by appropriately varying $F(t)$ we can find infinitely many periodic gaits (Fig. 3.1a) with all manner of complicated trajectories (Methods). Of those periodic gaits, we wish to find those that minimize the cost C .

The optimal solutions have cost arbitrarily close to zero unless the optimization is further constrained. The cost can be made arbitrarily small by growing the leg length (and the locomotion becomes akin to the rolling of a giant multi-spoked

wheel), so we set the maximum length to be l_{max} , representing the leg length. Because we have no leg-swing cost, C can be reduced to zero by taking very small steps (Alexander, 1992; Ruina et al., 2005; Kuo, 2001) so we optimize for various fixed values of step length d . Finally, C has a non-anthropomorphic lower bound (corresponding to standing on one leg for an infinite time mid-step), approached as the average speed v goes to zero, so we constrain v .

After nondimensionalizing using m , g and l_{max} , no free parameters remain. We seek solutions as two conditions are varied: the dimensionless average speed² $V = v/\sqrt{gl_{max}}$ (V^2 is the so-called Froude number) and the dimensionless step length $D = d/l_{max}$. For given values of V and D , the optimal periodic gait is determined with numerical optimal control methods that are more or less standard (Methods).

All optimizations converged toward one of three stereotypical collisional gaits, depending on V and D , but never to a smooth collisionless gait. First, at low V , the classic inverted-pendulum walking gait (Figs. 3.1b and 3.2b) is optimal. Second, at high V , an impulsive running gait is optimal (Figs 3.1c and 3.2c). Third, at intermediate V , a new gait, pendular running (Figs. 3.1d and 3.2d), is optimal. Pendular running has a flight phase between extended inverted-pendulum stance phases. Pendular running is a generalization of, and a connection between, walking and running: with no flight phase it is inverted-pendulum walking; with an infinitesimal pendular phase it is impulsive running.

The numerical optimization, unbiased by an expectation of what the optimal gaits might be, has thus discovered the classic gaits that caricature walking and running. The new third gait might be the model's way of running with a non-zero stance phase, given the model's lack of tendons. A tentative prediction would be the existence of a ground force versus time curve with two humps during the stance phase for, perhaps, weak or obese people running slowly. The respective regions of optimality of the three gaits are shown in Fig. 3.3.

Alexander (Alexander, 1976, 2003) argued that inverted-pendulum walking is limited to those speeds at which the centripetal acceleration of a body pivoting over a straight leg is less than gravity, ensuring that the body does not vault off the ground. However, walking becomes energetically non-optimal at speeds lower than the above limit (Alexander, 1976, 2003) (Fig. 3.3³). Indeed, people switch from a walk to run (Thorstensson and Robertson., 1987; Minetti et al., 1994) at about $V=0.65$ and $D=0.95$, close to the boundary at which walking ceases to be optimal (Fig. 3.3) in this model.

The numerical optimization results are buttressed by heuristic considerations. The cost C is an integral of the leg power (Methods). There are two ways of setting this power to zero: setting $\dot{l} = 0$ (corresponding to inverted-pendulum

²The published version had $V = v/\sqrt{gl_{max}}$, a typo.

³In Fig. 3.3 of the published version, the y-intercept of the dashed line was at about 1.7. The y-intercept should be at about 1.5 as shown in Fig. 3.3 in this corrected version.

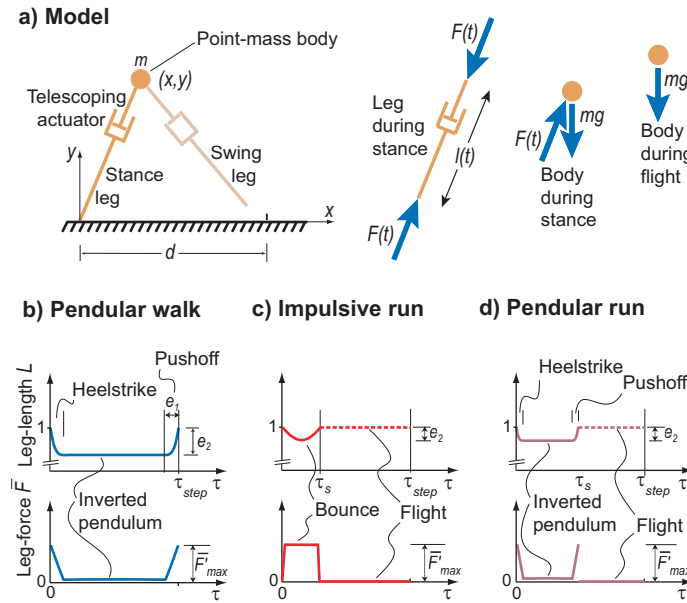


Figure 3.2: **Point-mass biped model and its optimal solutions.** (a) The configuration shown is part way through the stance phase. The next stance leg is oriented to prepare for a new contact at a distance d from the last. (b-d) Dimensionless force and length shown as functions of dimensionless time, for the three optimal gaits, (b) pendular walk; (c) impulsive run; (d) pendular run), before full convergence of the numerical optimization. The finite forces in the figures are approximations to the converged impulsive (collisional) forces. In the extrapolated optimum, as the grid size $h \rightarrow 0$ and the allowed force upper bound F_{max} , the optimizations find that $e_1, e_2 \rightarrow 0$ and that the maximum forces used go to infinity (Methods). In these limits the walking gait (b) is an inverted pendulum with heelstrike and push-off impulses, the running gait (c) is an impulsive bounce between free flights, and the pendular run (d) has constant-length pendulum phases and flight phases separated by impulses.

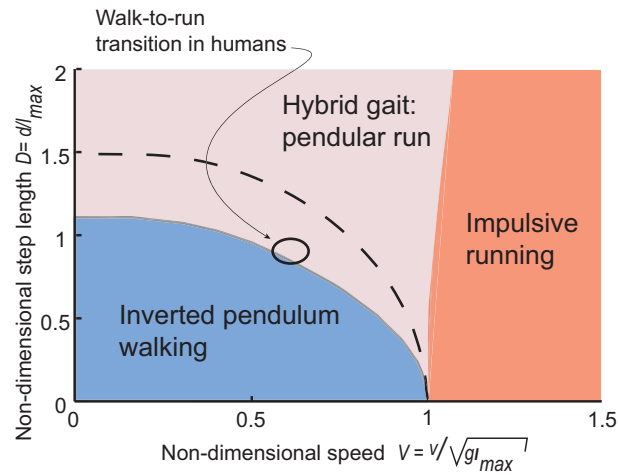


Figure 3.3: The regions in which each of the three collisional gaits are optimal. Inverted-pendulum walking ceases to be locally optimal at the pendular-run interface. The oval indicates the approximate speed and step length range at which humans switch from walking to running (Thorstensson and Robertson., 1987; Minetti et al., 1994). The dashed line indicates where compression-only inverted-pendulum walking becomes mechanically infeasible (typically approximated Alexander, 1976, as $V = 1$, which is correct for small D). At the right part of the intermediate region, the pendular run is almost impulsive running; at the left edge, it is almost inverted-pendulum walking.

motion) or setting $F = 0$ (corresponding to free flight). Thus, the flight phase ($F = 0$) of running is an energy-saving analogue of the pendular ($\dot{l} = 0$) motion of walking; both phases involve no work. All the work is crowded into brief impulses at appropriate times.

Inverted-pendulum walking, pendular running and impulsive running all have work-free motions, punctuated by impulses (collisions). The costs of these collisional gaits can be calculated directly (Alexander, 2003; Kuo, 2002; Ruina et al., 2005). For inverted-pendulum walking, positive work performed during push-off is evaluated as the difference in kinetic energy just before and after the push-off (Alexander, 1976, 2002a; Ruina et al., 2005). $C_{walking} = DV_I^2/(8 - 2D^2)$, where V_I is the magnitude of the velocity vector just before push-off. For impulsive running, cost is equal to the vertical kinetic energy that is lost and regained in every bounce (Ruina et al., 2005; Kuo et al., 2005) ($C_{running} = D/8V^2$). For a given V and small values of D , the cost for the collisional gaits is proportional (Ruina et al., 2005) to the square of the kink-angle in the trajectory (Fig. 3.4c). The energetic trade-off between inverted-pendulum walking and impulsive running (Fig. 3.4a, b) can be understood as a minimization of collision angles (Ruina et al., 2005) for a specific step length D . At low speeds the circular arc of walking has shallower collisions than the parabolic free-flight of running, and at high speeds the situation is reversed (Fig. 3.4c).

The optimizations here show that smooth collisionless gaits require more work than the optimal collisional gaits. For example, consider a flat walk (Alexander, 1976, 2003), in which the body moves at constant height. This gait has (Alexander, 1976, 2003) $C_{flat} = D/8\sqrt{1 - D^2}$. Figure 3.4a, b shows that the exceptionally smooth, flat walk is never optimal (Methods). Recent human experiments (Ortega and Farley, 2005; Gordon et al., 2003) also show that a flat walk uses more energy than normal walking.

As has been found for a gait model that assumes collisions *a priori* (Ruina et al., 2005), the more general model here shows that it is advantageous to simulate elasticity during running, even with no genuine elasticity (tendons). Indeed, real human legs do approximately simulate an elastic spring during running (McMahon and Cheng, 1990; Blickhan and Full, 1993). More generally, the model here, as well as simpler models (Alexander, 1980, 1976; Ruina et al., 2005), indicates that the energetic utility of running probably does not depend on genuine elasticity in the legs. However, such elasticity, neglected here, would further decrease the cost of running (Alexander, 1980, 1992; Cavagna et al., 1977), supporting the idea (Bramble and Lieberman, 2004) that human ancestors could have started to run before the modern human long Achilles tendon was fully evolved.

To maximize simplicity of calculation and interpretation, we have neglected various crucial features including a cost for leg-swing (Ruina et al., 2005; Kuo, 2001; Marsh et al., 2004), a more realistic model of muscle cost (Minetti and Alexander, 1997; Anderson and Pandy, 2001a), allowance of a non-infinitesimal double-stance phase (Alexander, 1980, 1992, 1997), elastic and dissipative elements in series with the actuator (Alexander, 1980, 1992; Minetti and Alexander, 1997;

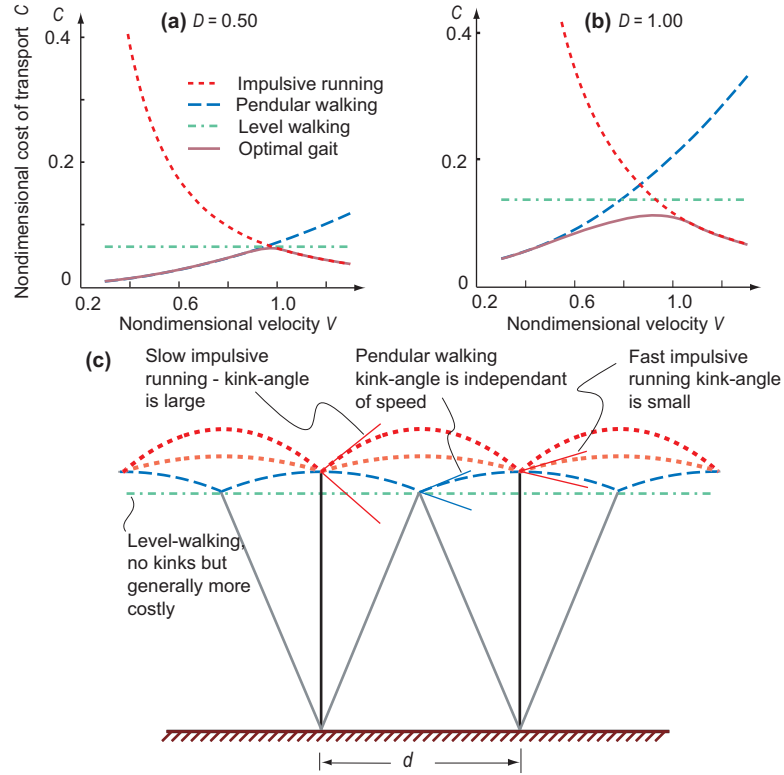


Figure 3.4: **Cost of transport versus speed.** (a) For small D ($= 0.50$), all periodic gaits (that do not involve leg tension) have nearly equal costs near $V = 1$. Inverted-pendulum walking is optimal at low speeds, pendular running at a narrow range of intermediate speeds, impulsive running at high speeds, and flat walking is never optimal. b, However, for large D ($= 1.00$) and for $V \approx 0.8 - 0.9$, flat walking, perhaps like a ‘Groucho walk’ (Bertram et al., 2002), although not optimal, has lower cost than both inverted-pendulum walking and impulsive running. The colors used in (a) and (b) indicate the following gaits: red, impulsive running; blue, pendular walking, green, level walking; purple, optimal gait. (c) Body trajectories for a pendular walking gait (blue; kink angle is independent of speed), a low-speed impulsive running gait (red; kink angle is large), a high-speed impulsive running gait (orange; kink angle is small) and level walking (green; no kinks, but generally more costly), all with the same step length.

Bramble and Lieberman, 2004), the possibility of higher-period gaits (for example skipping (Minetti, 1998)), an extended foot instead of a point foot (Anderson and Pandy, 2001a), and other anatomical realism (Anderson and Pandy, 2001a).

The simplest way of including a leg-swing cost would be to assume that it is a function of frequency and amplitude which is independent of gait. The leg-swing cost is then a function of V and D , has no effect on which gait uses less energy at a given V and D , and therefore has no effect on which gait is optimal at that V and D . Figure 3.3 would be exactly unchanged. The simplest way of incorporating elastic recovery is to assume that a fixed fraction of the leg work is from elastic energy storage and hence should have no cost in the optimization. This would scale the costs of all gaits by the same constant (less than 1) and would therefore have no effect on any of the relative costs of various gaits. Thus, leg-swing and elastic-recovery effects can affect gait choice only through more complex dependencies.

We do not know which neglected effects are the most important for explaining the deviations of observed human behavior from the model predictions here, particularly the prediction of the pendular-running gait, which seems little used by humans. Nonetheless, this model, having no free parameters, might most simply explain why we choose walking and running over the plethora of other possible gaits.

3.1 Methods

3.1.1 Formulation

The governing equations are

$$m\ddot{x} = F(x - x_c)/l, \quad m\ddot{y} = -mg + Fy/l \quad (3.1)$$

for stance with duration t_s , and

$$\ddot{x} = 0, \quad \ddot{y} = -g \quad (3.2)$$

for flight with duration t_f , where $l = \sqrt{(x - x_c)^2 + y^2}$. Time $t = 0$ is the beginning of a stance phase with foot-contact point $x_c = 0$. The initial conditions are $x(0) = x_0, y(0) = y_0, \dot{x} = \dot{x}_0$ and $\dot{y} = \dot{y}_0$. At $t = t_f + t_s$, periodicity requires that $x_f = x_0 + d, y_f = y_0, \dot{x}_f = \dot{x}_0$ and $\dot{y}_f = \dot{y}_0$. The numerical integration then determines v, d, l_{max} and C . For given l_{max}, d and v , we seek the control strategy $(x_0, \dot{x}_0, y_0, \dot{y}_0, F(t), t_s)$ that minimizes the work-based specific mechanical cost of transport

$$C = \int_0^{t_{step}} \frac{[F(t)l]^+}{mgd} dt \quad (3.3)$$

where $[\]^+$ is non-zero only for positive values ($[p]^+ = p$ if $P = 0$ and $[p]^+ = 0$ if $p < 0$). The only cost is for mechanical work ($dW = Fdl$).

3.1.2 Numerical solution of the optimal control problem

We nondimensionalize all quantities by l_{max} , M and g . We seek

$$(X_0, \dot{X}_0, Y_0, \dot{Y}_0, \bar{F}(\tau), \tau_s) = \\ (x_0/l_{max}, \dot{x}_0/\sqrt{gl_{max}}, y_0/l_{max}, \\ \dot{y}_0/\sqrt{gl_{max}}, F(t)/mg, t_s\sqrt{gl_{max}})$$

where τ is the non-dimensional time, that produce the optimal periodic gait with given V and D , and with the non-dimensional step-length satisfying $0 \leq L(\tau) \leq 1$.

The infinite-dimensional search space for this optimization problem contains the set of all possible functions $\bar{F}(\tau)$. We restrict our search to the set of piecewise linear functions, defined on an evenly spaced time-grid ($0 = \tau_0, \tau_1, \tau_2, \dots, \tau_N = \tau_s$), with grid spacing⁴ $\tau_i - \tau_{i-1} = h = \tau_s/N$. So the search space becomes $z = (X_0, \dot{X}_0, Y_0, \dot{Y}_0, \bar{F}_{i=0\dots N}, \tau_s)$, where⁵ $\bar{F}_i = \bar{F}(\tau_i)$. The linear constraints are $\epsilon \leq \tau_s \leq \tau_{step}$, $\bar{F}_{min} \leq \bar{F}_i \leq \bar{F}_{max}$. We need $\epsilon > 0$ because a periodic step requires a stance phase. In addition, although the forces are allowed to be unbounded conceptually, for numerical optimization they need to be bounded: we choose a bound $\bar{F}_{max} \gg 1$ and $\bar{F}_{min} = 0$. Ultimately \bar{F}_{max} is allowed to grow arbitrarily, so that it is not a parameter in the solutions we present. Interestingly, choosing $\bar{F}_{min} < 0$, allowing tensional leg-forces, does not affect the optima. The leg-length constraint, $0 \leq L(\tau) \leq 1$, is enforced at the grid points $\tau = \tau_i$. Gait periodicity is another nonlinear constraint.

For given z , C and the constraint violations are evaluated by integration of the differential equations. $C(z)$ is to be minimized subject to the various linear and nonlinear equality and inequality constraints: $g_{eq}(z) = 0$ and $g_{ineq}(z) \leq 0$. We smooth $C(z)$ with h as a smoothing parameter. We used a particularly robust implementation of Sequential Quadratic Programming SQP (Gill et al., 2002) for the optimization.

Convergence to the idealized collisional gaits is discovered by letting $N \rightarrow$ large, $\bar{F}_{max} \rightarrow$ large and $\epsilon \rightarrow$ small. At high V , if \bar{F}_{max} is set large enough for a given ϵ , \bar{F}_{max} has no effect on C . The optimization then always finds $\tau_s = \epsilon$ as $\epsilon \rightarrow 0$, thus converging to impulsive running. We assure ourselves of the convergence to the collisional walking by Richardson extrapolation. That is, we solve the problem for grids of sizes $N = N_1, N_2, N_3, \dots$ assuming that the cost is a smooth function of N^{-1} , and extrapolating the cost to $N^{-1} \rightarrow 0$. \bar{F}_{max} is maintained high enough and ϵ low enough to be unused constraints. The ODE solutions are accurate to about 10^{-14} over a grid interval (obtained by integrating from grid-point to grid-point with an adaptive RK-45 method, benchmarked by a Taylor-series method) and accurate to less than $10^{-14}N$ over the whole step. We thus avoid significant sources of error not related to the finiteness of N and can therefore treat the convergence as dependent only on N . The convergence is observed to be linear in N^{-1} . The

⁴The published version had $\tau_i - t_{i-1} = h = \tau_s/N$, a typo

⁵The published version had $\bar{F}_i(\tau) = \bar{F}(\tau_i)$, a typo.

linearly extrapolated limit of the sequence of C values is found to differ from the cost of the corresponding analytically determined inverted-pendulum collisional walking gait by a relative error of about 10^{-3} .

For each V and D , multiple optimization runs, each started with a different initial seed, all converged towards the same control strategy, indicating the likely uniqueness and globality of each collisional minimum. To determine the regions in which each gait is optimal more precisely (Fig. 3.3) we repeated the optimization over the space of (analytically calculable) collisional gaits.

Pontryagin’s maximum principle Pontryagin’s maximum principle (Bryson and Ho, 1975) can be used over the stance phase, neglecting the leg-length constraint, to get necessary conditions on the optimal solutions. This calculation shows that during stance, if the optimal control is not singular, the leg-forces must be maximum (F_{max} , apparently corresponding to heel-strike or push-off), or zero (stance simulating flight by having no force). This much agrees with our full optimizations and heuristics. The pendular stance portions we found, with $\dot{l} = 0$, seem to be singular arcs of the optimal control.

Note: *The verbatim text of Srinivasan and Ruina (2006) ends here.*

3.2 Further comments about Srinivasan and Ruina (2006)

3.2.1 A consequence of periodicity on the objective function

In Chapter 1, we presented a simple model of the energetic cost for muscle (Eq. 1.1). In essence, this simple model posits that the energetic cost of muscle use is proportional to a linear combination of the positive and negative work performed by the muscle. That is :

$$\text{Cost} = b_1 |\text{positive muscle work}| + b_2 |\text{negative muscle work}|$$

Since our minimal biped model has no external dissipation:

$$\text{Change in energy} = \text{positive work} - |\text{negative work}|$$

In particular, over a full period of a the minimal biped, there is no change in energy, which means that:

$$\text{positive work} = |\text{negative work}|$$

This means that:

$$\begin{aligned} & b_1 |\text{positive muscle work}| + b_2 |\text{negative muscle work}| \\ & = (b_1 + b_2) (\text{positive muscle work}) \end{aligned}$$

for a full period of the minimal biped. In other words, minimizing (any multiple of) the total positive work is exactly equivalent (here) to minimizing some linear combination of the positive and the negative work. All such minimizations will give exactly the same optimal solution, independent of the values of b_1 and b_2 . Of course, the optimal value of the objective function will depend on the particular values of b_1 and b_2 .

3.2.2 Description of the optimal control problem

Here, we provide a mathematically precise description of the optimal control problem described in the first part of this chapter. Note that each optimal control problem is defined for a given value of the nondimensional step-length D and the nondimensional step-period τ_{step} , and hence the nondimensional average speed V . In the following, the derivative of a quantity, say x , with respect to the nondimensional time τ is denoted by x' : that is, $x' = \frac{dx}{d\tau}$.

The goal is to determine the nondimensionalized initial conditions (X_0, X'_0, Y_0, Y'_0) , the nondimensionalized leg-force $\bar{F}(\tau)$, and the nondimensionalized duration of the stance phase τ_s , such that C , defined as follows, is minimized.

$$C = \frac{1}{2D} \int_0^{\tau_s} \left| \bar{F}(\tau) \frac{XX' + YY'}{\sqrt{X^2 + Y^2}} \right| d\tau \quad (3.4)$$

The expression for C in Eq. 3.3 is different from that in the above equation Eq. 3.4. We have replaced the $\int [P]^+$ in Eq. 3.3 by $\int |P|/2$ in the above equation. This replacement is equivalent to $b_1 = b_2 = 0.5$ in the discussion of the previous section – and as such does not make any difference to the optimal solutions obtained, as noted in the previous section.

Given the initial conditions, $X(0) = X_0$, $Y(0) = Y_0$, $X'(0) = X'_0$, $Y'(0) = Y'_0$, the state $(X(\tau), X'(\tau), Y(\tau), Y'(\tau))$ over the complete duration of a step, that is, $0 \leq \tau \leq \tau_{step}$, can be determined by integrating the following piecewise-defined dynamical system:

When $0 \leq \tau \leq \tau_s$,

$$X'' = \frac{\bar{F}(\tau)X}{\sqrt{X^2 + Y^2}} \quad (3.5)$$

$$Y'' = -1 + \frac{\bar{F}(\tau)Y}{\sqrt{X^2 + Y^2}} \quad (3.6)$$

When $\tau_s < \tau \leq \tau_{step}$,

$$X'' = 0 \quad (3.7)$$

$$Y'' = -1 \quad (3.8)$$

Finally, there is the (periodicity) constraint on the state at the end of a step $\tau = \tau_{step}$,

$$X(\tau_{step}) = X_0 + D, \quad Y(\tau_{step}) = Y_0, \quad X'(\tau_{step}) = X'_0, \quad Y'(\tau_{step}) = Y'_0 \quad (3.9)$$

We note here that the integrand, being the absolute value of the leg-power P is not a continuously differentiable function of P at $P = 0$ and therefore not a continuously differentiable function of whatever parameters P depends upon (typically). This non-smoothness of the integrand creates a similar non-smoothness in the integral — the objective function. We show numerical evidence for such non-smoothness in the objective function in a later section (Section 3.2.6). Non-smoothness of the objective function rules out the use of many powerful numerical optimization techniques that assume a certain degree of smoothness of the objective function. Since we wish to use these numerical techniques, we resort to two tricks that result in “smooth” optimization problems.

3.2.3 Trick-1: Smoothing the non-smooth integrand

The source of non-smoothness in the problem formulation above is that $|P|$ is a non-smooth function of P . Therefore, we can remove the non-smoothness by replacing the non-smooth $|P|$ by a smooth function $f(P, \epsilon)$, such that $|P| \approx f(P, \epsilon)$ for $\epsilon \ll 1$. Instead of minimizing C , we minimize C_ϵ :

$$C_\epsilon = \frac{1}{2D} \int_0^{\tau_s} f\left(\bar{F}(\tau) \frac{XX' + YY'}{\sqrt{X^2 + Y^2}}, \epsilon\right) d\tau \quad (3.10)$$

$$= \frac{1}{2D} \int_0^{\tau_{step}} f(P, \epsilon) d\tau \quad (3.11)$$

Here are some examples of the smoothing function f :

1. Arctan smoothing (Fig. 3.5a): $f_1(P, \epsilon) = \frac{2}{\pi} P \tan^{-1}(P/\epsilon)$.
2. $f_2(P, \epsilon) = \sqrt{P^2 + \epsilon^2}$ illustrated in Fig. 3.5b is related to the so-called Chen-Harker-Kanzow-Smale smoothing function (Taji and Miyamoto, 2002). We will call this the square-root smoothing.
3. $f_3(P, \epsilon) = \epsilon \log(1 + e^{-P/\epsilon})$, $\epsilon > 0$ illustrated in Fig. 3.5c is related to the so-called neural network smoothing function (Taji and Miyamoto, 2002).

Respectively, the analogous smooth approximations of $[P]^+$ are:

1. $g_1(P, \epsilon) = \frac{P}{2} \left(\frac{2}{\pi} \tan^{-1}\left(\frac{P}{\epsilon}\right) + 1 \right)$,
2. $g_2(P, \epsilon) = \frac{P + \sqrt{P^2 + \epsilon^2}}{2}$
3. $g_3(P, \epsilon) = P + |\epsilon| \log(1 + e^{-P/|\epsilon|})$

We qualify C_ϵ by a subscript — $C_{1,\epsilon}$, etc. — depending on which of the three smoothing functions is used in its definition. Now note that while $f_2(P, \epsilon)$ and $f_3(P, \epsilon)$ are greater than $|P|$ for all P and $\epsilon > 0$, $f_1(P, \epsilon)$ is less than $|P|$ (Fig. 3.5). That is,

$$0 \leq f_1(P, \epsilon) \leq |P| \leq f_2(P, \epsilon), f_3(P, \epsilon) \quad (3.12)$$

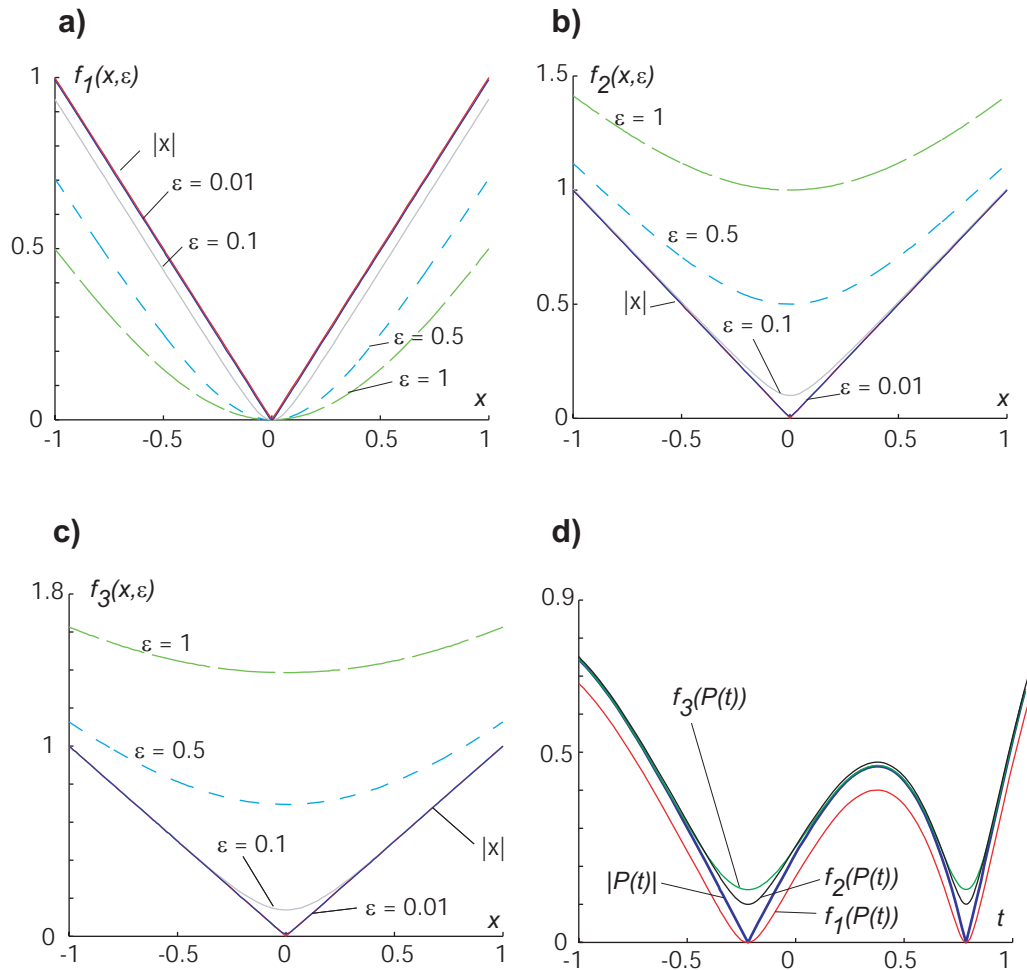


Figure 3.5: **Three smoothings of $|x|$.** (a) $f_1(x, \epsilon) = \frac{2}{\pi}x \tan^{-1}(x/\epsilon)$ approaches $|x|$ from below as ϵ goes to zero. (b) $f_2(x, \epsilon) = \sqrt{x^2 + \epsilon^2}$ and (c) $f_3(x, \epsilon) = x + |\epsilon| \log(1 + e^{-x/|\epsilon|})$ approach $|x|$ from above as ϵ goes to zero. In these figures, the smoothed versions are visually indistinguishable from $|x|$ for $\epsilon = 0.01$. (d) The smoothed and unsmoothed versions of a hypothetical $|P(t)|$ are shown. $\epsilon = 0.1$ was used for the smoothing.

Integrating the above equation over the stance phase, noting that P is the leg-power, we get:

$$0 \leq C_{1,\epsilon} \leq C \leq C_{2,\epsilon}, C_{3,\epsilon} \quad (3.13)$$

for any particular value of the control parameters. This means that minimizing each of these above quantities over the *same* search-space preserves the ordering of the costs. In other words,

$$0 \leq \min C_{1,\epsilon} \leq \min C \leq \min C_{2,\epsilon}, \min C_{3,\epsilon} \quad (3.14)$$

This above equation provides a smooth and well-conditioned way to bound the optimal value of C from above and below. Solving the above optimal control problems for different values of ϵ , gives us a sequence of upper and lower bounds on the optimal C . Further, assuming that C_ϵ depends smoothly on ϵ , the optimal value of the objective function at $\epsilon = 0$ can be obtained by smooth extrapolation. We shall present the results of such extrapolation in the section on the numerical solution of this optimal control problem (section 3.2.5).

3.2.4 Trick-2: Assume the non-smoothness away

Here we make the assumption that the trajectory of the center of mass is symmetric about mid-stance (when the leg is assumed vertical and touching the ground). Further we assume that only positive work is done in the second part of the stance (after mid-stance).

Since the gait is assumed symmetric, we consider only half a step — from mid-stance to the end of the step. The goal is to determine the nondimensionalized initial conditions (X'_0, Y_0) , the nondimensionalized leg-force $\bar{F}(\tau)$, and the nondimensionalized duration of the stance phase τ_s that minimize the cost function

$$C_{symm} = \frac{1}{D} \int_{\tau_{step}/2}^{\tau_s} P(\tau) d\tau \quad (3.15)$$

where,

$$P(\tau) = \bar{F}(\tau) \frac{XX' + YY'}{\sqrt{X^2 + Y^2}} \quad (3.16)$$

subject to the inequality constraint that

$$P(\tau) \geq 0 \quad \text{for} \quad \frac{\tau_{step}}{2} \leq \tau \leq \tau_{step} \quad (3.17)$$

The system dynamics are governed by the same differential equations as before. When $\tau_{step}/2 \leq \tau \leq \tau_s$,

$$X'' = \frac{\bar{F}(\tau)X}{\sqrt{X^2 + Y^2}} \quad (3.18)$$

$$Y'' = -1 + \frac{\bar{F}(\tau)Y}{\sqrt{X^2 + Y^2}}. \quad (3.19)$$

When $\tau_s < \tau \leq \tau_{step}$,

$$X'' = 0 \tag{3.20}$$

$$Y'' = -1 \tag{3.21}$$

The initial conditions for this piecewise system of equation is:

$$X(\tau_{step}/2) = 0, Y(\tau_{step}/2) = Y_0, X'(\tau_{step}/2) = X_0', Y'(\tau_{step}/2) = 0 \tag{3.22}$$

And for periodicity, the state at time $\tau = \tau_{step}$ is required to be:

$$X(\tau_{step}) = D/2, Y'(\tau_{step}) = 0 \tag{3.23}$$

There are no constraints on $Y(\tau_{step})$ and $X'(\tau_{step})$.

We note again that the C_{symm} is a smooth function of the control parameters, and so are all the constraints. We have removed the non-smoothness due to the absolute value function, by assuming it away. We have assumed symmetry of the optimal solution, and it is not a priori clear that the solution to the original problem will be symmetric about mid-stance. But numerical investigations (using say the smoothed version of the optimization problem, as discussed in the previous section) suggest that it is so. So we are justified making the above restrictions post-hoc.

3.2.5 Convergence of the numerical optima

The numerical methods used to solve the ϵ -smoothed optimal control problem (not assuming symmetry) essentially follow the short description in Section 3.1.2. The numerical method for the symmetric-therefore-smooth optimization problem is analogously formulated in an obvious manner – the boundary conditions for the symmetric problem are a little different, and there is the extra state constraint that the leg-power is positive through the second part of the stance phase. That the power is positive is enforced at a finite number of points on the grid: $P_i \geq 0$.

As mentioned earlier, we used SNOPT, a robust implementation of a sequential quadratic programming algorithm for solving nonlinear finite-dimensional optimization problems. SNOPT requires specification of a number of parameters – for example, information about how accurately the objective function and non-linear constraint violations can be calculated and how accurately the first-order optimality conditions need to be satisfied. We used MATLAB's ode45 for the numerical integration of the differential equations. Overall, the absolute error in the solution to the differential equations was maintained at about 10^{-13} for the state. This accuracy translates to a similar accuracy in the evaluation of the objective function and the constraint violation for the symmetric problem, which has a well-conditioned integrand for the objective function. For the ϵ -smoothed problem, the absolute errors in the constraint evaluation are again about 10^{-13} . However, we used a lower accuracy in the objective function evaluation of only about 10^{-8} , because the integrand in the objective function is not particularly smooth for small ϵ .

We discuss below the convergence of the numerical solutions of the two optimal control problems to the “true” optimum. Please see related discussion in Srinivasan and Ruina (2006). We present all the convergence results for the specific values $V = 0.5$ and $D = 0.5$. At these values of V and D , the optimal gait *seems* to be converging to inverted pendulum walking. The cost of transport of inverted pendulum walking at $V = 0.5$ and $D = 0.5$ can be calculated quite accurately using Eq. 2.8, without solving any optimization problem. We find this cost to be about 0.019913159 (accurate to about 10^{-8}). We show below that the numerical solution of the optimal control problems approach this cost as we let ϵ and $1/N$ tend to zero.

For the symmetric problem, we believe that the numerical solution to the optimal control problem should approach the true optimal solution as the grid-size $N \rightarrow \infty$. Table 3.1 shows the difference between the optimal values for a range of N and the accurate collisional value noted above. We note that the optimal values obtained from multiple runs of the optimization (for a given N) with substantially different initial guesses of the optimum differed only in the 8-th (or later) decimal place. This suggests reliable convergence of the optimizations with an accuracy of about 8-9 digits in the optimal value (given the particular discretization). Plotting the optimal value with respect to $h = 1/N$, we find that the optimal value essentially varies linearly with h . We take advantage of this observation to extrapolate to $h = 0$ by (least-squares) fitting a line to the h vs optimal value data. We find good agreement between the extrapolated cost and the accurate collisional value to be about 10^{-5} .

For the smoothed optimal control problem, we first extrapolate to $\epsilon = 0$ for given N (see Figure 3.6) and then extrapolate the ϵ -extrapolated optimal values for a sequence of N to $h = 0$ (see Table 3.2). Switching the order of convergence (first $h \rightarrow 0$ then $\epsilon \rightarrow 0$) resulted in poorer comparison with the accurate collisional value. Similar poor comparison of the extrapolated value with the accurate collisional cost was found when we tried to co-vary ϵ and h linearly to zero $\epsilon = h/5$ (see Table 3.3). The changing of the quality of the extrapolations with how the extrapolation is done is presumably related to the behavior of the underlying function relating the optimal value, h and ϵ .

3.2.6 Non-smoothness of the objective function

Much of the preceding discussion was motivated by the necessity to avoid the non-smoothness of the objective function. Here we show (numerically) that indeed the objective function is non-smooth (Figure 3.7). To obtain this figure, we started from the optimal solution of the symmetric smooth problem (Section 3.2.4) for $V = 0.5, D = 0.5$ and $N = 12$. We then changed the objective function in Equation 3.15 by replacing P with a $|P|$. Then we varied the value of the force at the first and second grid point, about their respective optimal values, to obtain Figure 3.7. Note that no constraints (periodicity or any other) were enforced as these force values were changed. So the non-smoothness is not somehow an artifact

Table 3.1: **Symmetric smooth problem.** Optimal value for various N for $V = 0.5$, $D = 0.5$ is shown in terms of its difference from the accurate cost obtained for inverted pendulum walking (0.019913159). Optimal value for $N \rightarrow \infty$ is obtained by extrapolation using a linear and quadratic curve-fits. The mean square errors for the two curve-fits are respectively about 5×10^{-5} and 1×10^{-5} (a cubic fit does not do any better). The accuracy of the extrapolations seem to be consistent with these mean square errors.

N	$h = 1/N$	Difference of the optimal value from the collisional value
4	0.25	-7.567×10^{-3}
8	0.125	-3.749×10^{-3}
16	0.0625	-1.873×10^{-3}
32	0.03125	-9.315×10^{-4}
64	0.015625	-4.647×10^{-4}
Linear Extrapolation	0	$+1.788 \times 10^{-5}$
Quadratic Extrapolation	0	-4.265×10^{-6}

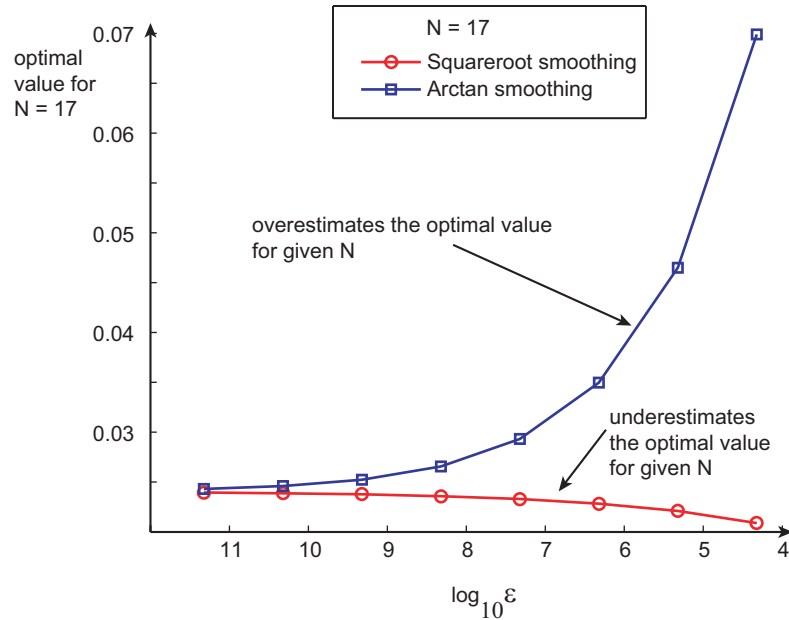


Figure 3.6: **Convergence of the smoothed optimal control problem in ϵ .** Optimal value for a sequence of ϵ -smoothed optimal control problems for fixed $N = 17$. As before, $V = 0.5$, $D = 0.5$. Two types of smoothing were used to obtain, respectively, a sequence of overestimates of the optimal value for $N = 17$ and a sequence of underestimates. Such sequences are extrapolated to $\epsilon = 0$ for a range on N for use in Table 3.2.

Table 3.2: **Convergence of the smoothed optimal control problem in N .** Optimal values for a sequence of N for $V = 0.5$, $D = 0.5$ are plotted in terms of their differences from the accurate collisional walking cost. Each of these numbers were obtained by solving a sequence of ϵ -smoothed optimal control problems (with the smoothing function f_1) and extrapolating to $\epsilon = 0$ as in Figure 3.6. We note that the extrapolation to $h = 0$ and $\epsilon = 0$ is different from the result of the collisional value by about 10^{-5} — somewhat higher than would be expected superficially from the mean-square errors of the linear (error: 5×10^{-6}) and quadratic (error: 5×10^{-7}) curve-fits. The source of this inconsistency is not clear.

N	Differences of ϵ -extrapolations from the accurate collisional value
10	-5.432×10^{-3}
14	-3.869×10^{-3}
16	-3.385×10^{-3}
18	-3.010×10^{-3}
20	-2.711×10^{-3}
Linear Extrapolation in $h = 1/N$	1.47×10^{-5}
Quadratic Extrapolation in $h = 1/N$	-5.61×10^{-5}

Table 3.3: **Co-vary ϵ and N in smoothed optimal control problem.** ϵ and N were varied according to the relation $\epsilon = \frac{1}{5N}$. The optimal values are then extrapolated to $\epsilon = 1/N = 0$ by fitting a cubic polynomial to the data. Mean-square error of the cubic fit was about 10^{-7} — the agreement of the extrapolation with the accurate collisional value of the walking cost is only about 10^{-4} .

N	Difference of optimal value from accurate collisional value
11	-2.275×10^{-2}
13	-1.922×10^{-2}
15	-1.666×10^{-2}
17	-1.471×10^{-2}
19	-1.317×10^{-2}
23	-1.090×10^{-2}
Cubic Extrapolation	-1.638×10^{-4}

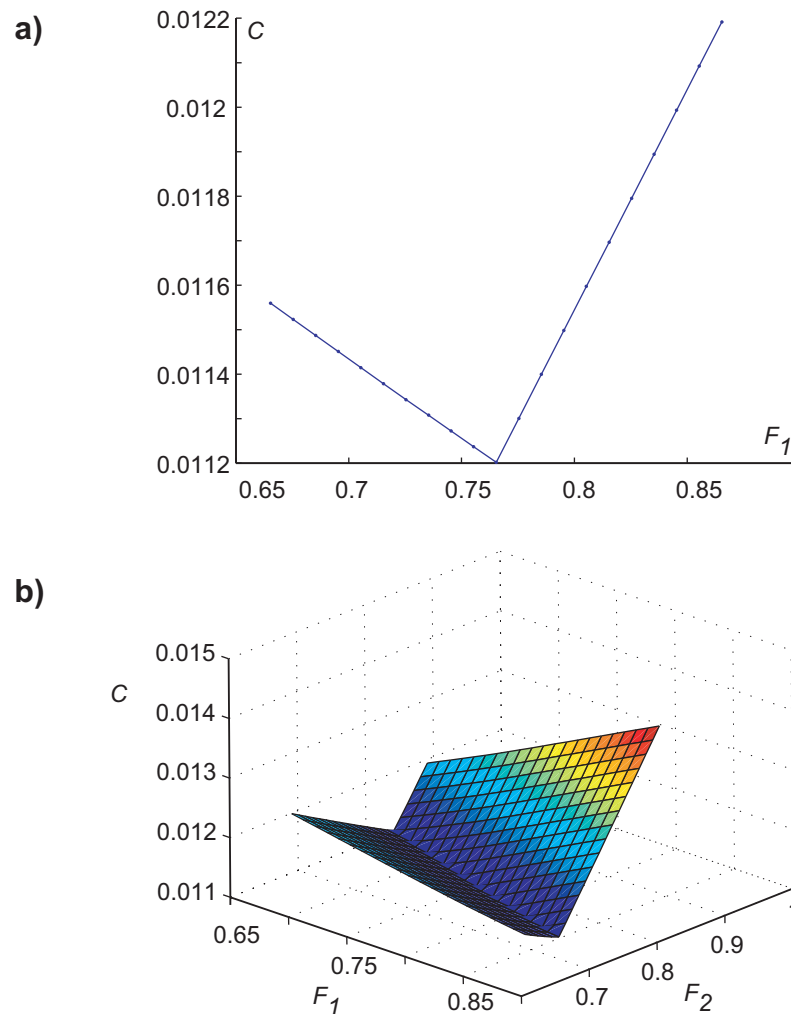


Figure 3.7: **Non-smoothness of the objective function.** Shown is the variation of the objective function when (a) one or (b) two control parameters are varied with all other parameters are kept fixed at their optimal values. The objective function does not seem continuously differentiable at the optimum – in both (a) and (b), the optimum lies at the kink. We solved the symmetric smooth problem ($N = 12$, $V = 0.5$, $D = 0.5$), found the optimum, then changed the objective function to include an absolute value sign, and obtained this plot as the force values at the first and second grid points were changed. The function looks non-smooth at finer scales as well.

of any of the constraints.

Note that had the non-smoothness been bounded away from the minimum, instead of being exactly at the minimum (as suggested by the figure), smooth optimization programs such as sequential quadratic programming would have had much better local convergence properties close the minimum.

3.2.7 Discovering level walking in the optimizations

In Figure 3.3, we claim inverted pendulum walking is optimal for a specific range of V and D , and no other gait is optimal in this region. This claim, as mentioned before, was based on numerical experiments where we started the optimization with different initial guesses and found that the optimization always converged to walking. To further bolster this claim, we wished to find out what the optimization would find if we explicitly ruled out walking at low speeds. During the stance of phase of inverted pendulum walking, the body goes up and then down. So to rule out inverted pendulum walking, we enforced an artificial constraint that the body should go down and then up during the stance phase (as in running). Interestingly, under this constraint we found that the level walking gait with no double stance (see section 2.3.5) was optimal at low speeds, instead of inverted pendulum walking. When we imposed the converse artificial constraint (that the body should go up then down during stance phase) for V and D values in the region where running was originally optimal, we again found that a level walking gait was optimal⁶.

3.2.8 Cost of pendular running

Recall that pendular running consists of a walking-like inverted pendulum stance phase and a running-like flight phase. The transition from the stance phase to the flight phase is accomplished by an impulsive push-off, which redirects the body velocity from downward to upward. Over a single step, all the positive work is performed during the impulsive push-off. The cost of one step of pendular running, therefore, is proportional to this positive work. Let α be the angle the leg makes with the vertical at the end of the stance phase. See Fig. 3.8. v_I is the velocity magnitude just before push-off. Let v_f be the velocity magnitude at the beginning of the flight phase and ϕ be the angle that the velocity at the beginning of flight phase makes with the horizontal. Then, $v_f \cos(\alpha + \phi) = v_i$ by linear momentum balance in the direction perpendicular to the push-off impulse. The positive work is, therefore,

$$W_p = m(v_f^2 - v_i^2)/2 \tag{3.24}$$

$$= mv_f^2(1 - \cos^2(\alpha + \phi))/2 \tag{3.25}$$

$$= mv_f^2 \sin^2(\alpha + \phi)/2 \tag{3.26}$$

⁶These are the results of very limited numerical experiments with the symmetric version of the optimal control problem.

As we have mentioned before, inverted pendulum walking and impulsive running may be viewed as limiting special cases of pendular running. Pendular running reduces to impulsive running when $\alpha = 0$ and reduces to inverted pendulum walking when $\phi = 0$. Away from these limits, pendular running – symmetric pendular running – is characterized by 3 non-dimensional parameters: the duty factor in addition to V and D . While duty factor is typically defined as the ratio of the stance time of a single leg to the time duration of a complete stride (two steps) of walking or running. In the following, we define μ_d to be twice this duty factor — that is the ratio of the stance time of a single leg to the time duration of a single step (half a stride).

Alternatively, the specification of three numbers v_i, α, ϕ completely describes a pendular run: v_i and α define the inverted pendulum stance phase, and v_f (a function of v_i, α, ϕ) and ϕ define the flight phase. The cost of transport can be evaluated, and so can the three nondimensional parameters μ_d, V and D as functions of v_i, α and ϕ . Conversely, we can determine the cost of transport given μ_d, V and D by numerical root-find.

3.2.9 Optimal duty factor for pendular running at small step-lengths

Small step-lengths imply that ϕ and α are small. Using this in the expression for the positive work in a pendular run:

$$W_p = \frac{m}{2} v_f^2 \sin^2(\alpha + \phi) \quad (3.27)$$

$$\approx \frac{m}{2} v_f^2 (\alpha + \phi)^2 \quad (3.28)$$

Noting that the $v_f \approx v \approx v_i$ to $O(1)$, time of flight $t_f = (2v_f \sin \phi)/g \approx 2vg\phi/g$, the time of stance is $t_s = (2l_{max} \sin \alpha)/v \approx 2l\alpha/v$ and $\mu_d = t_f/(t_f + t_s)$, we have $\alpha \approx t_s v / 2l_{max}$ and $\phi \approx gt_f / (2l_{max})$. Substituting this in W_p above:

$$W_p \approx \frac{m}{2} v^2 \left(\frac{t_s v}{2l_{max}} + \frac{gt_f}{2v} \right)^2 \quad (3.29)$$

$$= \frac{m}{2} v^2 t_{step} \left(\frac{g}{2v} \right)^2 \left(\frac{t_s}{t_{step}} V^2 + \frac{t_f}{t_{step}} \right)^2 \quad (3.30)$$

$$= \frac{m}{2} v^2 t_{step} (\mu_d V^2 + (1 - \mu_d))^2 \quad (3.31)$$

$$= \frac{m}{2} v^2 t_{step} (\mu_d (V^2 - 1) + 1)^2 \quad (3.32)$$

The optimal duty factor is that which minimizes $(\mu_d (V^2 - 1) + 1)^2$ subject to the condition $0 \leq \mu_d \leq 1$. $(\mu_d (V^2 - 1) + 1)^2$ is quadratic in μ and has exactly one stationary point $\mu_{stat} = 1/(1 - V^2)$ – a minimum – in the extended domain $-\infty < \mu_d < \infty$.

1. When $V < 1$, $\mu_{stat} > 1$. This means that in the domain $0 \leq \mu_d \leq 1$, the quadratic is decreasing. The minimum cost is when $\mu_d = 1$. That is, inverted pendulum walking is optimal.
2. When $V > 1$, $\mu_{stat} < 1$. This means that in the domain $0 \leq \mu_d \leq 1$, the quadratic is increasing. The minimum cost is when $\mu_d = 0$. That is, impulsive running is optimal.
3. When $V = 1$, the quadratic $(\mu_d(V^2 - 1) + 1)^2$ becomes independent of μ . All duty factors $0 \leq \mu_d \leq 1$ give the same cost!

These conclusions agree with the more elaborate optimization results obtained here by numerical optimization, and analytically in the next chapter.

3.2.10 Generating the phase boundaries

Given V and D , the cost of transport for a pendular run depends on the single-step duty factor μ . And for every V and D , there exists a value of the single-step duty factor μ that minimizes the cost of transport. We perform numerical optimization to obtain the optimal duty factor at a given V and D : this optimal duty factor decides whether the optimal gait is inverted pendulum walking, impulsive running or neither (proper pendular running).

Fig. 3.3 shows the regions over which each of these gaits seem to be optimal. How were these phase boundaries obtained? The walk-to-pendular-run boundary was determined more exactly by performing a binary search on where the optimal duty factor changed from 1 to something less than 1. This binary search was performed two different ways: 1) searching along constant- D lines – this is good for determining the boundary at low D . 2) searching along a constant- V lines – this is good for determining the boundary at low V , where the boundary seems to have a horizontal tangent.

The pendular-run-impulsive-run boundary was similarly determined. We compare the phase boundaries thus obtained with the optimal control solutions in Figure 3.9.

3.2.11 Possible discontinuity at the boundary between pendular running and impulsive running

Fig. 3.3 shows the regions over which each of these gaits seem to be optimal. In the region denoted as pendular running, the duty factor lies strictly between 0 and 1: $0 < \mu < 1$. However this figure (Fig. 3.3) does not provide any information about the variation of the duty factor within the pendular running region. To shed some light on this, we plot in Fig. 3.10 the duty factor as a function of nondimensional velocity V for a constant D . We notice that for low V , $\mu \equiv 1$ corresponding to inverted pendulum walking. And for high V , $\mu \equiv 0$ corresponding to impulsive running. The intermediate region with $0 < \mu < 1$ is pendular running. We notice

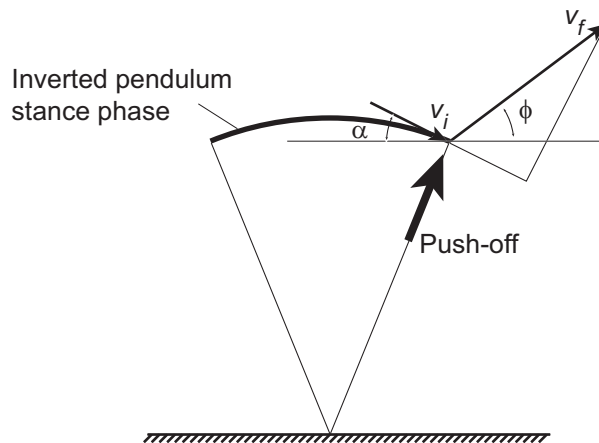


Figure 3.8: **Pendular run.** The impulsive change in velocity due to push-off at the end of a pendular stance phase is shown.

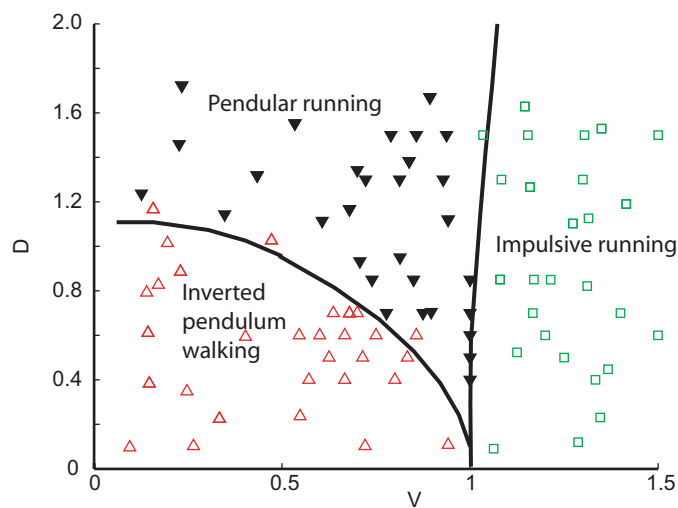


Figure 3.9: **Classified optimal gaits** We solved the symmetric optimal control problem with $N = 11$ for a number of different (V, D) combinations and classified the resulting optimal solution as inverted pendulum walking, impulsive running or pendular running. Because of the low grid-size, the regions over which a given gait is optimal is slightly different from that obtained by solving the more-restricted optimization problem of Section 3.2.10.

that the duty factor seems to vary continuously except possibly at the apparent interface of pendular running and impulsive running. The duty factor seems to drop precipitously from about 0.4 to zero. Is this a true discontinuity? Or is this an artifact of a vertical tangent that is generally hard to resolve numerically?

Some insight into this rapid change in the optimal duty factor is obtained by looking at Fig. 3.11. This figure is drawn for $D = 1$. Fig. 3.11a shows the variation of the cost of transport for $D = 1$ and $V = 0.97$. We see clearly that there is only one minimum: around $\mu = 0.5$. Fig. 3.11c shows a similar plot at $D = 1$ and a somewhat greater speed $V = 1.04$. Again we see only one minimum: now at $\mu = 0$. Fig. 3.11b shows the variation of the cost at an intermediate speed $V = 1.0255$. Careful examination of this plot indicates the presence of two minima. One at $\mu = 0$ and another at just over $\mu = 0.3$. The figure does show that the cost is almost flat – so the presence of two distinct minima is not completely evident from the figure. However the deviation from flatness seems much less than the small error in the evaluation of the cost: so we deem the non-uniqueness of the optimum a genuine feature of the problem, rather than a numerical artifact. Recall that the almost-flatness of the cost with respect to the duty factor near $V = 1$ was anticipated in the previous section, where we show that for small step-lengths cost is independent of μ when $V = 1$.

Fig. 3.11d shows the contours of the objective function as a function of the speed V and the duty factor μ . Fig. 3.11e shows a zoomed-in version of Fig. 3.11a. These contours were obtained by evaluating the cost on a grid and using MATLAB's `contour` function. The dark arrows in Fig 3.11d indicate the directions of function increase. The contours are therefore based on interpolation between the grid points, and therefore will not be as accurate as the function accuracy at the grid points. Figs. 3.11a,b,c correspond to variation of cost along vertical section in Fig. 3.11e. Three such vertical slices are shown (though not corresponding to Figs. 3.11a,b,c). The local minima along each of the sections are indicated by open circles. The contours indicate that there are indeed two minima for the intermediate speed: section CC. Examination of the contours in Fig. 3.11e suggests that the region where there are two locally optimal duty factors might be quite small. Further, it seems like the two minima arise independently. The vanishing of one minimum seems unrelated to the creation of the other – implying the presence of a discontinuous jump in the optimal duty factor.

In conclusion, despite our previous numerical claim of uniqueness of optimal solution for a given V and D , the above considerations indicate existence of non-uniqueness in a small range of V and D . This is not surprising given that at $V = 1$ and $D = 0^+$, there exist infinitely many solutions (same cost for all duty factors). On the other hand, we must point out that the above evidence for non-uniqueness comes from the analysis of a restricted optimization problem (optimal duty factor for a pendular run). It is still possible that the original optimal control problem has unique solutions in the $V - D$ region of interest (but bounded away from the $D = 0$ limit).

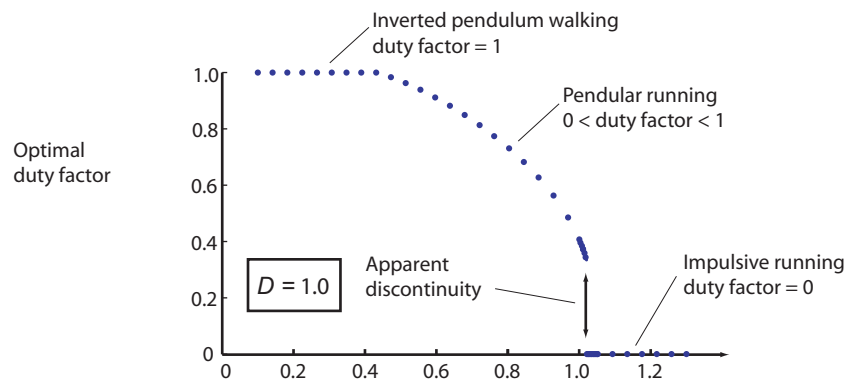


Figure 3.10: **Optimal pendular running** The optimal duty factor given that the gait is a pendular run is plotted as a function of V at a constant $D = 1.0$.

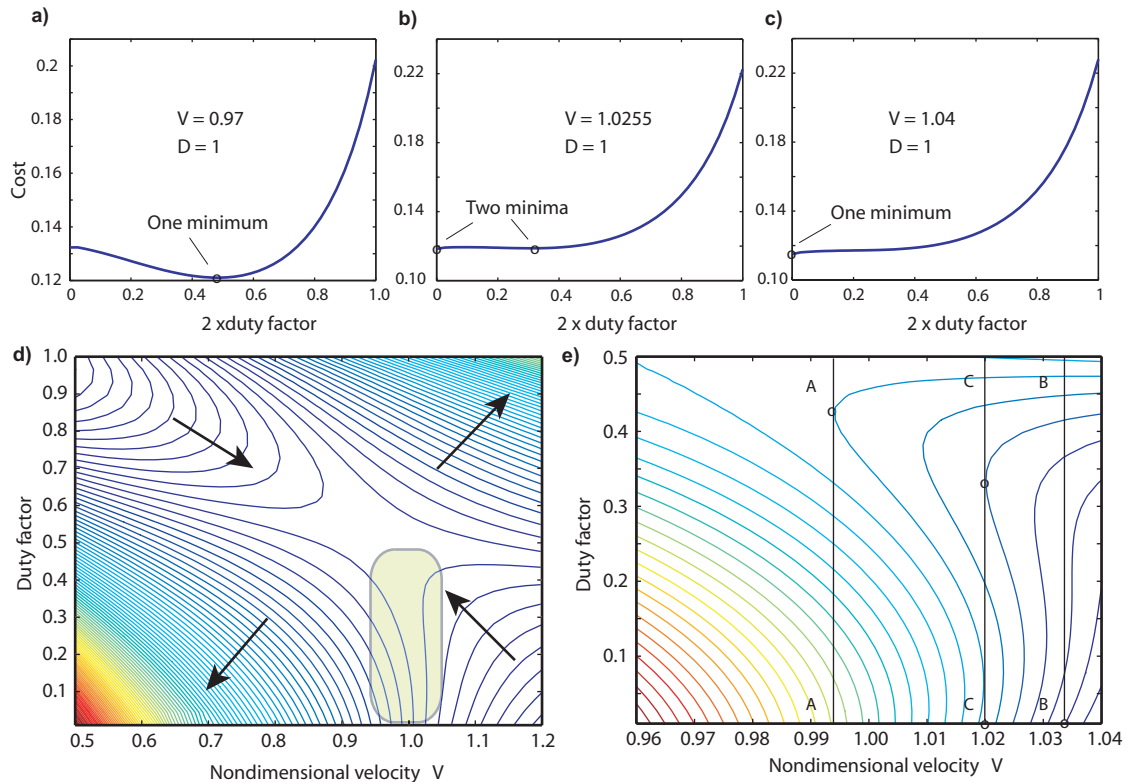


Figure 3.11: **Unique optimal duty factor?** Or are there multiple local minima? (a) shows only one minimum. (b) shows two minima, while (c) again shows one minimum. Thus there seems to be a very small window of non-uniqueness. (d) shows the contour plot of the cost with respect to V and the duty factor at a constant D . (e) zooms in on the region shaded yellow in (d). Vertical sections through this region are depicted in (a), (b), and (c). The contours in (e) were created using MATLAB's contour, with 30 grid points on each axis.

Chapter 4

Minimal biped model at small step lengths: a heuristic proof of optimality of walking and running

4.1 Introduction

In the previous chapter, we computed the optimal gaits of the simple biped model by numerical optimization and showed that (for the minimal model) walking is indeed energetically optimal at low speeds and running at high speeds. To better understand this gait choice, we consider another simpler optimization problem that is closely related to the original optimization problem in the limit of small step-lengths. This simplified optimization problem is amenable to analytical solution. This analytical solution confirms the results of the computer optimization.

Note that while animals do not naturally prefer small step lengths, we see in Fig. 3.3a that, for the minimal model of Chapter 3, the gait transition from walking to running seems to be preserved even at low step-lengths. Therefore, it is reasonable to explore gait choice for a given small step length and a given forward speed.

Broadly, this chapter is divided into five conceptual pieces:

- We simplify the original optimal control problem by various symmetry assumptions, resulting in **Problem A**.
- We replace the radial telescoping leg in Problem A by a vertical telescoping leg to get **Problem B**.
- We then show that ratio of the objective function values for equivalent gaits in Problem A and Problem B approaches 1 as the step length goes to zero, for the case of finite leg-forces. This result suggests that solving Problem B might give us some insight into the solution of Problem A at small step-lengths.
- We simplify problem B to **the elevator problem**, in which all the motion is constrained to one dimension.
- We find the optimal solutions for the elevator problem, and note that the optimal solutions are similar to inverted pendulum walking and impulsive running in the original problem, Problem A.

The results of this chapter cannot be construed as a complete rigorous proof of optimality of walking and running in the limit of small step-lengths, although it might be possible to fill the gaps in the arguments here. This chapter might be considered as a detailed heuristic device to understand, what we hope, is the essential structure of the optimization problem.

4.2 Problem A: Symmetry assumptions.

Assumption 1 As in the previous chapters, each “step” consists of the (periodic) action of a single leg with a given foot-contact point. However, unlike in chapter 3, we do not restrict the number of flight phases per step in any manner. The two legs are assumed to perform identically during their respective steps. Given these assumptions, we only need to consider a *single step* (of either leg) for a complete analysis of the gait.

Assumption 2 Define “mid-step” as when the body has the same horizontal position as the foot-contact point. We assume that the trajectory of the center of mass is symmetric about mid-step (e.g., Figure 4.1a). This assumption implies that only *half a step* — from mid-step till the end of the step — contains all the information about the gait. The complete gait can be generated from only half a step by appropriate time reversal and time translation of the half-step.

Constraints on the leg force The idealized gaits such as inverted pendulum walking and impulsive running, discussed in Chapters 2-3, require infinite forces. Since unbounded forces can be troublesome analytically, we impose simple bounds on the leg forces $F_A(t)$: $F_{min} \leq F_A(t) \leq F_{max}$.

Ideally, we would like to solve a sequence of minimization problems such that the force bounds go to infinity: $F_{min} \rightarrow -\infty$ and $F_{max} \rightarrow \infty$. But for now, we assume that the forces are bounded.

Implications of the symmetry assumptions The boundedness of the leg force $F_A(t)$ implies that the acceleration is always bounded and that the velocity of the body is continuous. Because the velocity vector along the gait-trajectory is continuous, the symmetry conditions above basically require that the vertical component of the velocity vanish both at mid-step and at the end of the step (Figure 4.1b).

Problem A in equations We seek the optimal gait for given horizontal speed v and step length d . In Chap. 3, we enforced a limit on the length of the leg l_{max} . Here, for analytical simplicity, we replace the leg-length constraint with a specification of the height of the center of mass at mid-step l_0 .

We slightly modify the notation used in Chapter 3. Here $t = 0$ corresponds to mid-step here and therefore, the end of step corresponds to $t = \frac{t_{step}}{2} = \frac{d}{2v}$. All the variables are subscripted with A to denote that they correspond to problem A. e.g., x_A , F_A , etc. Further, the costs here are not normalized by step-length here (such normalization is superfluous for the purposes of optimization when both v and d are fixed).

We wish to determine that $\dot{x}_A(0)$ and $F_A(t)$ over $t \in [0, \frac{t_{step}}{2}]$ that together minimize the total positive work C_A , where

$$C_A = \int_0^{\frac{t_{step}}{2}} [F_A \dot{l}_A]^+ d\tau, \quad (4.1)$$

subject to the constraints that $x_A(0) = 0$, $y_A(0) = l_0$, $x_A(\frac{t_{step}}{2}) = \frac{d}{2}$, $\frac{dy_A}{dt}(0) = 0$ and $\frac{dy_A}{dt}(\frac{t_{step}}{2}) = 0$. The differential equations governing the position of the point-mass x_A and y_A are

$$m\ddot{x}_A = F_A \frac{x_A}{l_A}, \text{ and} \quad (4.2)$$

$$m\ddot{y}_A = -mg + F_A \frac{y_A}{l_A} \quad (4.3)$$

where F_A , x_A , y_A and l_A are all functions of time t and $l_A = \sqrt{x_A^2 + y_A^2}$.

Trajectories can be completely specified by v , d , and $\ddot{y}_A(t)$ A given gait trajectory is completely described by the specification of the initial conditions and the leg-force $F_A(t)$. We will show below that given average speed v and step length d , a gait trajectory is completely determined by the specification of the vertical acceleration $\ddot{y}_A(t)$.

Noting that $y_A(0) = l_0$ and $\dot{y}_A(0) = 0$, we can integrate a given vertical acceleration to obtain the vertical velocity component $\dot{y}_A(t)$ and the vertical position $y_A(t)$. Only those vertical acceleration functions that satisfy the symmetry condition $\dot{y}_A(0) = \dot{y}_A(\frac{t_{step}}{2}) = 0$ are considered relevant.

Having determined $y_A(t)$, we can determine $\frac{F_A(t)}{l_A(t)}$ from Eq. 4.3:

$$\frac{F_A(t)}{l_A(t)} = \frac{m\ddot{y}_A(t) + mg}{y_A(t)} \quad (4.4)$$

$$= f(t), \text{ say} \quad (4.5)$$

We can use this $f(t)$ in Eq. 4.2 to obtain the following equation for x_A .

$$m\ddot{x}_A = f(t)x_A \quad (4.6)$$

Solving for $x_A(t)$ requires two initial conditions. One of these, the horizontal position at mid-step, is known: $x_A(0) = 0$. We will now show that the other initial condition can uniquely be determined as a function of $f(t)$, v and d .

First, observe that Eq. 4.6 is linear in x for a given $f(t)$. This linearity, taken together with the initial condition $x_A(0) = 0$ implies that the final horizontal position $x_A(\frac{t_{step}}{2})$ will simply be proportional to the initial speed $\dot{x}_A(0)$. That is, $x_A(\frac{t_{step}}{2}) = k\dot{x}_A(0)$, where k depends on $f(t)$. This proportionality allows us to uniquely choose the initial horizontal speed $\dot{x}_A(0)$ to obtain any given step length $d = 2x_A(\frac{t_{step}}{2})$, and thus obtain any given speed v , given $f(t)$ and t_{step} .

Determination of $x_A(t)$ completes the description of the trajectory. The leg-force $F_A(t)$ can be determined from the knowledge of $x_A(t)$, $y_A(t)$ and $f(t)$

In summary, specification of v , d and $\ddot{y}_A(t)$ uniquely and completely describes a trajectory in Problem A. Conversely and perhaps more obviously, every (meaningful) trajectory has a unique v , d and $\ddot{y}_A(t)$.

4.3 Problem B: Riding a circular arc with vertical telescoping legs

Two key observations help motivate the description of Problem B.

1. In Problem A, no work is done whenever the (radial) leg-length does not change – that is, the point-mass moves in a circular arc. We would like a similar property for Problem B – that is, moving in a circular arc must be work-free.
2. Recall that we will eventually consider only the limit of small step lengths. In the limit of small step lengths, the leg is almost vertical. So perhaps a reasonable simplifying approximation would be to have an exactly vertical leg.

We combine these two ideas in Fig 4.2a. Imagine a circular track of radius l_0 centered at $(0,0)$ in the sagittal plane as in Fig 4.1a. And imagine a point-mass body riding the circular track with a *vertical telescoping leg*. The foot of the vertical telescoping leg rides on the circular track with *constant horizontal speed*. This constant horizontal velocity component is assumed to be enforced externally, without any energetic cost to the biped.

As shown in Fig 4.2a, y_B is the vertical position of the point-mass from the ground. $y_V(t)$ is the length of the vertical telescoping leg and $y_C(t) = y_B(t) - y_V(t)$ is the height of the circular track from the ground, corresponding to where the point-mass is at time t . F_B is the vertical force transmitted by the vertical telescoping actuator.

Problem B in equations The goal is to minimize the positive work C_B of the vertical telescoping actuators, where

$$C_B = \int_0^{t_{step}/2} [F_B(t)\dot{y}_B(t)]^+ dt \quad (4.7)$$

subject to the same boundary conditions as Problem A:

$$y_B(0) = l_0, \frac{dy_B}{dt}(0) = 0, \text{ and } \frac{dy_B}{dt}\left(\frac{t_{step}}{2}\right) = 0. \quad (4.8)$$

Note that the two extra boundary in Problem A, namely $x(0) = 0$ and $x(t_{step}/2) = d/2$ are automatically taken care of in Problem B by the assumption of constant

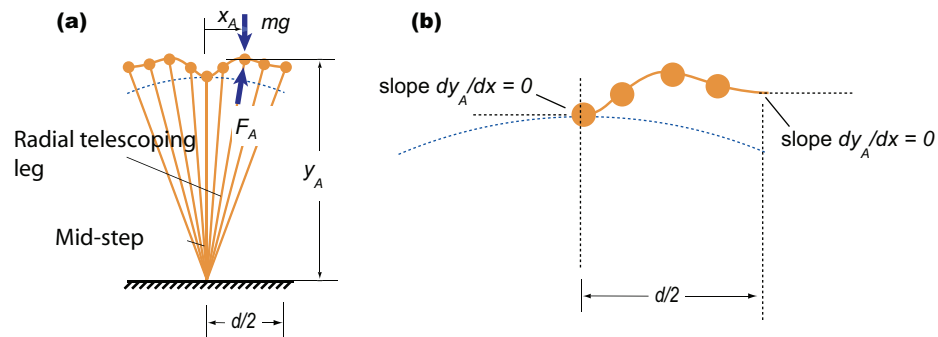


Figure 4.1: **Problem A** (a) One step of a gait that is symmetric about the mid-step. (b) Assumptions that all steps are identical and that each step is symmetric about mid-step imply that the vertical component of the velocity is zero at mid-step and the end of the step.

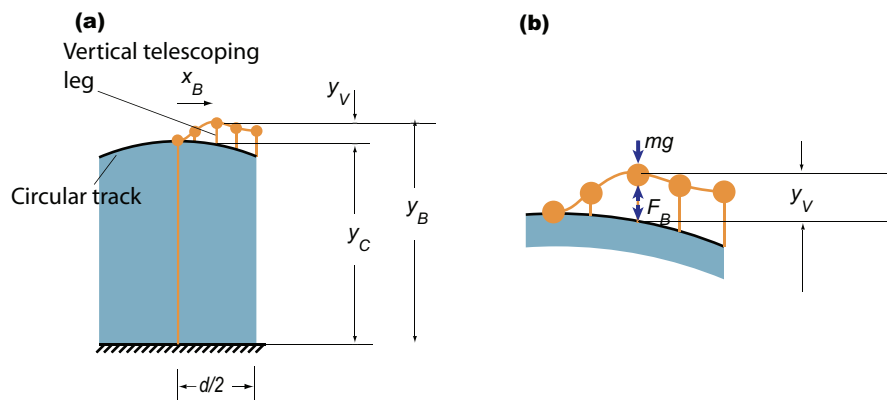


Figure 4.2: **Problem B: riding a circular track** (a) The radial telescoping leg of Problem A has been replaced by a vertical telescoping leg in Problem B. The foot of the vertical telescoping leg moves on a circular track. (b) The action of the vertical telescoping leg riding on a circular track is shown in detail. Note that the vertical velocity components vanish at mid-step and end of step.

horizontal speed $v = d/t_{step}$. The only governing dynamics equation is for the vertical motion:

$$m\ddot{y}_B = m(\ddot{y}_V + \ddot{y}_C) = F_B - mg \quad (4.9)$$

because a constant speed is enforced in the horizontal direction: $x_B(t) = vt$. A formula for \ddot{y}_C in the above equation might be obtained by twice differentiating $y_C = \sqrt{l_0^2 - x_B^2}$ with respect to time, where $x_B(t) = vt$. The vertical force $F_B(t)$ is bounded: $F_{min} \leq F_B(t) \leq F_{max}$.

4.4 Small step lengths: Problem B is “similar” to Problem A

Definition: analogous trajectories Recall that every trajectory in Problem A is completely described by the specification of the speed v , step length d and the vertical acceleration $\ddot{y}_A(t)$. For every such trajectory in (the feasible region of) Problem A, we define a unique *analog* in (the feasible region of) Problem B as having the same speed v , the same step length d and the same vertical motion $y_B(t) = y_A(t)$ (noting that a trajectory in problem B can be uniquely described thus).

Feasible trajectories in Problems A and B Note that the vertical component of the leg-force in Problem A is always less than or equal to the magnitude of the total leg-force and that the vertical forces are equal for analogous trajectories in problem A and B (because the vertical motions are the same: see lemma 3). That is, $|F_B(t)| \leq |F_A(t)|$. This implies that if the total leg-force $F_A(t)$ for a trajectory in Problem A obeys the appropriate force bounds, the vertical (total) force $F_B(t)$ for an analogous trajectory in Problem B also obeys the corresponding force bounds. Evidently, the converse is not true. In other words, the feasible region of Problem A is mapped strictly into the feasible region of Problem B. If we wish to show that Problem A is in some sense related to Problem B, we should demonstrate that the set of feasible trajectories for the two problems are also, somehow, closely related. We will ignore this aspect here for simplicity, at the cost of completeness. Indeed, we will show the “similarity” of Problems A and B in only one limited sense (see below). Therefore the results of this chapter cannot be construed as a rigorous proof of optimality of walking and running in the limit of small step-lengths. But rather as a detailed heuristic device to understand, what we hope, is the essential structure of the optimization problem.

A one parameter family of gaits In Problem A, given a particular trajectory with speed v , step-length d_0 , step-duration t_0 and vertical acceleration $g(t)$, we can generate a one-parameter family of gaits, all with the same average speed v , but with different step-lengths by simply using a time-stretched version of the vertical acceleration $g(t)$. That is, the vertical acceleration for a gait with step-length d is

given by $\ddot{y}_A(t) = g(td_0/d)$. Clearly, this one parameter family is uniquely defined for every v , d_0 , and $g(t)$, following our earlier observation that a gait is completely characterized by specification of v , d and $y_A(t)$.

Having defined a one parameter family of gaits parameterized by the step length, we can meaningfully ask how the energetic costs scale as $d \rightarrow 0$. We formalize the idea of small step lengths by taking $d = O(\epsilon)$, as ϵ , a convenient small quantity, approaches zero.

Proposition 1: For analogous trajectories of Problems A and B, we have $\frac{C_A}{C_B} = 1 + O(\epsilon)$ when $d = O(\epsilon)$. That is, we claim that

$$\int_0^{t_{step}/2} [F_A(t)\dot{l}_A]^+ dt = (1 + O(\epsilon)) \int_0^{t_{step}/2} [F_B(t)\dot{y}_V]^+ dt \quad (4.10)$$

for analogous trajectories of Problems A and B. Simply showing that $C_A \rightarrow C_B$ is not meaningful as both C_A and C_B can approach zero as $d \rightarrow 0$.

Proof: Noting that the integrands in Equation 4.10 are essentially products of two terms, we shall simply show that the analogous multiplicands in the integrands are respectively equal up to a factor of at most $(1 + O(\epsilon))$. In particular, lemma 2 shows that $\dot{l}_A = (1 + O(\epsilon^2))\dot{y}_V$ and lemma 3 shows that $F_A = (1 + O(\epsilon^2))F_B$ for all analogous trajectories. We now state and prove two other lemmas, 1a and 1b, which will be used in lemma 2.

Lemma 1a: For any given $g(t)$ and v , the fluctuations in the leg-length are much smaller than the initial leg-length in the limit of small step-lengths. That is, $l_A(t) = l_0(1 + O(\epsilon^2))$.

Proof: Noting that $\ddot{y}_A(t) = g(td_0/d)$, we have

$$y_A(t) = l_0 + \int_0^{t_{step}} \int_0^{t'} g\left(\frac{t''d_0}{d}\right) dt'' dt' \quad (4.11)$$

$$= l_0 + O(\epsilon^2), \quad (4.12)$$

noting that $t' \leq t_{step} = O(\epsilon)$ and that $g(t)$ is bounded and independent of d . Combining this with $x_A(t) \leq d$ and $l_A(t) = \sqrt{y_A^2 + x_A^2}$, we have $l_A(t) = l_0 + O(\epsilon^2) = l_0(1 + O(\epsilon^2))$.

Lemma 1b: For any given $g(t)$ and v , the fluctuations of the horizontal velocity component become much smaller than the average horizontal speed in the limit of small step-lengths. That is, $\dot{x}_A = v(1 + O(\epsilon))$.

Proof: $g(t)$ determines $y_A(t)$, which in turn determines $f(t)$ in the differential equation for $\dot{x}_A(t)$: $\ddot{x}_A = f(t)x_A$. This gives

$$\dot{x}_A(t) = \dot{x}_A(0) + \int_0^t f(t')x_A(t')dt' \quad (4.13)$$

$$= \dot{x}_A(0) + O(\epsilon^2) \quad (4.14)$$

Because the average horizontal speed is a constant v , this equation implies that $\dot{x}_A(0) = v + O(\epsilon^2)$ and consequently that, $x_A(t) = vt + O(\epsilon^2) = v(1 + O(\epsilon^2))t$.

Lemma 2: $\dot{l}_A = \dot{y}_V(1 + O(\epsilon^2))$ for analogous trajectories.

Proof:

1. $l_A = \sqrt{x_A^2 + y_A^2}$. Differentiating this equation with respect to t , we have $\dot{l}_A = x_A\dot{x}_A/l_A + y_A\dot{y}_A/l_A$. Noting that $l_A = l_0(1 + O(\epsilon^2)) = y_A(1 + O(\epsilon^2))$ from lemma 1a, we have $\dot{l}_A = (x_A\dot{x}_A/l_0 + \dot{y}_A)(1 + O(\epsilon^2))$.
2. The equation for the circular track of radius l_0 gives $y_C = \sqrt{l_0^2 - x_B^2}$. So $\dot{y}_C = -(1 + O(\epsilon^2))x_B\dot{x}_B/l_0$.
3. $y_V = y_B - y_C$ and $y_B = y_A$ for analogous trajectories. Therefore,

$$\dot{y}_V = \dot{y}_B - \dot{y}_C = \dot{y}_A - \dot{y}_C \quad (4.15)$$

Substituting items (1) and (2) into this equation, we have

$$\dot{y}_V = (1 + O(\epsilon^2)) \left(\dot{l}_A - \frac{x_A\dot{x}_A}{l_0} \right) + \frac{x_B\dot{x}_B}{l_0}(1 + O(\epsilon^2)) \quad (4.16)$$

$$= (1 + O(\epsilon^2)) \left(\dot{l}_A + \frac{x_A\dot{x}_A}{l_0} - \frac{x_B\dot{x}_B}{l_0} \right) \quad (4.17)$$

But by lemma 1b, we have $\dot{x}_A(t) = v(1 + O(\epsilon^2)) = \dot{x}_B(1 + O(\epsilon^2))$ and as a corollary, $x_A(t) = x_B(t)(1 + O(\epsilon^2))$. Using these, we have

$$\dot{y}_V = (1 + O(\epsilon^2)) \left(\dot{l}_A + \frac{x_B\dot{x}_B(1 + O(\epsilon^2))^2}{l_0} - \frac{x_B\dot{x}_B}{l_0} \right) \quad (4.18)$$

$$= (1 + O(\epsilon^2)) \dot{l}_A \quad (4.19)$$

Lemma 3: $F_A = F_B(1 + O(\epsilon^2))$

Proof: If F_{Ay} is the component of F_A in the vertical direction,

$$F_{Ay} = \frac{y_A F_A}{l_A} = \frac{y_A F_A}{\sqrt{y_A^2 + x_A^2}} \quad (4.20)$$

$$= (1 + O(\epsilon^2)) F_A \quad (4.21)$$

Further, by definition, the vertical accelerations for analogous trajectories are identical. This means that the vertical forces are equal: that is, $F_{Ay} = m\dot{y}_A + mg = m\dot{y}_B + mg = F_{By}$. But $F_{By} = F_B$ by definition of F_B . So $F_B = F_{Ay} = F_A(1 + O(\epsilon^2))$.

As mentioned before, we combine these lemmas 2 and 3 to show that the energetic costs of analogous trajectories in Problem A and Problem B are different only by a factor $1 + O(\epsilon^2)$. Note that we have assumed bounded leg-forces and accelerations in this proof.

4.5 The “elevator problem”: Riding a constant acceleration vertical elevator.

Replace circle by a parabola Only item 2 of lemma 2 above uses anything about the foot of the vertical telescoping actuator traveling in a circular path in Problem B. And $y_C(t)$ enters the proof of lemma 2 only as its first derivative \dot{y}_C . Differentiating $y_C(t) = \sqrt{l_0^2 - x_B^2(t)} = \sqrt{l_0^2 - (vt)^2}$ with respect to t , we have

$$\dot{y}_C = -\frac{v^2 t}{y_C} \quad (4.22)$$

We now replace the circular track by a parabolic track, $y_p(t) = l_0 - \frac{v^2 t^2}{2l_0}$. To see that $y_p(t)$ describes a parabolic track, simply substitute for time $t = x_B/v$ in the expression for $y_p(t)$. If the foot of the vertical telescoping actuator travels with constant horizontal speed on this parabolic track, the corresponding vertical velocity component of the foot will be

$$\dot{y}_p = -\frac{v^2 t}{l_0} \quad (4.23)$$

$$= -\frac{v^2 t}{\sqrt{y_C^2 + x_B^2}} \quad (4.24)$$

$$= -\frac{v^2 t}{(1 + O(\epsilon^2)) y_C} \quad (4.25)$$

$$= (1 + O(\epsilon^2)) \dot{y}_C \quad (4.26)$$

So replacing the circle y_C by the parabola y_p will not change the truth of lemma 2. We make this replacement because the vertical acceleration of the foot is conveniently a constant when traveling on the parabolic track with constant horizontal speed. That is

$$\ddot{y}_p = -\frac{v^2}{l_0} = \text{a constant} \quad (4.27)$$

Summarizing, we want to find the path of the body over half a step that entails the least positive work done by the vertical telescoping legs riding on a *parabolic* arc with constant horizontal velocity. The constraint is that the initial and final vertical speeds must be zero.

Galilean relativity Since the horizontal speed is assumed to be a constant in Problem B, the body will have no horizontal motion observing from an inertial frame moving with horizontal speed v . Since the foot of the vertical telescoping actuator is riding the parabolic arc, when the constant speed is subtracted out, the foot will be simply seen to be accelerating downwards with $-\ddot{y}_p$. Let us call this downward acceleration e .

$$e = -\ddot{y}_p \tag{4.28}$$

$$= \frac{v^2}{l_0} \tag{4.29}$$

Note further that the cost to be minimized (Equation 4.7) and the boundary conditions (Equation 4.8) also depend on only the vertical motion of the telescoping leg. Therefore, we can rewrite problem B with the parabolic track, just in terms of the vertical coordinates. This gives us what we will call the “elevator problem”.

The foot moving downwards with constant downward acceleration $e = -\ddot{y}_B = -\frac{v^2}{l_0}$ is most conveniently represented as being attached to an elevator moving downwards with constant acceleration e . Fig. 4.3 shows how we reformulate Problem B with a parabolic track in terms of a person riding the vertical elevator: a person has vertical telescoping legs and his foot is glued to the top of an elevator moving downwards with constant acceleration e . At time $t = 0$, both the person and the elevator are at the same position (without loss of generality). This initial state corresponds to mid-step — the apex of the parabolic (circular) arc. The person can push or pull on the elevator with his vertical telescoping legs. The person must have zero vertical velocity at time $t = \frac{t_{step}}{2}$. The objective is to meet this zero vertical velocity constraint by reacting against the elevator in a way that requires the least positive work.

Elevator problem in equations Fig. 4.3 shows the key variables in the elevator problem. Downward displacements and velocities are considered positive. y_e is the position of the elevator, y_m is the position of the mass m , and $y_r = y_e - y_m$ is the relative position of the elevator with respect to the mass. We find it convenient to visualize the motion of the particle in terms of y_r . In particular, most of the following discussions will use representation of the dynamics of the point-mass in the $y_r - \dot{y}_r$ plane.

At mid-step $t = 0$, the positions and the velocities of both the elevator and the mass are equal to zero: $y_e(0) = y_m(0) = y_r(0) = 0$ and $\dot{y}_e(0) = \dot{y}_m(0) = \dot{y}_r(0) = 0$. Thus this starting configuration is represented by the origin O in the $y_r - \dot{y}_r$ plane (Fig. 4.4a, b, c).

Since the elevator is accelerating downward constantly, $\dot{y}_e(t) = et$ and $y_e(t) = et^2/2$. In particular, $\dot{y}_e(\frac{t_{step}}{2}) = \frac{et_{step}}{2}$. Since a constraint is that the mass have zero vertical velocity at the end of the step, we have $\dot{y}_m(\frac{t_{step}}{2}) = 0$ and therefore, $\dot{y}_r(\frac{t_{step}}{2}) = \frac{et_{step}}{2}$. In other words, the final state at $t = \frac{t_{step}}{2}$ should lie somewhere on the line AB corresponding to $\dot{y}_r = \frac{et_{step}}{2}$ in the $y_r - \dot{y}_r$ plane (Fig. 4.4a, b, c). Thus goal in the elevator problem can be stated as being to take the state of the mechanical system from the origin O in the $y_r - \dot{y}_r$ plane to any point on the line AB in a given amount of time $\frac{t_{step}}{2}$, and with minimum positive work.

The vertical motion of the point-mass is governed by the equation: $m\ddot{y}_m = mg - F$, where F is the force exerted by the leg on the elevator (or vice versa). The differential equation for the relative position y_r is

$$m\ddot{y}_r = m\ddot{y}_e - m\ddot{y}_m \quad (4.30)$$

$$= me - mg + F \quad (4.31)$$

We wish to minimize the total positive work

$$C_e = \int_0^{t_{step}/2} [F(t)\dot{y}_r]^+ dt \quad (4.32)$$

Limit of infinite force-bounds Similar to our numerical calculations in Chapter 3, formally, we wish to determine the limit of the sequence of optimal solutions as the force-bounds in elevator problem increase without bound ($F_{max} \rightarrow \infty$ and $F_{min} \rightarrow -\infty$), for every combination of speed v and step-length d . However, we find it more convenient in the presentation below to informally allow infinite leg-forces, in particular, impulses that instantaneously change the vertical speed. The energetic costs of such impulses can be easily calculated.

Note that to show the similarity of Problem A with Problem B, and eventually with the elevator problem in the limit of small step-lengths, we assumed that the leg-forces, and consequently, the accelerations were bounded. We have not shown the similarity of the energetic costs of Problems A and B if the force-bounds go to infinity *before* the step-lengths go to zero. In fact, such a result is not true in general. However we imagine that asymptotic similarity of the energetic costs will fail only for gaits with irrelevantly large costs.

4.6 Optimal “gaits” in the elevator problem.

Walking and running in the elevator problem Forgetting our technical definition of analogous trajectories for a moment, “inverted pendulum walking” in the elevator problem can be most naturally described as riding the elevator till $t = \frac{t_{step}}{2}$ and then pushing-off impulsively against the elevator at exactly $t = \frac{t_{step}}{2}$ so that the vertical velocity of the person gets reset to zero. “Impulsive running”, on the other hand, is jumping impulsively off the elevator at $t = 0$ giving the point-mass an initial vertical velocity that ensures that the vertical speed at $t = \frac{t_{step}}{2}$ equals zero.

We will show below that these two elevator riding strategies are indeed the optimal solutions to the elevator problem (proposition 2). However, before we state and prove this result, we present some results about the structure of the problem in the $y_r - \dot{y}_r$ plane.

Constant energy contours Rearranging equation 4.31, we get

$$F = m(\ddot{y}_r + g - e) \quad (4.33)$$

The instantaneous mechanical power of this force (as used in equation 4.32) is given by:

$$P = F\dot{y}_r \quad (4.34)$$

$$= m(\ddot{y}_r + g - e)\dot{y}_r \quad (4.35)$$

$$= \frac{d}{dt} (m\dot{y}_r^2/2 + m(g - e)y_r) \quad (4.36)$$

$$= \frac{dE}{dt} \quad (4.37)$$

The final equation above simply notes that the leg power P is the time derivative of the total energy $E = m\dot{y}_r^2 + m(g - e)y_r$. Contours of constant energy E in the $y_r - \dot{y}_r$ plane play a key role in the proof of optimality of walking and running below. Generically, the constant energy contours are parabolas in the $y_r - \dot{y}_r$ plane. When $g > e$, the parabolas open leftward (Figure 4.4a), when $g < e$ the parabolas open rightward (Figure 4.4b), and when $g = e$, the parabolas degenerate into straight lines (Figure 4.4c). Note that the constant energy contours coincide with the trajectories corresponding to gravitational free-fall, with $F(t) = 0$ and $P(t) = 0$.

Note also that the total cost C_e can also be rewritten in terms of E .

$$C_e = \int_0^{t_{step}/2} [P]^+ dt \quad (4.38)$$

$$= \int_0^{t_{step}/2} \left[\frac{dE}{dt} \right]^+ dt \quad (4.39)$$

Feasible directions in the $y_r - \dot{y}_r$ plane The trajectory of the point-mass in the $y_r - \dot{y}_r$ plane is determined by the following equations (the second equation among which is the same as Equation 4.31).

$$\begin{aligned} \frac{dy_r}{dt} &= \dot{y}_r \\ \frac{d\dot{y}_r}{dt} &= e - g + \frac{F}{m} \end{aligned} \quad (4.40)$$

The tangent vector at some point (y_r, \dot{y}_r) on a given trajectory will be $\dot{y}_r \mathbf{i} + (e - g + \frac{F}{m}) \mathbf{j}$ where $\{\mathbf{i}, \mathbf{j}\}$ is the natural coordinate basis for the corresponding vector space.

The first element of this tangent vector tells us that the trajectory can only move to the right in the upper half plane ($\dot{y}_r > 0$) and to the left on the lower half-plane ($\dot{y}_r < 0$), clearly a property of all such phase planes. Since we impose no bounds on the force F , the second element of the tangent vector can be any real number. The set of feasible tangent vector directions is shown in Fig. 4.4d. All rightward directions are accessible in the upper half-plane and all leftward directions are accessible in the lower half-plane. The trajectory can only have a vertical tangent when at $\dot{y}_r = 0$. Note however that Fig. 4.4d is slightly misleading. The vectors in Fig. 4.4d are drawn to equal lengths only for convenience. They indicate only the feasible *directions*, but say nothing about the feasible *magnitudes* of the tangent vectors. Not every tangent-vector magnitude is possible in a given tangent vector direction. This means that while the tangent vectors of every trajectory must lie within the appropriate cone in Fig. 4.4d, the converse is not true (not every curve that has the tangent vector at every point pointing in the right directions can be a solution to Equations 4.40).

Time duration of a given trajectory in the $y_r - \dot{y}_r$ plane The time taken to go between two points P_1 and P_2 along a given trajectory in the $y_r - \dot{y}_r$ plane is given by

$$\text{Time duration} = \int dt = \int_{y_r(P_1)}^{y_r(P_2)} \frac{dy_r}{\dot{y}_r} \quad (4.41)$$

given that $\dot{y}_r \neq 0$ anywhere along the trajectory. We will now discuss how to modify this formula if the trajectory does intersect the $\dot{y}_r = 0$ axis. Note first that by choosing $F = mg - me$, the right hand sides of the Equations 4.40 become identically zero. For this choice of force, the $\dot{y}_r = 0$ becomes a fixed line. That is, arbitrary lengths of time can be spent on this line. So given some trajectory intersecting or starting from the $\dot{y}_r = 0$ axis, we cannot determine the time taken for the trajectory without knowing exactly how long was spent on $\dot{y}_r = 0$. So if a trajectory P_1P_2 intersects the $\dot{y}_r = 0$ axis at a point R , then the total time duration for the trajectory needs to be formally calculated as:

$$\text{Time duration} = \int_{y_r(P_1)}^{y_R(R^-)} \frac{dy_r}{\dot{y}_r} + \text{Time spent at } R + \int_{y_r(R^+)}^{y_r(P_2)} \frac{dy_r}{\dot{y}_r} \quad (4.42)$$

We will use this formula later in the proof of case 2 of proposition 2. We do not discuss the convergence properties of the improper integrals in Eq. 4.42 because the specific instances of this integral that we will consider will either be convergent by construction or their bounded-ness (or otherwise) will not affect the ensuing arguments.

Proposition 2. For the elevator problem, when $e > g$, “impulsive running” minimizes and when $e < g$, “inverted pendulum walking” is optimal.

Case 1. $g > e$ The goal is to move from the origin O to the line AB with the least positive work. We claim that the optimal strategy is to “walk”: that is, riding the elevator performing no work, and then at the last moment push-off impulsively to make the vertical velocity of the point-mass \dot{y}_m zero. In Fig. 4.4a this trajectory is represented by OM: riding the elevator with zero relative speed is equivalent to remaining at the origin O. And the line OM represents the change in vertical speed because of the impulsive push-off at the end. In other words, we claim that the optimal path from O to AB is the vertical line OM (Fig. 4.4a).

How do we show that OM is the optimal strategy? From the explanation in the previous paragraph, it is clear that OM is a feasible trajectory by construction. We now need to establish that every other feasible trajectory such as the dotted lines ON and OPQ (Figure 4.4a) necessarily require greater positive work. We shall consider two types of feasible trajectories.

1. **Trajectories entirely in the upper half-plane** Trajectories entirely in the upper half-plane can never move leftward, as discussed earlier. Starting from O, such a trajectory can reach any point on AB in the right half-plane. Clearly it is best to go straight up to M, because any point N to the right of M will lie on a higher-energy parabolic contour. So reaching N will have required higher positive work.
2. **Trajectories not entirely in the upper half-plane** We can extend the proof to paths not entirely lying in the upper half-plane by noting that for such paths, for example OPQ, where PQ is the part of the path that lies entirely in the upper half-plane.

$$\text{Cost OPQ} = \text{Cost OP} + \text{Cost PQ} \quad (4.43)$$

$$\geq \text{Cost OP} + \text{minimum cost from P to AB} \quad (4.44)$$

The cost for going from P to AB when restricted to the upper half-plane is minimized if Q is directly above P (repeating arguments from item 1). And this cost will be the same as that of OM (because the parabolas are equally spaced). Therefore

$$\text{Cost OPQ} \geq \text{Cost OP} + \text{Cost OM} \quad (4.45)$$

$$> \text{Cost OM} \quad (4.46)$$

Thus the any such path OPQ will necessarily be worse than OM as well.

Case 2. $g < e$ We claim that the optimal strategy in this case is to “run”: impulsive jump at $t = 0$ from O to R, then fly freely to S without doing any further work along a constant- E parabola. That is, we claim that ORS is the optimal trajectory.

Now consider an alternate path, say OT. A necessary condition for OT to have a lower positive work than ORS is that OT never touches an E -contour of higher

energy than RS. Consider such a path (Fig. 4.4d). This path will lie entirely below the path ORS. We will now show that any such a path that has lower positive work cannot satisfy all the constraints of the optimization problem.

One constraint of the optimization problem is that the total time take to go from O to AB is $t_{step}/2$. Therefore, candidate path OT needs to last for exactly the same time duration as the path ORS. We use the formula we derived earlier for the time taken (Equation 4.42). By construction, the time spent at O for the trajectory ORS is equal to zero (the impulse OR is applied immediately). So the time duration for path ORS is simply given by

$$\text{Time duration ORS} = \int_{y_r(O^+)}^{y_r(S)} \frac{dy_r}{\dot{y}_r} \quad (4.47)$$

Noting that $y_r(S) < y_r(T)$ and that

$$\dot{y}_r(y_r) \text{ on OT} \leq \dot{y}_r(y_r) \text{ on ORS.} \quad (4.48)$$

we have

$$\int_{0^+}^{y_r(S)} \frac{dy_r}{\dot{y}_r} < \int_{0^+}^{y_r(T)} \frac{dy_r}{\dot{y}_r} \quad (4.49)$$

Therefore,

$$\text{Time for ORS} < \text{Time for O}^+\text{T} \leq \text{Time for OT} \quad (4.50)$$

Summarizing, no path that has a lower cost than ORS can simultaneously reach AB in time. Thus the path ORS is the optimal strategy.

Case 3. $e = g$ We show below, by construction, that there are infinitely many globally optimal trajectories.

Consider trajectories that go from O to AB over which \dot{y}_r never decreases; that is, $\ddot{y}_r \geq 0$. Such “non-backtracking” trajectories also necessarily have $\dot{y}_r \geq 0$. Examples of such trajectories are OF, OG, OH in Fig. 4.4c.

How many such non-backtracking trajectories exist that go from O to AB in $t = t_{step}/2$? The equation of motion when $e = g$ reduces to $m\ddot{y}_r = F$. So all we need for such non-backtracking trajectories to exist is that, for $F > 0$:

$$\int_0^{t_{step}/2} \frac{F(t)}{m} dt = \frac{et_{step}}{2} \quad (4.51)$$

Clearly infinitely many $F(t)$ satisfy this equation. Now we will show that all these non-backtracking trajectories have the same cost, equal to the minimum possible cost.

When $e = g$, the power P simplifies to $P = m\ddot{y}_r\dot{y}_r$, which for non-backtracking trajectories is greater than zero by definition. But for $P \geq 0$, $[P]^+ = P$.

$$C_p = \int_0^{t_{step}} P dt \quad (4.52)$$

$$= \int_0^{t_{step}/2} m\ddot{y}_r\dot{y}_r dt \quad (4.53)$$

$$= \frac{m\dot{y}_r\left(\frac{t_{step}}{2}\right)^2 - m\dot{y}_r(0)^2}{2} \quad (4.54)$$

$$= \frac{m}{2} \left(\frac{et_{step}}{2}\right)^2 \quad (4.55)$$

A lower bound on the cost of going from O to AB is given by the energy difference between O and AB (note that AB is a constant energy contour for $e = g$). And every non-backtracking trajectory accrues a cost (Eq. 4.55) exactly equal to this lower bound.

Summarizing, all feasible gaits with non-tensional leg-forces ($F \geq 0$) are optimal when $e = g$.

4.7 Discussion

We have noted that e is just the centripetal acceleration while travelling on a circular arc: $e = \frac{v^2}{l_0}$. Thus the conditions $e > g$, $e < g$ and $e = g$ reduce to conditions on the classical Froude number $V = v^2/(gl_{max})$ as defined in Chapters 2 and 3.

When $V < 1$ and $e < g$, the elevator problem suggests that the best strategy is to ride the parabolic arc and push off at the last moment. This is essentially the description of the classic inverted pendulum walking.

Similarly, when $V > 1$ and $e > g$, the elevator problem suggests that the best strategy is impulsively push-off at mid-step, and fly through the air for the rest of the step. This is essentially the description of the classic impulsive running.

At speed $V = 1$ or $e = g$, the elevator problem suggests that all gaits that use only non-tensional leg forces ($F > 0$) have the same cost. The cost landscape is perfectly flat for a large part of the domain. This flatness of the cost-landscape suggests structural instability of the conclusion of non-uniqueness of the optimum strategy — that the optimal solution might be very sensitive to small changes in the model.

These results agree both qualitatively and quantitatively with the variety of optimization results presented in Chapters 2 and 3. However, we do not claim to have rigorously proved the optimality of walking and running for Problem A in the limit of small step-lengths. Nevertheless, the detailed similarity between the elevator problem and the original locomotion optimization problem is clear and possibly useful in aiding the intuition.

Repeating the observation we made in the previous chapter, whenever work is to be minimized, the optimal strategy seems to consist of largely passive work-free motions with brief periods of impulsive work. There are two ways to have zero leg power $P = F\dot{l}$. One is to set $F = 0$ and the other is to set $\dot{l} = 0$. Walking and running seem to utilize exactly these two mechanisms. In walking the body rides on a stiff-leg of constant length ($\dot{l} = 0$), not doing any work until the final moment when the trailing leg pushes off. In running, all the work is done in a brief impulse during mid-stance, and no further work is done during the flight phase ($F = 0$). We will encounter this optimal solution structure (consisting of brief impulses and mostly work-free motions) again in the next chapter, where we derive work-optimal strategies for swinging a pendulum (leg).

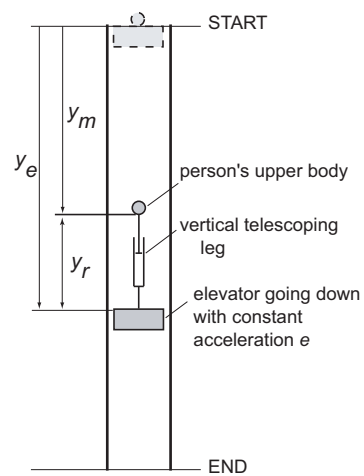


Figure 4.3: **Problem C: Riding an accelerating elevator.** Both the point-mass and the elevator start at the same position (START) with zero vertical speeds. The elevator maintains a constant downward acceleration e . The point-mass can react push or pull against the elevator using arbitrarily strong vertical telescoping legs. When the elevator reaches END, the vertical speed of the point-mass should again be zero. The objective is to ensure this by doing the least amount of work with the vertical telescoping legs.

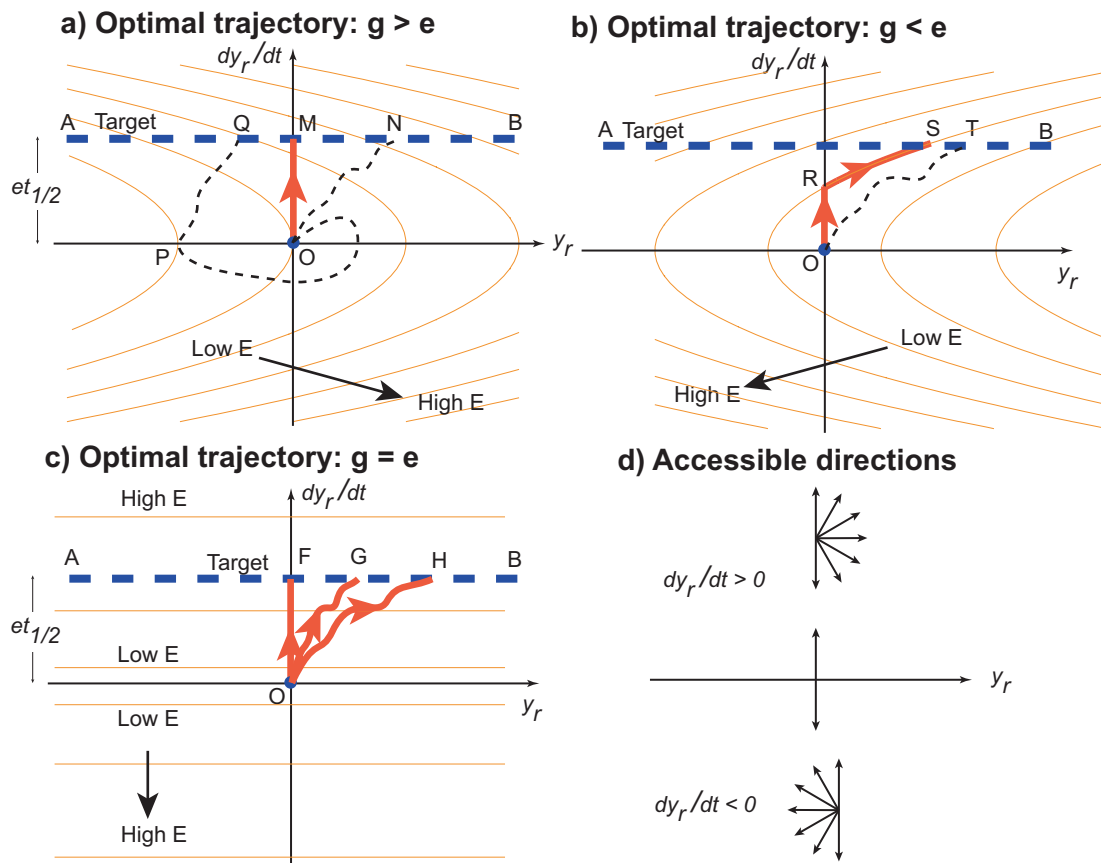


Figure 4.4: **Solution to the elevator problem.** (a), Case 1: $g > e$. The thin parabolic contours are constant energy lines. The goal is to go from the origin O to the dotted line AB with the least positive work. Optimal strategy is the vertical line OM . Two alternate suboptimal strategies ON and OPQ are shown as thin dashed lines. (b) Case 2: $g < e$. Optimal strategy is the path ORS . An alternate path OT is shown as a thin dotted line. (c), Case 3, $g = e$. All trajectories (e.g., OF , OG , OH) that do not backtrack have the same cost and hence are optimal. (d) shows the set of accessible velocity directions – directions in which the trajectory can proceed. In the upper half-plane, the trajectories can never move left. In the lower half plane, the trajectories can never move to the right. No magnitude information is intended by the equal length of the arrows.

Chapter 5

Cost of swinging the leg.

5.1 Introduction

During walking, the vertical position of the hip is nominally periodic at the same frequency as the the step frequency. A natural conjecture is that the motion of the swing leg during walking is powered entirely by the vertical motion of the hip. However, it has been shown that the motion of the the swing leg during walking is powered, in part, by the hip muscles (Braune and Fischer, 1895-1904) and requires some energy (Marsh et al., 2004).

The amount of energy required by the hip muscles to swing the leg through a given angle in a given amount of time will depend to an extent on the motion of the hip. Nevertheless, it may useful to understand how much energy a person takes to swing his leg when his hip is held at rest. Here we will discuss some simple models of the energetics of swinging.

5.2 Model of leg-swinging: No tendons

Following Doke et al. (2005), we model the leg as a compound pendulum attached via a torque motor to an immovable object of infinite inertia (Fig. 5.1). The pendulum has mass m , moment of inertia I about the center of mass, and the center of mass is situated at a distance r away from the pivot. The motor effectively models all the muscles articulating the hip — both the agonists and the antagonists. For simplicity, this motor is assumed to be able to produce arbitrarily high torques, and arbitrary time-histories of torque. So, for example, impulsive torques that change the angular speed instantaneously are assumed to be possible.

When the torque time-history $Q(t)$ is bounded, the motion of the leg can be described by

$$(I + mr^2)\ddot{\theta}(t) + mgr \sin \theta = Q(t). \quad (5.1)$$

A particular gait might require the legs to move in a periodic manner with specified amplitude and frequency. Given that the motor in this model can produce arbitrary torque time-histories, we wish to determine the torque time-history that minimizes the total positive work per period of oscillation of the pendulum — for a given time period of swing $t_s = 1/f_s$ and given swing amplitude θ_{max} . The positive work over a period is:

$$W_p = \int_0^{t_{swing}} [Q(t)\dot{\theta}(t)]^+ dt, \quad (5.2)$$

where $\dot{\theta}(t)$ is the angular velocity.

We will consider only swinging that is symmetric about the vertical. We require the pendulum to go from $\theta = -\theta_{max}$ to $\theta = \theta_{max}$ and back in one swing.

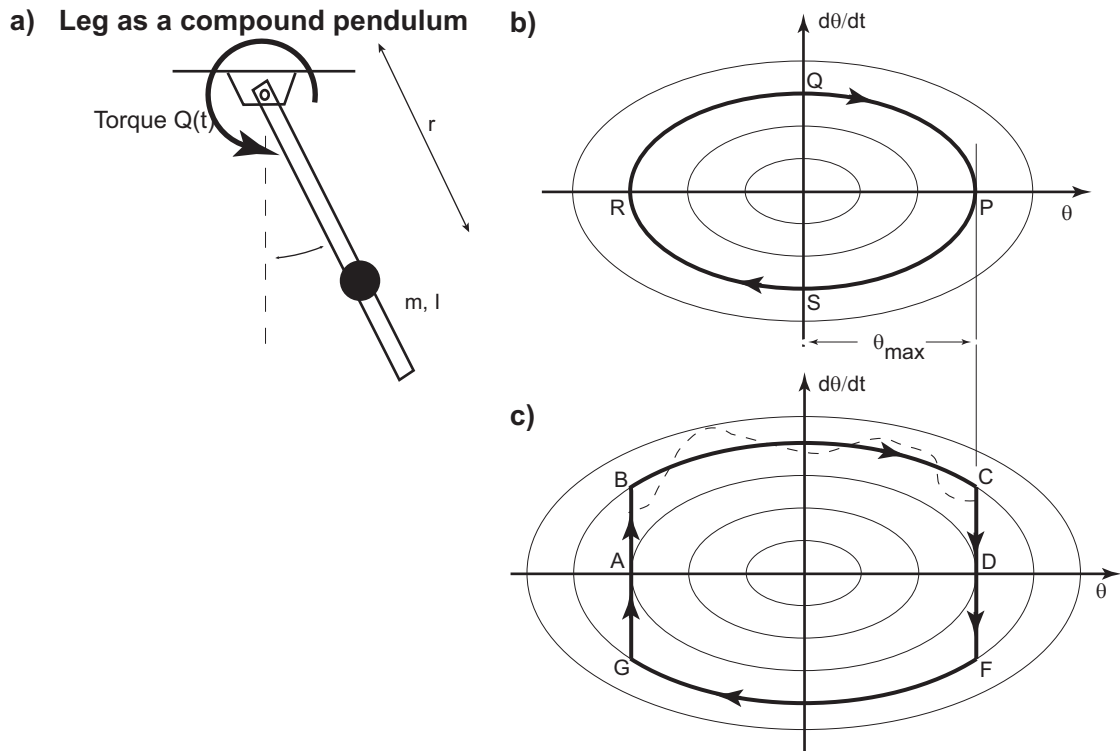


Figure 5.1: **Mechanics of leg-swinging.** (a) The leg is modeled as a compound pendulum attached to a rigid support. (b) Phase portrait θ vs. $\dot{\theta}$ for the pendulum. The concentric ellipses denote constant energy contours for the mechanical system; the ellipses coincide with the trajectories of unforced oscillations of the pendulum. Thick solid line is the optimal motion for amplitude θ_{max} when the required swing frequency is less than or equal to the natural frequency at this amplitude. (c) Thick solid line is the optimal motion for a swing frequency greater than the natural frequency at the given θ_{max} .

5.2.1 Strategies for the total positive work

Since we are dealing with a compound pendulum, and not a simple harmonic oscillator, the natural frequency of oscillation f_n depends on the amplitude θ_{max} ; that is, $f_n = f_n(\theta_{max})$. And for any specific amplitude of oscillation, we can discuss three different cases: swinging the pendulum at a frequency that is 1) equal to, 2) less than, or 3) greater than the natural frequency of oscillation. As we shall see below, the optimal solutions for case-2 and case-3 are qualitatively different from each other and case-1 is at the interface of these other two cases.

Case 1: $f_s = f_n$, swinging at the natural frequency Clearly swinging at the natural frequency requires no actuator work, positive or negative. Completely passive swinging is work-free and hence optimal. In Fig. 5.1a curve PQRSP is the passive oscillation corresponding to given amplitude θ_{max} , and therefore optimal.

Case 2: $f_s < f_n$, swinging slower than the natural frequency Symmetric swinging slower than the natural frequency can be achieved with zero actuator work as well. The optimal strategy is to let the swinging be completely passive. However, with no intervention, passive swinging would take less time than the required oscillation period t_s , because $f_s < f_n$. To use up the extra time to get a slower swinging frequency, the torque actuator can simply hold the pendulum motionless for the appropriate amount of time (a total time of $\frac{1}{f_s} - \frac{1}{f_n}$) at the end of each swing. Since the natural oscillatory motion has zero velocity at the end of each swing, the motor does not have to perform mechanical work to bring the velocity to zero. All it has to do is provide some additional torque to hold the pendulum at rest at one of its extreme positions. Thus in Fig. 5.1b, the trajectory PQRSP is again the optimal trajectory, except that the pendulum spends some time at points P and R.

Case 3: $f_s > f_n$, swinging faster than the natural frequency Swinging faster than natural frequency requires non-zero work. We claim that the work-optimal strategy corresponding to a specified amplitude θ_{max} is ABCDFGA, as shown in Fig. 5.1c. In this work-optimal strategy, the pendulum is momentarily at rest at state A. The torque actuator impulsively accelerates the pendulum to state B — a finite change in velocity in infinitesimal time. The pendulum then swings passively from state B to state C. This passive swing, because it happens with a higher speed, covers the same oscillation amplitude in less time than the ellipse directly connecting states A and D — so that the appropriate high frequency f_s can be achieved. When $\theta = -\theta_{max}$ is reached, the trajectory discontinuously jumps to state A and so on.

In summary, we claim that the optimal motion has basically passive motions BC and FG for all time but for brief periods at the beginning and end of a swing when there is rapid acceleration and deceleration. It is at these brief periods that all the work is done and all the cost is incurred.

How do we prove that this strategy minimizes the positive work? Consider, for simplicity but with no loss of generality, the problem of going from A to D with minimum positive work. Let us consider an alternative route from A to D, suggested by the dotted line in Fig. 5.1. Any such alternate route cannot lie entirely below ABCD. An alternate route lying entirely below ABCD (that is, one that has lower $\dot{\theta}$ for every θ) can be shown to have a time duration that would be longer than of ABCD. Therefore for the alternate route to last for the same duration as the path ABCD, the alternate route must necessarily go above ABCD by at least a little bit (or be identical to ABCD).

We shall now show that any such alternate route will necessarily require more positive work. Note that the concentric ellipses are also constant total energy contours and bigger ellipses correspond to greater energy. Therefore, moving from an inner ellipse to an outer ellipse requires some positive work (equal to the difference in their energies). Since the dotted path necessarily touches an outer ellipse, the pendulum on the dotted path has at some point a higher total energy than it ever has on ABCD. This means that it required more positive work than ABCD (where no negative work is performed until the last moment).

Overall, this optimization problem is qualitatively similar to minimizing the positive work required to move a mass on a frictionless floor through a given distance in a specified amount of time, starting from rest and ending at rest. The strategy again is to accelerate impulsively to the required average speed, coast for the entire distance, and impulsively decelerate to a stop at the last moment. The key is that the accelerations and the decelerations are impulsive. If they are not impulsive, the speed of the mass will have to be higher than the (specified) average speed at some point during the motion — and achieving this higher speed will require more positive work than simply reaching exactly the average speed impulsively.

5.3 Analytical expressions for the cost of impulsive work.

We now derive an approximate expression for the cost of the work-optimal swinging described above. The equations of motion for the passive oscillation of a pendulum can be solved in closed form in terms of elliptic functions. However, it is easier and perhaps more enlightening to consider the small amplitude approximation of the dynamics of the pendulum with a simple harmonic oscillator. The equation for the approximating simple harmonic oscillator is:

$$\ddot{\theta} + \omega_n^2 \theta = \frac{Q(t)}{I + mr^2}, \quad (5.3)$$

where $\omega_n = \sqrt{mgr/(I + mr^2)}$ and $f_n = \frac{\omega_n}{2\pi}$ is the natural frequency of oscillation. This equation has a family of oscillatory solutions given by $\theta(t) = \theta_0 \sin(\omega_n t)$, each θ_0 corresponding to a different ellipse in the small angle version of Fig. 5.1b,c.

The positive work done on the path ABCDFG in Fig. 5.1b is simply equal to twice the energy difference between the inner ellipse motion with swing amplitude θ_{max} and the outer ellipse of which BC and FG are segments. Let the swing amplitude corresponding to the bigger ellipse (BC-FG) be θ_b . The passive oscillatory solution corresponding to this ellipse has $\theta(t) = \theta_b \sin \omega_n t$. Since the motion ABCDFG takes time t_s , BC should require a duration $t_s/2$. And θ at C is equal to θ_{max} . This gives $\theta_{max} = \theta_b \sin(\frac{\omega_n t_s}{4})$.

The maximum angular speed corresponding to a constant energy ellipse corresponding to $\theta(t) = \theta_0 \sin \omega_n t$ is $\omega_n \theta_0$. The energy corresponding to this constant energy ellipse is equal (up to a constant) to the maximum kinetic energy: $0.5(I + mr^2)(\omega_n \theta_0)^2$. Therefore, the total positive work over ABCDFG is given by:

$$W_{p/ABCDFG} = 2 \cdot \frac{1}{2} (I + mr^2) \omega_n^2 (\theta_b^2 - \theta_{max}^2) \quad (5.4)$$

$$= mgr \theta_{max}^2 \left(\frac{\theta_b^2}{\theta_{max}^2} - 1 \right) \quad (5.5)$$

where $\theta_b = \theta_{max} / \sin(\omega_n t_s / 4)$. In Fig. 5.2, we plot the non-dimensional quantities $W_{p/ABCDFG} / (mgr \theta_{max}^2)$ and f_s / f_n .

A useful comparison case is work-optimal oscillation in the absence of gravity. This problem is identical to the problem of moving a block on the frictionless floor discussed earlier. The positive work of the impulses in this case is given by

$$W_{p/nogravity} = \frac{(I + mr^2) \theta_{max}^2 \omega_s^2}{\pi^2} = mgr \theta_{max}^2 \frac{4 \omega_s^2}{\pi^2 \omega_n^2}. \quad (5.6)$$

For swing frequencies sufficiently larger than the natural frequency, the cost of work-optimal leg-swinging in the presence of gravity is essentially different by only an additive constant from the cost of optimal leg-swinging in the absence of gravity.

We can compare the optimal swinging cost derived above with the cost for an exactly sinusoidal oscillation at the appropriate frequency f_s as derived in Doke et al. (2005),

$$W_{p/sinusoid} = mgr \theta_{max}^2 \frac{|\omega_n^2 - \omega_s^2|}{\omega_n^2}. \quad (5.7)$$

So far, we have considered the cost to be proportional to only positive work. What happens when we add to this work-cost, a cost for muscle force proportional to the integral of the force, in this case the torque $Q(t)$: $\int_0^{t_s} |Q(t)| dt$? For swinging at the natural frequency, the optimal cost will still be equal to zero. For $f_s < f_n$, presumably, there will now be a non-zero optimal cost and the optimal swinging strategy may not be the same as the work-optimal strategy. On the other hand, for $f_s > f_n$, the new optimal swinging strategy will be the same as the work-minimizing strategy (as perhaps alluded to in Kuo, 2001). The optimal energetic cost will now have an extra component proportional to the integral of the impulsive torques.

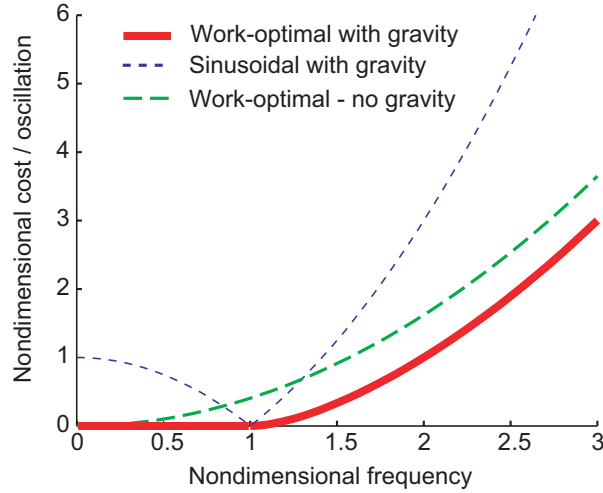


Figure 5.2: Nondimensional positive work $W_{p/oscillation}/mgr\theta_{max}^2$ as a function of the ratio of swing frequency and natural frequency $\frac{\omega_s}{\omega_n}$. Three cases are shown. Solid curve is the cost of work-minimizing strategy in the presence of gravity. Thick long-dashed curve is work-minimizing in the absence of gravity. Thin short-dashed curve is the cost of a sinusoidal oscillation at the required frequency.

5.4 Effect of tendons

We will now briefly discuss the effect that elastic tendons might have on the energetics of swinging the leg. The mechanical system in Fig. 5.1a can be augmented with a torsional spring (tendon) in series with the torque motor (muscle). The mechanical system shown in Fig. 5.3b is formally equivalent to the small angle approximation of such a mechanical system. The mass M in Fig. 5.3b corresponds to the rotational inertia about the pivot of the pendulum in Fig. 5.1a. Other system components in the pendulum model have similar obvious analogs in Fig. 5.3b. Here, the tendon is represented as a linear spring in series with the muscle, which is now represented as a linear telescoping actuator. Gravity can be treated as a spring of effective stiffness k_g in parallel with the muscle. Absence of gravity can be studied by removing this parallel spring from the model, as in Fig. 5.3a.

Discussion of the work-optimal swinging of the mass M in the context of these models is beyond the scope of this chapter. Instead we will simply consider the energetic cost required for sinusoidal oscillation of the mass. Further, we will consider only the no-gravity case in detail. Assume that the motion of the mass is sinusoidal with amplitude A and frequency $\omega_s/(2\pi)$: $x_m(t) = A \sin(\omega_s t)$. Noting that the equation of motion for the mass is $m\ddot{x}_m + k(x_m - x_f) = 0$, we have

$$x_f = \frac{A(k - M\omega_s^2)}{k} \sin(\omega_s t) \quad (5.8)$$

The positive work performed by the muscle over a single oscillation is given by

$$W_{muscle}^+ = \int_0^{\frac{2\pi}{\omega_s}} [F\dot{x}_f]^+ dt \quad (5.9)$$

$$= \int_0^{\frac{2\pi}{\omega_s}} [M\ddot{x}_M\dot{x}_f]^+ dt \quad (5.10)$$

$$= \int_0^{\frac{2\pi}{\omega_s}} \left[\frac{MA^2}{k} \omega_s^3 (k - M\omega_s^2) \sin(\omega_s t) \cos(\omega_s t) \right]^+ dt \quad (5.11)$$

$$= MA^2\omega_s^2 \left| 1 - \frac{M\omega_s^2}{k} \right| \quad (5.12)$$

As would be expected, the energetic cost per oscillation is zero when $\omega_s = \sqrt{k/M}$, the natural frequency of the spring-mass system. But more significantly, we see that for large swing frequencies $\omega_s \gg \sqrt{k/M}$, the positive work per swing scales like ω_s^4 . Thus the positive work increases much faster with the frequency than in the no-tendon case discussed earlier, in which the cost per swing scales like ω_s^2 (Eq. 5.6).

The key observation here is that the positive work done by just the muscle can be (and is) very different from the total work done on the mass (by the muscle-tendon complex). The total work performed on the mass is given by

$$W_{total}^+ \text{ over one period} = \int_0^{\frac{2\pi}{\omega_s}} [F\dot{x}_m]^+ dt \quad (5.13)$$

$$= \int_0^{\frac{2\pi}{\omega_s}} [M\ddot{x}_M\dot{x}_m]^+ dt \quad (5.14)$$

$$= \int_0^{\frac{2\pi}{\omega_s}} [MA^2\omega_s^3 \sin(\omega_s t) \cos(\omega_s t)]^+ dt \quad (5.15)$$

$$= MA^2\omega_s^2 \quad (5.16)$$

From Eq. 5.12 and Eq. 5.16, we see that the muscle work scales differently from the total work on the leg. Taking the ratio of these two quantities,

$$\frac{W_{muscle}}{W_{total}} = \left| \frac{M\omega_s^2}{k} - 1 \right| \quad (5.17)$$

Eq. 5.17 shows that for sufficiently high values of ω_s , the positive muscle work can far exceed the total positive work on the leg. This suggests (as Alexander remarks elsewhere) that springs in series with the muscles can either be energetically beneficial or be energetically detrimental depending on the operating frequency range relative to the natural frequency of the system.

With the inclusion of gravity (Fig. 5.3b), there are two key “natural frequencies”. The first natural frequency $\omega_{n1} = \sqrt{k_g/M}$ is due to gravity acting in isolation when the muscle not activated (and therefore the spring is slack). The second

natural frequency $\omega_{n2} = \sqrt{(k + k_g)/M}$ is with the muscle activated isometrically (no change in length), so that the two springs act in parallel. When the swing frequency is sufficiently higher than this second frequency, we suppose that the energetic cost per oscillation will scale like ω_s^4 as in the no-gravity case discussed above.

5.5 Discussion

There is electromyographic evidence that during walking (Basmajian and De Luca, 1985) and during isolated leg-swingin (Doke et al., 2005), the swing-leg muscle activity is large at the beginning and end of the swing phase, but relatively small during most of the swing phase. This muscle activation strategy seems similar to the work-optimal strategy discussed here in the absence of tendons. On the other hand, we note that muscles act like low-pass filters and impulsive forces are not really possible.

Doke et al. (2005) has pointed out that positive work alone cannot explain the rapidity of the rise in metabolic cost as a function of frequency. And that the rapid increase in metabolic cost could be explained with a dependence of cost on a higher derivative of force. To support these conjectures, subjects were asked to swing their leg at various frequency-amplitude combinations that ensure that the *total* work done on the leg is approximately a constant. It was found that although the total work rate on the leg was kept constant, the metabolic rate still increased with frequency. While this result is indeed consistent with a cost proportional to the rapidity of the changes in muscle forces, it is also consistent with the behavior of a work-based energetic cost in the presence of tendons, as discussed in the previous section (muscle work can be much more than the work on the leg). Eq. 5.17 indicates that when the total work is kept a constant, the muscle work increases with the second power of frequency — similar to the $\omega_s^{2.5}$ suggested by Doke. Of course, for this purely work-based theory to be relevant, recall that the swing frequencies need to be sufficiently higher than the effective natural frequency $\sqrt{(k_g + k)/m}$.

From the data in Doke et al. (2005), we can determine the ratio of the total work on the leg and the metabolic cost. This ratio is around 0.1 — this number can be treated as an upper bound on the muscle efficiency if there were no tendons (no spring work). This unusually low muscle efficiency can then be explained by a cost for rapid force production. But as before, this unusually low “apparent” muscle efficiency can, in theory, be explained by the presence of tendons, since the muscle work can be much higher than the actual work on the leg at high enough swing frequencies. We conclude that distinguishing the energetic costs of work and force production requires that the experimental swing frequencies not be much higher than, and preferably lower than, the effective natural frequency of the human leg $\omega_{n2} = \sqrt{(k_g + k)/m}$.

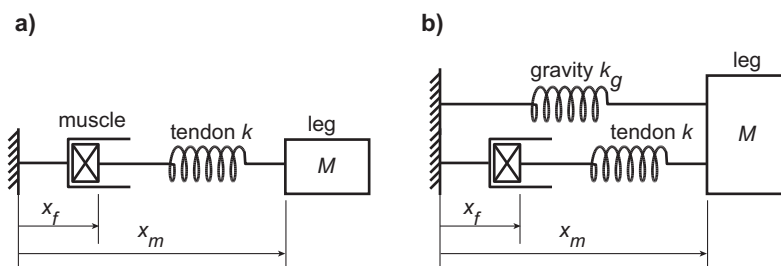


Figure 5.3: **Leg-swinging with tendon springs** (a) shows a model for the leg in the absence of gravity. (b) gravity in a simple pendulum model is equivalent to a spring in parallel to the muscles.

Chapter 6

Power laws: why cost of swinging is approximately a constant proportion of the total cost of locomotion.

6.1 Introduction

The total metabolic cost of legged locomotion can be approximately partitioned into two parts – one corresponding to the energy required to swing the legs, and another for the work and force of the leg muscles during stance. As an animal moves faster, both the stance cost and the leg-swing cost typically increase. Marsh et al. (2004) show that as the speed of locomotion (in running turkeys) is varied, the ratio of these two cost components is approximately constant, as measured by blood flow to the respective muscles¹.

Assuming a generic power law relation for each of the cost components, we show that the constancy of the ratio of stance cost and leg-swing cost can be qualitatively explained by metabolic cost optimization. This constancy of the ratio follows from a general property of power laws, and is independent of any specific details of the actual power laws assumed for the metabolic cost components.

6.2 Optimal trade-off between two power laws

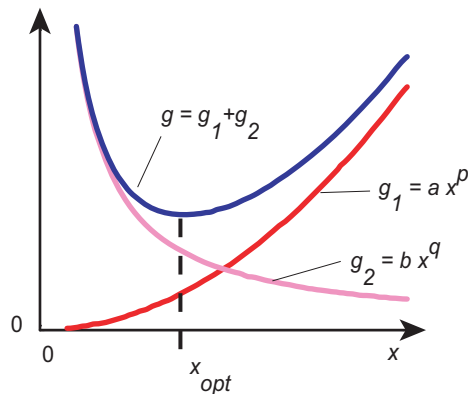


Figure 6.1: Minimum of the sum of two power law functions.

First we present an elementary calculus result about power laws we shall use later. Why are we interested in power laws? Because as we will discuss later, the individual cost components seem to be approximated well by power laws.

¹Muscles that are active during a leg's stance phase seem to be largely inactive during the swing phase and vice versa.

Consider two functions $g_1(x)$ and $g_2(x)$ (Fig. 6.1). g_1 is a simple increasing power-law function of x : that is, $g_1(x) = ax^p$ with $p > 0$. And $g_2(x)$ is a simple decreasing power-law function of x : that is, $g_2(x) = bx^q$ with $q < 0$. Clearly $x = 0$ minimizes g_1 , and $x = \infty$ minimizes g_2 . The sum of these two functions, $g(x) = g_1(x) + g_2(x)$, has a minimum x_{opt} somewhere in between. x_{opt} is obtained by differentiating g with respect to x and setting the result equal to zero:

$$\frac{dg}{dx} = apx_{opt}^{p-1} + bqx_{opt}^{q-1} = 0 \quad (6.1)$$

The above equation is easily solved for x_{opt} . Multiplying Eq. 6.1 by x_{opt} and rearranging, we obtain an expression for the ratio of g_1 and g_2 at x_{opt} .

$$\begin{aligned} apx_{opt}^p + bqx_{opt}^q &= 0 \\ \frac{ax_{opt}^p}{bx_{opt}^q} &= \frac{-p}{q} = \frac{g_1(x_{opt})}{g_2(x_{opt})} \end{aligned} \quad (6.2)$$

So the ratio of the two components ax_{opt}^p and bq_{opt}^q is $-p/q$, a constant that does not depend on the weights a and b .

For example, the ratio of the first and second term at the minimum of $F_1(x) = 0.01x^{-2} + 1000x^4$ is exactly the same (equal to $\frac{2}{4} = \frac{1}{2}$) as the ratio of the first and second term at the minimum of $F_2(x) = 1000x^{-2} + 0.01x^4$, despite the widely different weights on the power laws.

6.3 Metabolic cost components can be approximated by power laws

The basic hypothesis is that animals move in a manner that minimizes the metabolic cost of locomotion per unit distance. The relevant cost of locomotion E_{loc} can be defined as the total metabolic cost during locomotion minus the resting metabolic cost. As discussed in the introduction above, we model E_{loc} as the sum of the two terms, the stance cost E_{stance} and the swing cost E_{swing} , both per unit distance. The magnitude of these terms will depend both on the speed v of locomotion and on the stride rate f , or equivalently, the step-length d . For example, keeping the speed constant and varying the stride rate, or vice versa, changes the magnitudes of the costs. While swing cost and stance cost will depend on many other details of the muscular coordination as well, for simplicity, they can be assumed to be functions of only the speed and the stride rate. This assumption is equivalent to using the costs for the gait with optimal muscle-use for a given speed and stride rate.

In some simple mathematical models of animal mechanics, and in experiments, the individual cost terms seem to be relatively well-approximated by power laws. The stance cost per unit distance is of the form:

$$E_{stance} = b_1 v^\alpha f^\beta. \quad (6.3)$$

Simple curve-fits to running data (Kram and Taylor, 1990) and simple models of running (for instance, Equation 2.34 for impulsive running here; see also, Ruina et al., 2005; Srinivasan and Ruina, 2006) give a power law dependence for the cost. Also, assuming a metabolic cost proportional to work, maximum force, integral of force, or any other plausible physical quantity, each separately results in such a power law for the cost of the so-called step-to-step transition in walking (Eq. 2.11 here and also, Kuo, 2001; Ruina et al., 2005). The power law dependence described above for the cost of stance can be lost if more than one of these cost mechanisms (work, force, etc) has a substantial contribution – that is, if we imagine that stance cost as the sum of two or more cost components.

The swing cost per unit distance is assumed to have the same power-law functional form, $E_{swing} = b_2 v^\gamma f^\delta$. This is again approximately true, especially for not-too-small frequencies, as suggested by Doke et al. (2005). Also, our simpler work-based estimations of the leg-swing cost in the previous chapter, are amenable to approximation by power laws.

Both simple models of leg-swinging and simple experiments indicate that $\delta > 0$. i.e., leg-swinging cost at any given speed increases with stride frequency. Similarly, in reality and in models, for a given speed, E_{stance} decreases with increasing f , so $\beta < 0$. The total cost of locomotion E_{loc} is given by,

$$E_{loc} = E_{stance} + E_{swing} = b_1 v^\alpha f^\beta + b_2 v^\gamma f^\delta. \quad (6.4)$$

6.4 Optimal trade-offs between the stance and leg-swing cost

For a given velocity v , humans and animals tend to pick the step length f_{opt} that minimizes their cost of locomotion (Högberg, 1952; Zarrugh et al., 1974; Bertram and Ruina, 2001; Kuo, 2001). The optimal stride frequency f_{opt} for a given speed v might be obtained by differentiating Eq. 6.4 with respect to f , and setting it equal to zero. Thus,

$$\frac{dE_{loc}}{df} = \beta b_1 v^\alpha f_{opt}^{\beta-1} + \delta b_2 v^\gamma f_{opt}^{\delta-1} = 0. \quad (6.5)$$

Following the derivation of Eq. 6.2, we obtain an expression for the ratio of E_{swing} to E_{stance} .

$$\frac{E_{swing}(v, f_{opt})}{E_{stance}(v, f_{opt})} = \frac{b_2 v^\gamma f_{opt}^\delta}{b_1 v^\alpha f_{opt}^\beta} = -\frac{\delta}{\beta}. \quad (6.6)$$

The ratio E_{swing}/E_{stance} is a positive constant because $\delta > 0$ and $\beta < 0$, as noted earlier. Since the ratio E_{swing}/E_{stance} depends only on the constant exponents of the step length in the power laws, the constant is independent of the speed v , weighting coefficients b_1 , b_2 , or the exponents of v .

From Eq. 6.6 we deduce that $E_{stance}/E_{loc} = \beta/(\beta - \delta)$ i.e., the simple model predicts that the stance cost (and the swing cost) are constant fractions of the total cost as the speed is varied. The stance cost and swing cost increase in direct proportion to the total cost. In particular, if the costs were proportional to mechanical work of the muscles, positive work during stance should be proportional to the total metabolic cost.

6.5 Discussion

Running turkeys. In a recent experimental study, Marsh et al. (2004) performed detailed measurements of blood flow to various muscles in turkeys running at different speeds. They found that the leg-muscles that are most active during stance are relatively inactive during swing, and vice versa. This observation enabled them to estimate the ratio of the metabolic cost for these two activities from the ratio of the total blood flow to the muscles contributing to leg swing and stance, respectively. They found this ratio to be roughly constant (approximately equal to 1/3) as the velocity is varied, just as our simple theory predicts.

Interestingly enough, the simple energetic models of both walking and running give the same fraction $E_{swing}/E_{stance} = 1/3$. For walking, the simplest model suggests $\beta = -1$ (Kuo, 2001; Ruina et al., 2005; Srinivasan and Ruina, 2006, and Chapters 2 and 3 here) and for running the simplest model again suggests $\beta = -1$ (Ruina et al., 2005). Doke et al. (2005) gives the scaling for leg swing ($\delta = 3$). Using these numbers in Eq. 6.6, we again obtain $E_{swing}/E_{stance} = -\delta/\beta = 1/3$. The quality of these predictions is perhaps too good for the simple model here, and more experimental data is needed to test the validity of the simple explanation here.

External work and metabolic cost in walking and running The so-called “external work” is often used as an approximate estimate of the work done by the legs during stance (Cavagna, 1975, also see relevant section in chapter 2). We could check if this estimate of stance cost is proportional to the total metabolic cost as the speed of locomotion is changed. Experiments in running have shown that the “external work” is indeed approximately proportional to the total metabolic cost as the speed is varied (Cavagna et al., 1964, and Figure 2.7). The situation for walking seems to be similar. Re-analyzing published data (Bobbert, 1960; Kuo et al., 2005) we find that there is not as good a proportionality between the measured metabolic cost and the external work as the speed is increased (Fig. 2.4). However, in both cases, the actual constant of (approximate) proportionality suggests an excessively high muscle efficiency (again Fig. 2.7), thus implying an elastic work component (much more so in running than in walking).

When costs are not quite power laws. We must emphasize that the power law description of the cost is merely a crude approximation. More complete models

of cost, that do not exactly give power laws, might show deviations from proportionality (e.g., 10-15% deviation in walking, Kuo, 2001)) over the relevant range of speeds.

6.6 Conclusions

We have presented a simple way of understanding the apparently constant partitioning of the metabolic cost of legged locomotion suggested by some experiments. This explanation is especially powerful as it requires very little information about the specific trends in the metabolic costs.

Chapter 7

Conclusions

We have presented arguably the simplest first-principles models of the various aspects of legged locomotion. A key contribution is the presentation of a minimal model of a bipedal animal (chapters 2–3 and Alexander, 1980), which could locomote in a variety of different ways. When appropriately nondimensionalized, the minimal model has exactly zero parameters. This makes the model amenable to extensive analysis: the chapters 2–4 were essentially an elaboration of what happens when this minimal animal moves in specific ways, and how this minimal animal ought to move if it wished to move in a manner that minimized the work done by its muscles.

In particular, we found that in chapter 2, the classical descriptions of walking (inverted pendulum walking) and running (impulsive running and the pogostick model of running) were special cases of this more general minimal model. We then used the model to describe some less familiar gaits such as level walking and skipping. We found that if the only gaits the animal could use were walking, running, skipping, or level-walking – it was best to walk when going slow, and run when going faster, and maybe level-walk at a small range of intermediate speeds. Skipping was always a little worse than running.

We then formulated a more general question – which gait among all the periodic gaits (with a certain reasonable structure) the minimal model is capable of, requires the least positive work for a given speed and step-length. This question and its answer in Chapter 3 was another key contribution of this thesis. Alexander had explored this question with a three parameter family of gaits that was somewhat based on what animals perform already. We extended this work, answered a more general question, explored a greater variety – conceptually infinite-dimensional space – of gaits, not in any significant way informed by experimental observations.

By asking a more general question, we obtained simpler results. Numerical optimization found that the two classic descriptions of walking and running are actually two of the three optimal gaits for this minimal model. This is an especially satisfactory result – the optimization of the simplest model discovers its simplest special cases as optima. The result is also somewhat amusing because there is no way anyone could have known, without doing the calculations reported here, that the simplest descriptions (over 1940 - 1975) of walking and running were actually energetically optimal in any sense, let alone for the same model.

A curious aside in this story was the discovery of a third (optimal) gait by the optimization, that we have dubbed the pendular run. While this prediction might well turn out to be an artifact of the model defects, its discovery is indicative of the optimization’s ability to generate novel hypotheses.

Discovery of impulsive running by the optimization, for instance, indicates that elasticity in the leg-muscle-tendons is not necessary for running to energetically beneficial. And even without elasticity, running should “look” elastic to be energetically optimal. A classic hypothesis in biomechanics was that the smoothest

level-walking gait would be perfectly optimal. This, we showed in chapter 2, is far from being the case. Indeed, normal walking and running – especially their optimal idealizations – while consuming much less energy than the smoother gaits, are also particularly non-smooth with rapid changes in velocity during some parts of the stance phase.

We confirmed the results of the extensive numerical optimizations of Chapter 3, by providing an analytical proof of optimality for walking and running in a tractable simplification of the minimal model (chapter 4). It turns out that we can obtain some insight into perhaps the fundamental question in the study of bipedal locomotion (why are particular gaits preferred over others?) by essentially elementary, and somewhat informal, mathematical arguments.

The structure of the optimal solutions described in Chapters 3, 4, 5 serves as a textitpost hoc rationalization of a recent trend in robotics, especially the sub-field of robotics that concerns itself with the development of legged robots – the development of the so-called *passive dynamic robots*. Pioneered by Tad McGeer (McGeer, 1990b,c,d, 1992), these passive dynamic robots were initially designed as going downhill powered only by gravity, but have since been minimally modified to walk on level ground (Collins et al., 2005). The first robots were completely passive (powered by gravity) and the more recent robots have largely passive motions, with minimal injections of motor power. One motivation for the building of such robots is energy efficiency. However, why having largely passive motions (in a periodic motion that is not completely passive) would be energy efficient is not obvious a priori. That passivity might imply energy efficiency was initially motivated by observation of human gait (Mochon and McMahon, 1980) and later experimentally demonstrated by the building of these robots. It is in this context that we must note that the minimum-work solution (Chapters 3, 4, 5) in this thesis all consist of largely passive motions with brief periods where all the work is performed (impulsively). It is likely that some of the energetic benefits of these optimal solutions are inherited by the passive robots by their designers requiring most of the motion to be passive. Thus rather than attributing the energetic economy of the passive dynamic robots to some imagined but ill-defined notion of “natural dynamics” (by which passive dynamics is meant), their energy efficiency should be attributed to similarity to work-optimal motions. For instance, it might be possible to invent a world, where energy-optimal motions are far away from work-optimal motions, where passive dynamics would be far from being efficient – perhaps a world in which the energetic cost is dominated by a cost for force.

In summary, we hope that the analysis and appreciation of the simple models presented here will provide a minimal template to base our more complex thoughts upon, either for the building of robots, or more usefully, for the understanding, augmentation and modification of human and animal performance.

Chapter 8

Future work

8.1 Less restrictive calculations with the minimal model

In Chapter 3, for combinatorial simplicity of the optimal control problem, we considered only gaits with certain structure. For instance, we only considered gaits that had no double stance. We could relax this restriction, and repeat the optimizations including gaits with double stance. We also assumed that the two legs of the bipedal animal alternately go through the same motions. This assumption of symmetry between the two legs rules out gaits in which the two legs perform asymmetrically, as in unilateral skipping (see Chapter 2.5). We also ruled out higher periodic gaits such as bilateral skipping. We believe that the relaxation of all these constraints will produce no change in the optimal gaits except perhaps near the gait-transition region (around $V = 1$), where the metabolic cost landscape seems quite flat (that is, many gaits have very similar costs).

Although we believe that the relaxation of these constraints will produce no changes in the optimal solutions, we now briefly discuss how to relax these constraints. There are many ways to relax these restrictions on the structure of the gaits, but the relaxation must be done carefully. One way to relax these restrictions is to first enumerate separately each of the various distinct permutations of the flight, single stances and double stances. And then one can seek the optimal gait among gaits that have a particular permutation of stance and flight phases. Such a combinatorial approach is likely to get out of hand very quickly with the depth of the explored tree of possibilities. Another (less combinatorial) way to describe the structure of the various stance and flight phases is to specify the start and end times of each of the stance phases. But such parametrization of the phase-structure of a gait has its own issues. Using a separate grid to represent each of the leg-forces is no longer a good idea: relative movement of the two grids will mean that even a constant step-size integrator will be “inconsistent” (that is, a different sequence of arithmetic operations will be performed for arbitrarily small changes in some parameter). A solution to this problem might be to use high-accuracy integrators (say, using Taylor series methods) in conjunction with high-degree splines. Or avoid discretization using grids entirely and use C^∞ approximations such as those due to Fourier or Chebyshev as appropriate.

8.2 More calculations with the minimal model

We have clearly not exhausted all the possibly interesting calculations that could be performed with the minimal model. We have considered only steady locomotion on level ground. It would be interesting to see how predictions about gait transitions change with the slope of the ground. One could also use the model in the context of actually travelling a given distance in a given amount of time — starting from

rest and ending at rest. Of course, if we are trying to solve this problem for exactly the minimal model, one needs to impose further constraints such as average step lengths as in Chapter 3.

8.2.1 Optimal state-based feedback control

Even in steady locomotion, animals' gaits are not strictly periodic (Chapter 2) — external perturbations of various kinds need to be constantly corrected for. The principle of energetic optimality can be applied to these incessant corrective actions. How does one actuate the legs when knocked off a nominal optimal trajectory (such as inverted pendulum walking) so as to still minimize the cost per unit distance, but given the current perturbed state. The answer to this question will be a “control policy” or a state-based feedback control. The solution method (in the absence of incessant stochastic perturbations) will involve some numerical implementation of dynamic programming (Bertsekas, 1995; Morimoto et al., 2003). On the other hand, much of the stabilizing control authority in legged locomotion probably comes from appropriate foot-placement (Bauby and Kuo, 2000; Carver, 2003). So it is not clear if an attempt to find the optimal corrective action will be particularly insightful.

8.2.2 Adding force and power constraints

The minimal model can be minimally modified in a number of ways. For example, the minimal model had conceptually no force bounds — that is, infinite forces are possible. And this possibility of infinite forces were taken advantage of by three optimal gaits (inverted pendulum walking, etc.). In human walking and running, the leg-forces hardly exceed a small multiple of the body-weight. We could specify such an upper bound on the force, and compute the optimal gaits once again. Presumably, walking and running will still be optimal. But the impulses in inverted pendulum walking and impulsive running would be replaced by much lower forces — and the optimal gaits would be a little smoother. Constraints on the force-rate or the leg-power would presumably have a similar smoothing effect. In particular, we believe that such constraints would discover a running gait that would superficially look compliant and springy even though the mechanical model has no springs in it. Further, we believe that an extended double stance in walking might be energetically favored under these constraints, as it is in human walking.

8.2.3 Adding a cost for force

Alternative to (or in addition to) adding various constraints on force, we could modify the model of metabolic cost to incorporate a cost for force instead of a constraint on the force as in Equation 1.2 or variations thereof. A high-enough cost for high forces would have a smoothing effect on the optimal gaits, similar

to the smoothing effects of constraints on the leg-forces, presumably discovering a compliant running gait and a walking gait with an extended double stance phase.

8.2.4 Tendons in series with muscles

Real animal legs have tendons in series with the muscles. To model these tendons, we might add a spring in series with the telescoping actuator. But adding just a spring to the minimal model without appropriately adding a cost for force or adding passive dissipative elements will result in perfectly optimal zero-cost running motions (see 2.4.2). Dissipation is mechanically messy to incorporate into the model — and there is not much evidence for passive (non-collisional) dissipative mechanisms in a human leg (viscous dissipation is more likely dominant in a small insect). It seems more appropriate to add a cost for force instead to rule out passive cost-free motions. But what value of stiffness do we use for the spring? Perhaps we can use the effective spring constant displayed in Figure 2.8. The spring in series with the actuator will probably make walking a little more compliant. On the other hand, it would be interesting to see if running is indeed (as conjectured by some) a gait in which close-to-zero work is done by the muscle, most of the work done by the tendons, with most of the metabolic cost being due to the cost for isometric force.

8.3 A kinematically accurate minimal model of a bipedal animal

It is a common observation that we do not feel as tired standing with straight legs as we do standing with bent knees. Clearly standing requires the same vertical force ($= mg$) irrespective of how bent the legs are. However the kinematics of the knee is such that a straighter leg requires a much smaller knee-torque and hence much smaller forces from the muscles spanning the knee joint. This means that when the leg is straight, the cost of muscle force is likely to be small (Kuo et al., 2005).

Note that the addition of springs to the minimal model is likely to tilt the balance in favor of compliant gaits like running Alexander (1992). It seems plausible that the addition of a knee to the minimal model is likely to promote a straight-legged walking gait even in the presence of springs in series with the muscles.

So perhaps the minimal model that will capture most of the energetic aspects of human locomotion will be one that has a point-mass body, massless legs with actuated knees and ankles, springs in series with the actuators at the knee and the ankle, and a metabolic cost model that provides a cost for both work and force. If indeed energetic optimization with this model discovers walking and running, and predicts their respective metabolic costs quite accurately, we have reason to hope that it will explain why skipping is preferred by children and astronauts, but is more expensive than walking and running for human adults on earth.

BIBLIOGRAPHY

- R. K. Ahuja and J. B. Orlin. Inverse optimization. *Operations Research*, 49(5): 771–783, 2001.
- R. Alexander. Energy-saving mechanisms in walking and running. *J. Exp. Biol.*, 160:55–69, 1991.
- R. Alexander. A model of bipedal locomotion on compliant legs. *Phil. Trans. R. Soc. Lond.*, B338:189–198, 1992.
- R. Alexander. Invited editorial on “interaction of leg stiffness and surface stiffness during human hopping”. *J. App. Physiology*, 82:13–14, 1997.
- R. M. Alexander. Design by numbers. *Nature*, 412:591, 2001.
- R. M. Alexander. Work or force minimization as a criterion for the evolution of locomotion. In *Fourth World Congress of Biomechanics, Calgary, Canada*, August 2002a.
- R. M. Alexander. Tendon elasticity and muscle function. *Comparative Biochemistry and Physiology, Part A*, 133:1001–1011, 2002b.
- R. M. Alexander. *Principles of animal locomotion*. Princeton University Press, Princeton., 2003.
- R. M. Alexander. *Mechanics of bipedal locomotion.*, volume 1, pages 493–504. Pergamon Press, New York, 1976.
- R. M. Alexander. Optimum walking techniques for quadrupeds and bipeds. *J. Zool., Lond.*, 192:97–117, 1980.
- R. M. Alexander. *Elastic mechanisms in animal movement*. Cambridge University Press, Cambridge., 1988.
- R. M. Alexander. Optimization and gaits in the locomotion of vertebrates. *Physiol. Rev.*, 69:1199–1227, 1989.
- R. M. Alexander. *Energy for animal life*. Oxford University Press, UK, 1999.
- R. M. Alexander and G. M. O. Maloij. Stride lengths and stride frequencies of primates. *Journal of Zoology, London.*, 202:577–582, 1984.
- F. C. Anderson and M. G. Pandy. Dynamic optimization of human walking. *Journal of Biomechanical Engineering*, 123:381–390, 2001a.
- F. C. Anderson and M. G. Pandy. Static and dynamic optimization solutions for gait are practically equivalent. *Journal of Biomechanics*, 34:153–161, 2001b.

- F. C. Anderson and M. G. Pandy. A dynamic optimization solution for vertical jumping in three dimensions. *Computer Methods in Biomechanical and Biomedical Engineering.*, 2:201–231, 1999.
- J. V. Basmajian and C. De Luca. *Muscles Alive: Their Function Revealed by Electromyography*. Williams and Wilkins, Baltimore, MD, 1985.
- G. J. Bastien, P. A. Willems, B. Schepens, and N. C. Heglund. Effect of load and speed on the energetic cost of human walking. *Eur J Appl Physiol*, 94:76–83, 2005.
- C. E. Bauby and A. D. Kuo. Active control of lateral balance in human walking. *Journal of Biomechanics*, 33:1433–1440, 2000.
- M. Bekker. *Theory of Land Locomotion*. University of Michigan Press, Ann Arbor., 1956.
- J. Bertram, P. DAntonio, J. Pardo, and D. V. Lee. Pace-length effects in human walking: Groucho gaits revisited. *J. Motor Behavior.*, 34:309–318, 2002.
- J. E. A. Bertram and A. Ruina. Multiple walking speed-frequency relations are predicted by constrained optimization. *Journal of Theoretical Biology*, 209(4): 445–453, 2001.
- J. E. A. Bertram, A. Ruina, C. E. Cannon, Y. H. Chang, and M. Coleman. A point-mass model of gibbon locomotion. *J. Exp. Biol.*, 202:2609–2617, 1999.
- D. P. Bertsekas. *Dynamic programming and optimal control*. Athena Scientific, 1995.
- A. A. Biewener. Muscle-tendon stresses and elastic energy storage during locomotion in the horse. *Comparative Biochemistry and Physiology B*, 120:73–87, 1998.
- R. Blickhan and R. J. Full. Similarity in multilegged locomotion: bouncing like a monopode. *J. Comp. Physiol. A.*, 173:509–517, 1993.
- R. Blikhan. The spring-mass model for running and hopping. *J. Biomech.*, 22: 1217–1227, 1989.
- A. C. Bobbert. Energy expenditure in level and grade walking. *J. Appl. Physiol*, 15:1015–1021, 1960.
- J. Borelli. *On the movement of animals (De Motu Animalium, Pars prima)*. P. Maquet (trans.), 1989. Springer-Verlag, Berlin, p. 152., 1680.
- M. H. Bornstein and H. G. Bornstein. The pace of life. *Nature*, 259:557–558, 1976.

- D. Bramble and D. Lieberman. Endurance running and the evolution of homo. *Nature*, 432:345–352, 2004.
- W. Braune and O. Fischer. *Der Gang des Menschen (The Human Gait. Translated by P. Maquet, 1987)*. Springer-Verlag, Berlin, 1895-1904.
- G. A. Brooks, T. D. Fahey, T. P. White, and B. K. M. *Exercise physiology: Human bioenergetics and its applications*. Mayfield Publishing Company., 2000.
- L. S. Brotman and A. N. Netravali. Motion interpolation by optimal control. In *SIGGRAPH '88: Proceedings of the 15th annual conference on Computer graphics and interactive techniques*, pages 309–315, New York, NY, USA, 1988. ACM Press. ISBN 0-89791-275-6. doi: <http://doi.acm.org/10.1145/54852.378531>.
- A. Bryson and Y. Ho. *Applied Optimal Control*. John Wiley, NY, 1975.
- S. G. Carver. *Control of a spring mass hopper*. PhD thesis, Cornell University, Ithaca, 2003.
- G. A. Cavagna. Force platforms as ergometers. *J. Appl. Physiol.*, 39:174–179, 1975.
- G. A. Cavagna, F. P. Saibene, and R. Margaria. External work in walking. *J. Appl. Physiol.*, 18:1–9, 1963.
- G. A. Cavagna, F. P. Saibene, and R. Margaria. Mechanical work in running. *J. Appl. Physiol.*, 19:249–256, 1964.
- G. A. Cavagna, N. C. Heglund, and C. R. Taylor. Mechanical work in terrestrial locomotion: two basic mechanisms for minimizing energy expenditure. *Am. J. Physiol.*, 233:243–261, 1977.
- P. R. Cavanagh and K. R. Williams. The effect of stride length variation on oxygen uptake during distance running. *Med. Sci. Sports Exercise*, 14:30–35., 1982.
- C. Chevallereau, Y. Aoustin, and A. Formal'sky. Optimal walking trajectories for a biped. In *IEEE Robot Motion and Control*, pages 171–176, Kiekrz, June 1999.
- C. K. Chow and D. H. Jacobson. Studies of human locomotion via optimal programming. *Mathematical Biosciences*, 10:239–306, 1971.
- S. Collins, A. Ruina, R. Tedrake, and M. Wisse. Efficient bipedal robots based on passive dynamic walkers. *Science Magazine*, 307:1082–1085, 2005.
- R. Crowninshield and R. Brand. A physiologically based criterion of muscle force prediction in locomotion. *Journal of Biomechanics*, 14:793–801, 1981.
- D. T. Davy and M. L. Audu. A dynamic optimization technique for predicting muscle forces in the swing phase of gait. *J. Biomech.*, 20:187201, 1987.

- S. L. Delp and J. P. Loan. A computational framework for simulating and analyzing human and animal movement. *Computing in Science and Engineering [see also IEEE Computational Science and Engineering]*, 2:46–55, 2000.
- J. B. Dingwell and J. P. Cusumano. Nonlinear time series analysis of normal and pathological human walking. *Chaos*, 10(4):848–863, 2000.
- J. Doke, M. J. Donelan, and A. D. Kuo. Mechanics and energetics of swinging the human leg. *J. Exp. Biol.*, 208:439–445, 2005.
- J. M. Donelan, R. Kram, and A. D. Kuo. Mechanical and metabolic determinants of the preferred step width in human walking. *Proc. R. Soc. Lond. B*, 268:1985–1992, 2001.
- J. M. Donelan, R. Kram, and A. D. Kuo. Mechanical and metabolic costs of step-to-step transitions in human walking. *Journal of Experimental Biology*, 205:3717–3727, 2002a.
- M. J. Donelan, R. Kram, and A. D. Kuo. Simultaneous positive and negative external mechanical work in human walking. *J. Biomech.*, 35:117–124, 2002b.
- C. T. Farley and O. Gonzalez. Leg stiffness and stride frequency in human running. *J. Biomech.*, 29:181–186, 1996.
- C. T. Farley and C. R. Taylor. A mechanical trigger for the trot-gallop transition in horses. *Science*, 253:306–308, 1991.
- C. T. Farley, R. Blickhan, J. Saito, and C. R. Taylor. Hopping frequency in humans: a test of how springs set stride frequency in bouncing gaits. *J. Appl. Physiol.*, 71:2127–2132, 1991.
- W. O. Fenn. Work against gravity and work due to velocity changes in running: Movements of the center of gravity within the body and foot pressure on the ground. *Am J Physiol*, 93:433–462, 1930a.
- W. O. Fenn. Frictional and kinetic factors in the work of sprint running. *Am J Physiol*, 92:583–611, 1930b.
- T. Flash and N. Hogan. The coordination of arm movements: an experimentally confirmed mathematical model. *Journal of Neuroscience*, 5:1688–1703, 1985.
- M. Garcia, A. Chatterjee, and A. Ruina. Efficiency, speed, and scaling of two-dimensional passive-dynamic walking. *Dynamics and Stability of Systems*, 15(2):75–99, 2000.
- H. Geyer, A. Seyfarth, and R. Blickhan. Spring-mass running: simple approximate solution and application to gait stability. *J Theor Biol.*, 232:315–28, 2005.

- R. M. Ghigliazza, R. Altendorfer, P. Holmes, and D. Koditschek. A simply stabilized running model. *SIAM Review*, 47:519–549, 2005.
- P. E. Gill, W. Murray, and M. A. Saunders. Snopt: An sqp algorithm for large-scale constrained optimization. *SIAM J. Optim.*, 12:979–1006, 2002.
- M. Gomes and A. Ruina. A passive dynamic walking model that walks on level ground. In *International Society of Biomechanics XIX Congress, Dunedin, New Zealand*, 2003.
- M. Gomes and A. Ruina. A five-link 2d brachiating ape model with life-like zero-energy-cost motions. *Journal of Theoretical Biology*, 237(3):265–278, 2005a.
- M. Gomes and A. Ruina. A walking model with no energy cost. *Phys Rev E*, 2005b.
- K. Gordon, D. Ferris, and A. Kuo. Reducing vertical center of mass movement during human walking doesn't necessarily reduce metabolic cost. In *Proc. 27-th Annual Meeting. American Society Biomechanics, Toledo, OH*. American Society of Biomechanics, 2003.
- S. J. Gould and R. C. Lewontin. The spandrels of san marco and the panglossian paradigm: a critique of the adaptationist program. *Proceedings of the Royal Society of London, Series B.*, 205, 1979.
- S. Grillner. Neural networks for vertebrate locomotion. *Scientific American*, 274:64–69, 1996.
- S. Grillner, P. Wall, L. Brodin, and A. Lansner. Neuronal network generating locomotor behavior in lamprey: Circuitry, transmitters, membrane properties, and simulation. *Annual Review of Neuroscience*, 14:169–199, 1991.
- S. Grillner, T. Deliagina, A. E. Ekeberg, and Manira, R. Hill, A. Lansner, G. Orlovsky, and P. Wall. Neural networks that co-ordinate locomotion and body orientation in lamprey. *Trends in Neuroscience*, 18:270–279, 1995.
- D. Hardt. Determining muscle forces in the leg during human walking: an application and evaluation of optimization methods. *Journal of Biomechanical Engineering*, 100:72–78, 1978.
- M. Hardt, K. Kreutz-Delgado, and J. W. Helton. Optimal biped walking with a complete dynamical model. In *IEEE Conference on Decision and Control, Phoenix, AZ*, 1999.
- H. Hatze. The complete optimization of the human motion. *Mathematical Biosciences*, 28:99–135, 1976.

- J. M. Hausdorff, C. K. Peng, Z. Ladin, J. Y. Wei, and A. L. Goldberger. Is walking a random walk? evidence for long-range correlations in stride interval of human gait. *J. Appl. Physiol.*, pages 349–358, 1995.
- P. Högberg. How do stride length and stride frequency influence the energy-output during running? *Arbeitsphysiologie*, 14:437–441, 1952.
- D. F. Hoyt and C. R. Taylor. Gait and the energetics of locomotion in horses. *Nature*, 292:239–240, 1981.
- A. Hreljac. Preferred and energetically optimal gait transition speeds in human locomotion. *Med. Sci. Sports Exerc.*, 25:1158–1162, 1993.
- Y. Hurmuzlu and G. D. Moskowitz. Bipedal locomotion stabilized by impact and switching: I. two and three dimensional, three element models. *International Journal of Dynamics and Stability of Systems*, 2:73–96, 1987a.
- Y. Hurmuzlu and G. D. Moskowitz. Bipedal locomotion stabilized by impact and switching: Ii. structural stability analysis of a four-element model. *International Journal of Dynamics and Stability of Systems*, 2:97–112, 1987b.
- E. R. Kandel, J. H. Schwartz, and T. M. Jessell. *Principles of Neural Science*. McGraw-Hill Medical; 4 edition, 2000.
- R. Kram and C. R. Taylor. Energetics of running: a new perspective. *Nature*, 346:265–267, 1990.
- R. Kram, T. M. Griffin, J. M. Donelan, and Y. H. Chang. Force treadmill for measuring vertical and horizontal ground reaction forces. *Journal of Applied Physiology*, 85(2):764–769, 1998.
- T. M. Kubow and R. J. Full. The role of the mechanical system in control: a hypothesis of self-stabilization in hexapedal runners. *Philosophical transactions of the Royal Society B*, 354:849–861, 1999.
- A. D. Kuo. A simple model predicts the step length-speed relationship in human walking. *Journal of Biomechanical Engineering*, 123:264–269, 2001.
- A. D. Kuo. Energetics of actively powered locomotion using the simplest walking model. *J. Biomech. Eng.*, 124:113–120, 2002.
- A. D. Kuo, J. M. Donelan, and A. Ruina. Energetic consequences of walking like an inverted pendulum: step-to-step transitions. *Exer. Sport Sci. Rev.*, 33:88–97, 2005.
- H. D. Lee and W. Herzog. Force enhancement following muscle stretch of electrically and voluntarily activated human adductor pollicis. *Journal of Physiology*, 545:321–330, 2002.

- R. V. Levine and A. Norenzayan. The pace of life in 31 countries. *Journal of Cross-Cultural Psychology*, 30(2):178–205, 1999.
- C. K. Liu, A. Hertzmann, and Z. Popović. Learning physics-based motion style with nonlinear inverse optimization. In *ACM, SIGGRAPH.*, 2005.
- S. P. Ma and G. I. Zahalak. A distribution-moment model of energetics in skeletal muscle. *Journal of Biomechanics*, 24(1):21–35, 1991.
- E. Marder and D. Bucher. Central pattern generators and the control of rhythmic movements. *Current Biology*, 11:R986–R996, 2001.
- E. J. Marey. *Animal Mechanism. A treatise on terrestrial and aerial locomotion (2nd edition)*. Henry S. King & Co., London., 1874.
- R. Margaria. *Biomechanics and Energetics of Muscular Exercise*. Oxford, UK, Clarendon Press., 1976.
- R. L. Marsh, D. J. Ellerby, J. A. Carr, H. T. Henry, and C. I. Buchanan. Partitioning the energetics of walking and running: swinging the legs is expensive. *Science*, 303:80–83, 2004.
- T. McGeer. Passive dynamic walking. *International Journal of Robotics Research*, 9:62–82, 1990a.
- T. McGeer. Passive dynamic walking. *The International Journal of Robotics Research*, 9(2):62–82, 1990b.
- T. McGeer. Passive walking with knees. *Proceedings of 1990 IEEE International Conference on Robotics and Automation*, 3:1640–1645, 1990c.
- T. McGeer. Passive bipedal running. *Proceedings of the Royal Society of London B*, 240:107–134, 1990d.
- T. McGeer. Passive dynamic biped catalog. *Proceedings of Experimental Robotics II: The International Symposium*, pages 465–490, 1992.
- T. McMahon and G. Cheng. The mechanics of running: how does stiffness couple with speed? *J. Biomech.*, 23, Suppl.1:65–78, 1990.
- T. A. McMahon. *Mucles, reflexes, and locomotion*. Princeton university press, Princeton, NJ, 1984.
- L. Menegaldo, A. de Toledo Fleury, and H. Weber. Biomechanical modeling and optimal control of human posture, 2003. *Journal of Biomechanics*, in press.
- A. Minetti and R. M. Alexander. A theory of metabolic costs for bipedal gaits. *J. Theor. Biol*, 186:467–476, 1997.

- A. E. Minetti. The biomechanics of skipping gaits: a third locomotor paradigm? *Proc. R. Soc. B*, 265:1227–1235, 1998.
- A. E. Minetti, L. P. Ardigo, and F. Saibene. The transition between walking and running in humans: metabolic and mechanical aspects at different gradients. *Acta Physiol. Scand.*, 150:315–323, 1994.
- S. Mochon and T. McMahon. Ballistic walking. *Journal of Biomechanics*, 13:49–57, 1980.
- J. Morimoto, G. Zeglin, and C. G. Atkeson. Minimax differential dynamic programming: application to a biped walking robot. In *Proceedings of the 2003 IEEE/RSJ Intl. Conference on Intelligent Robots and Systems Las Vegas, Nevada*, 2003.
- A. Nagano, B. R. Umberger, M. W. Marzke, and K. G. M. Gerritsen. Neuro-musculoskeletal computer modeling and simulation of upright, straight-legged, bipedal locomotion of australopithecus afarensis (a.l. 288-1). *American journal of physical anthropology*, 126:2–13, 2005.
- R. Neptune, F. Zajac, and S. Kautz. Muscle force redistributes segmental power for body progression during walking. *Gait and Posture*, 19:194–205, 2004.
- R. R. Neptune, S. A. Kautz, and F. E. Zajac. Contributions of the individual ankle plantar flexors to support, forward progression and swing initiation during walking. *Journal of Biomechanics*, 34:1387–1398, 2001.
- H. F. Nijhout and D. J. Emlen. Competition among body parts in the development and evolution of insect morphology. *Proc. Natl. Acad. Sci. USA*, 95:3685–3689, 1998.
- J. D. Ortega and C. T. Farley. Minimizing center of mass vertical movement increases metabolic cost in walking. *J. Appl. Physiol.*, 2005. doi: 10.1152/jap-physiol.00103.2005.
- D. T. P. P H Channon, S H Hopkins. Simulation and optimisation of gait for a bipedal robot. *Mathematical and Computer Modelling*, 14:463–467, 1990.
- M. Pandy, B. A. Garner, and F. C. Anderson. Optimal control of non-ballistic muscular movements: A constraint-based performance criterion for rising from a chair. *Journal of Biomechanical Engineering*, 117:15–26, 1995.
- M. G. Pandy, F. E. Zajac, E. Sim, and W. S. Levine. An optimal control model for maximum-height human jumping. *Journal of Biomechanics*, 23:1185–1198, 1990.
- J. Perry. *Gait analysis: normal and pathological function*. SLACK, Thorofare, NJ, 1992.

- J. Pratt. *Exploiting Inherent Robustness and Natural Dynamics in the Control of Bipedal Walking Robots*. PhD thesis, MIT, 2000.
- C. Raasch, F. Zajac, B. Ma, and W. Levine. Muscle coordination of maximum-speed pedaling. *Journal of Biomechanics*, 30:595–602, 1997.
- V. Radhakrishnan. Locomotion: dealing with friction. *Proc Natl Acad Sci U S A.*, 95:5448–5455, 1998.
- M. H. Raibert. *Legged robots that balance*. MIT Press, Cambridge., 1986.
- H. J. Ralston. Energy-speed relation and optimal speed during level walking. *Int Z Angew Physiol.*, 17:277–283., 1958.
- H. J. Ralston. Energetics of human walking. In R. M. Herman, S. Grillner, P. S. G. Stein, and D. G. Stuart, editors, *Neural control of locomotion*. Plenum Press, New York, 1976.
- N. Rashevsky. Studies in the physicomathematical theory of organic form. *Bull. Math. Biophysics.*, 6:1–59, 1944.
- N. Rashevsky. On the locomotion of mammals. *Bull. Math. Biophysics.*, 10:11–23, 1948.
- J. L. Ringuest. *Multiobjective optimization : behavioral and computational considerations*. Kluwer Academic Publishers, Boston, 1992.
- T. J. Roberts, R. L. Marsh, P. G. Weyand, and C. R. Taylor. Muscular force in running turkeys: The economy of minimizing work. *Science*, 275:1113–1115, 1997.
- L. Roussel, C. C. de Wit, and A. Goswami. Generation of energy optimal complete gait cycles for biped robots. In *Proceedings of the 1998 IEEE International Conference on Robotics and Automation, Leuven, Belgium*, 1998.
- A. Ruina, J. Bertram, and M. Srinivasan. A collisional model of the energetic cost of support work qualitatively explains leg-sequencing in walking and galloping, pseudo-elastic leg behavior in running and the walk-to-run transition. *J. Theor. Biol.*, 14:170–192, 2005.
- J. B. D. Saunders, V. T. Inman, and H. D. Eberhart. The major determinants in normal and pathological gait. *Am. J. Bone. Joint. Surg.*, 35:543–558, 1953.
- J. Seipel and P. Holmes. Running in three dimensions: Analysis of a point-mass sprung-leg model. *Int. J. Robotics Research*, 24:657–674, 2005.
- W. I. Sellers, L. A. Dennis, W. J. Wang, and R. H. Crompton. Evaluating alternative gait strategies using evolutionary robotics. *J. Anat.*, 204, 2004.

- A. Seyfarth, H. Geyer, M. Gunther, and R. Blickhan. A movement criterion for running. *J Biomech.*, 35:649–55, 2002.
- J. M. Smith. Optimization theory in evolution. *Annual Review of Ecology and Systematics*, 9, 1978.
- J. M. Smith. *Evolution and the theory of games*. Cambridge University Press, Cambridge, 1982.
- M. Srinivasan and A. Ruina. Computer optimization of a minimal biped model discovers walking and running. *Nature*, 439:72–75, 2006.
- W. J. Sutherland. The best solution. *Nature*, 435:569, 2005.
- K. Taji and M. Miyamoto. A globally convergent smoothing newton method for nonsmooth equations and its application to complementarity problems. *Computational Optimization and Applications*, 22:81–101, 2002.
- S. Tashman, F. E. Zajac, and I. Perakash. Modeling and simulation of paraplegic ambulation in a reciprocating gait orthosis. *Journal of Biomechanical Engineering*, 117:300–308, 1995.
- A. Thorstensson and H. Robertson. Adaptations to changing speed in human locomotion: speed of transition between walking and running. *Acta. Physiol. Scand.*, 131:211–214, 1987.
- V. Tucker. The energetic cost of moving about. *Am. Sci.*, 63:413–419, 1975.
- J. R. Usherwood. Why not walk faster? *Biology letters*, 1:338 – 341, 2005.
- O. von Stryk. User’s guide for dircol (version 2.1): A direct collocation method for the numerical solution of optimal control problems. Technical report, Fachgebiet Simulation und Systemoptimierung, Technische Universit Darmstadt, November 1999.
- W. Wang, R. H. Crompton, T. S. Carey, M. M. Günther, Yu Li, R. Savage, and W. I. Sellers. Comparison of inverse-dynamics musculo-skeletal models of al 288-1 australopithecus afarensis and knm-wt 15000 homo ergaster to modern humans, with implications for the evolution of bipedalism. *Journal of Human Evolution*, 47:453–478, 2004.
- S. J. Wickler, D. F. Hoyt, E. A. Cogger, and M. H. Hirschbein. Preferred speed and cost of transport: the effect of incline. *The Journal of Experimental Biology*, 203:2195–2200, 2000.
- S. J. Wickler, D. F. Hoyt, E. A. Cogger, and G. Myers. The energetics of the trot-gallop transition. *The Journal of Theoretical Biology*, 206:1557–1564, 2003.

- S. Wright and P. Weyand. The application of ground force explains the energetic cost of running backward and forward. *J. Exp. Biol.*, 204:1805–1816, 2001.
- G. T. Yamaguchi and F. E. Zajac. Restoring unassisted natural gait to paraplegics via functional neuromuscular stimulation: a computer simulation study. *IEEE Transactions on Biomedical Engineering.*, 37:886–902, 1990.
- F. E. Zajac. Muscle and tendon: properties, models, scaling, and application to biomechanics and motor control. *Critical Review of Biomedical Engineering*, 17: 359–411, 1989.
- F. E. Zajac. Muscle coordination of movement: A perspective. *Journal of Biomechanics*, 26:109–124, 1993.
- M. Y. Zarrugh, F. N. Todd, and H. J. Ralston. Optimization of energy expenditure during level walking. *European Journal of Applied Physiology*, 33(4):293–306, 1974.